

An explanation of the **merced** code

Gerald Hedstrom
Nuclear Theory & Data Group
Lawrence Livermore National Laboratory

14 June 2017

Contents

1	Summary	1
2	Transfer matrices	2
2.1	Conservation of particle number	5
2.2	Conservation of energy	5
2.3	Conservation of both particles and energy	6
2.4	Control of the conservation option	7
2.5	Numerical quadrature	8
3	Interpolation of the data	9
3.1	Interpolation methods for a single variable	9
3.1.1	Histograms	9
3.1.2	Linear-linear	9
3.1.3	Log-linear	9
3.1.4	Linear-log	10
3.1.5	Log-log	10
3.2	Interpolation methods for probability densities	10
3.2.1	Direct interpolation	11
3.2.2	Unit-base interpolation	13
3.2.3	Interpolation by cumulative points	14
3.3	Unscaled interpolation of Kalbach-Mann data	15
4	Discrete two-body reactions	18
4.1	Newtonian mechanics of discrete 2-body reactions	18
4.1.1	The boost to the laboratory frame	20
4.2	Computation of the transfer matrix from data for discrete 2-body reactions	21
4.3	Format of data in the input file	23
4.3.1	Data for both forms of probability density	23
4.3.2	Angular probability density tables	23
4.3.3	Legendre coefficients of angular probability density	24
5	Isotropic energy probability densities in the laboratory frame	26
5.1	Computational aspects of incomplete gamma functions	26
5.2	Functional formulas for isotropic probability densities	27

5.2.1	Evaporation model	27
5.2.2	Maxwell model	29
5.2.3	Watt model	30
5.2.4	Madland-Nix model	31
5.3	Energy probability density tables	35
5.3.1	Input of isotropic energy probability tables	35
5.4	General evaporation of delayed fission neutrons	37
5.4.1	Input of data for the general evaporation model	37
6	Uncorrelated energy-angle probability densities	39
6.1	Input of data for uncorrelated energy-angle probability densities	40
7	Legendre expansions of energy-angle probability densities in the laboratory frame	42
7.1	Computation of the transfer matrices for data in the laboratory frame . . .	42
7.2	Form of the input file for Legendre coefficient data in the laboratory frame	43
7.2.1	Input of all Legendre coefficients together	43
7.2.2	Input of one Legendre coefficient at a time	44
8	Legendre expansions of energy-angle probability densities in the center-of-mass frame	47
8.1	Geometrical considerations	48
8.1.1	Assertion	48
8.2	Input of Legendre coefficients of energy-angle probability densities in the center-of-mass frame	49
8.3	Input of isotropic energy probability densities in the center-of-mass frame .	49
9	Joint energy-angle probability density tables	50
9.1	Input of $\pi(E'_{\text{lab}}, \mu_{\text{lab}} E)$ the form of a table, Eq. (9.1)	51
9.2	Input of $\pi(E'_{\text{lab}}, \mu_{\text{lab}} E)$ as a product, Eq. (9.2)	52
10	Formulas for double-differential energy-angle data	55
10.1	The Kalbach-Mann model for double-differential data	55
10.1.1	The Kalbach-Mann a parameter	56
10.1.2	Photo-nuclear reactions	58
10.1.3	Interpolation of Kalbach-Mann data	58
10.1.4	The input file for the Kalbach-Mann model	60
10.2	The n -body phase space model	63
10.2.1	Geometry of the n -body phase space model	64
10.2.2	Input file for the n -body phase space model	64
11	Data for incident gammas	66
11.1	Coherent scattering	66
11.1.1	A programming detail	67
11.1.2	The input file for coherent scattering	68

11.2	Compton scattering	69
11.2.1	The input file for Compton scattering	71
12	Usage of merced	73
12.1	Output file	73
12.2	Form of the input file	73
12.2.1	Comments	73
12.2.2	Parallel computing	74
12.2.3	Interpolation flags	74
12.3	Information used by all data models	75
12.3.1	The data model	76
12.3.2	Incident energy groups	76
12.3.3	Outgoing energy groups	76
12.3.4	Frames of reference	76
12.3.5	Relativistic kinetics	76
12.3.6	Approximate flux	77
12.3.7	Reaction cross section	77
12.3.8	Multiplicity	78
12.3.9	Model weight	78
12.4	Optional flags, output information	78
12.4.1	Legendre order of the output	79
12.4.2	Numerical precision of the output	79
12.4.3	Conservation flag	79
12.4.4	Consistency check	79
12.5	Optional inputs, quadrature methods	79
12.6	Optional inputs, numerical tolerances	80
12.6.1	Convergence of adaptive quadrature	80
12.6.2	Near equality of floating-point numbers	80
12.7	Physical constants	81
12.7.1	Conversion from \AA^{-1} to energy	81
12.7.2	Thompson scattering cross section	81
12.7.3	Electron rest mass	81
12.7.4	Neutron rest mass	81
12.8	Errors and warning messages	81
12.9	Model-dependent information	82
A	Relativistic 2-body problems	83
A.1	Initial collision	83
A.2	Mapping between frames	84
A.2.1	Incident photons	85
A.3	Outgoing particles	86
A.3.1	The boost to the laboratory frame	87
A.3.2	Photon emission	88

B	Proof of Assertion 8.1.1	89
B.1	An equivalent geometric condition	89
B.2	Proof of the assertion	91

1 Summary

The `merced` code is one of the computer programs used in the conversion of reaction data from the `GND` library [1] of evaluated nuclear data to input for deterministic particle transport codes. This data conversion is managed by the `fudge` python script [2], while the `merced` code performs the computation of transfer matrices used to approximate the kernel in the integral operator of the Boltzmann equation.

This document is organized as follows. Section 2 explains how the transfer matrix is used in the discretization of the Boltzmann equation. Section 3 examines the methods used for interpolation of data in `GND`. The remainder of the document is devoted to a discussion of the considerations involved in computing transfer matrices based on the various data formats used in the `GND` library.

For discrete 2-body reactions, the processing of angular probability density data given in the center-of-mass frame is discussed in Section 4. The treatment here is Newtonian, with a relativistic version presented in Appendix A.

Section 5 discusses the treatment of the data in `GND` used for isotropic energy probability densities given in the laboratory frame.

Sections 6 through 10 deal with double-differential, energy-angle probability density data. Uncorrelated energy-angle probability density data is presented in Section 6. One option for energy-angle probability density data is as coefficients of Legendre expansions. This option is discussed in Section 7 for data given in the laboratory frame and in Section 8 for center-of-mass data. The proof of a mathematical detail used in analysis of the boost for such data is given in Appendix B. Energy-angle probability densities may also be presented as tabulated data as discussed in Section 9. The final form of energy-angle probability density data is in the form of parameters of mathematical formulas, and these are taken up in Section 10.

Section 11 deals with special data for incident gammas, specifically, coherent scattering and Compton scattering.

Finally, the document closes in Section 12 with instructions on how to run `merced`, along with an explanation of the input parameters.

2 Transfer matrices

Deterministic particle transport codes solve a discrete version of the Boltzmann equation, and the transfer matrix approximates the kernel of the integral operator in this equation. If x denotes the position, t the time, E' the particle energy, Ω' the direction of motion, v the magnitude of the velocity (speed), and $n(x, t, E', \Omega')$ the number density, then the flux $\phi = vn$ satisfies the Boltzmann equation [3]

$$\frac{1}{v} \partial_t \phi(E', \Omega') + \Omega' \cdot \nabla \phi(E', \Omega') + \rho \sigma_t \phi(E', \Omega') = \frac{\rho}{4\pi} \int_{\Omega} d\Omega \int_0^{\infty} dE \mathcal{K}(E', \Omega' \cdot \Omega | E) \phi(E, \Omega). \quad (2.1)$$

The direction Ω' is relative to some given “north pole” Ω_0 , and ρ is the density of the material. The dependence on x and t is suppressed. The first two terms in Eq. (2.1) give the derivative with respect to distance of the flux in a coordinate system moving with the particles. The parameter σ_t is the microscopic total cross section, so the term $\rho \sigma_t \phi(E', \Omega')$ represents the rate of particle loss per particle path length.

The kernel $\mathcal{K}(E', \Omega' \cdot \Omega | E)$ in Eq. (2.1) gives the rate of production of outgoing particles with energy E' and direction Ω' corresponding to incident particles at energy E and direction Ω . Here, the energies E and E' and the directions Ω and Ω' are in the laboratory coordinate system. From here on, the notation

$$\mu = \Omega' \cdot \Omega$$

is used. It is significant that the dependence of $\mathcal{K}(E', \mu | E)$ on μ is axisymmetric, because the orientation of the target nucleus is unknown. The primes are placed where they are in Eq. (2.1), because the emphasis in this document is on approximation of the right-hand side of the equation. In that setting, it is natural that E denote the energy of the incident particle and E' the outgoing particle energy.

For a given target, the nuclear data in GND is given reaction by reaction, e.g., elastic scattering, neutron capture, fission, etc. The transfer matrix approximating \mathcal{K} is built up by summing over the reactions r

$$\mathcal{K} = \sum_r \mathcal{K}_r.$$

The reaction kernels \mathcal{K}_r themselves are not given in GND, but their component factors are given instead, namely,

1. $\sigma_r(E)$: the cross section for the r -th reaction,
2. $M_r(E)$: the multiplicity of the outgoing particle,
3. $w_r(E)$: the model weight for these data,

4. $\pi_r(E', \mu | E)$: the double-differential probability density of the energy and direction cosine for one outgoing particle.

In terms of this notation, \mathcal{K}_r is the product

$$\mathcal{K}_r(E', \mu | E) = \sigma_r(E) M_r(E) w_r(E) \pi_r(E', \mu | E). \quad (2.2)$$

The multiplicity $M_r(E)$ may be constant, e.g., 1 for elastic scattering and 2 for $(n, 2n)$ reactions, but the number of fission neutrons depends on the incident energy E . The default is $M_r(E) = 1$.

Model weight The model weight is usually $w_r(E) = 1$, and that is the default. One exception is that data for a single outgoing neutron in an $(n, 2n)$ reaction may have $M_r(E) = 2$ and $w_r(E) = 0.5$. The model weight is also used to handle the use of different interpolation rules over different ranges of incident energy. Thus, if the interpolation for $E_1 < E < E_2$ is different from that for $E_2 < E < E_3$, the data may be split into two sets, one with

$$w_r(E) = \begin{cases} 1 & \text{for } E_1 \leq E < E_2, \\ 0 & \text{for } E_2 \leq E \leq E_3, \end{cases}$$

and the other with

$$w_r(E) = \begin{cases} 0 & \text{for } E_1 \leq E < E_2, \\ 1 & \text{for } E_2 \leq E \leq E_3. \end{cases}$$

The GND nuclear data consist of tables of $\sigma_r(E)$ and $\pi_r(E', \mu | E)$ and possibly $M_r(E)$ and $w_r(E)$. The data for $\pi_r(E', \mu | E)$ take several forms, and the various data representations are dealt with individually.

The discretization of Eq. (2.1) is based, first, on the specification of a set of energy groups $\{\mathcal{E}_g\}$ for the incident particles and energy groups $\{\mathcal{E}'_h\}$ for the emitted particles. The energy groups for neutrons are typically different from those for gammas, and yet another set is usually used for charged particles. The flux $\phi(E, \Omega)$ inside the integral in Eq. (2.1) is discretized according to the energy groups of the incident particle, while $\phi(E', \Omega')$ on the left-hand side of Eq. (2.1) is discretized according to the energy groups of the outgoing particles. These energy groups are also called energy bins.

According to the normalization for Legendre expansions used in GND, the angular discretization of π_r in Eq. (2.2) is given by

$$\pi_r(E', \mu | E) = \sum_{\ell} \left(\ell + \frac{1}{2} \right) \pi_{r\ell}(E' | E) P_{\ell}(\mu)$$

with $P_{\ell}(\mu)$ denoting the ℓ -th Legendre polynomial and

$$\pi_{r\ell}(E' | E) = \int_{-1}^1 d\mu \pi_r(E', \mu | E) P_{\ell}(\mu). \quad (2.3)$$

The flux $\phi(E, \Omega)$ in Eq. (2.1) is expanded into spherical harmonics

$$\phi(E, \Omega) = \sum_{\ell, m} C_{\ell, m} \phi_{\ell, m}(E) Y_{\ell, m}(\Omega) \quad (2.4)$$

with normalization

$$C_{\ell, m} = \frac{1}{\int d\Omega [Y_{\ell, m}(\Omega)]^2}.$$

A discrete approximation to Eq. (2.1) may be obtained by expanding $\phi(E, \Omega)$ in spherical harmonics and integrating over the outgoing energy group \mathcal{E}'_h . This gives an equation for the vector of values

$$\phi_{\ell, m}(E'_h).$$

Note that $\phi_{\ell, m}(E'_h)$ is a histogram with respect to the energy E' of the outgoing particle, constant on each energy group \mathcal{E}'_h . Integration of the right-hand side of Eq. (2.1) over \mathcal{E}'_h gives

$$\mathcal{I}_{h, \ell} = \sum_r \int_0^\infty dE \phi_{\ell, 0}(E) \int_{\mathcal{E}'_h} dE' \int_{-1}^1 d\mu \mathcal{K}_r(E', \mu | E) P_\ell(\mu). \quad (2.5)$$

The integral Eq. (2.5) contains only the spherical harmonics with $m = 0$, because the kernel \mathcal{K}_r is axisymmetric.

The unknown flux ϕ appears in Eq. (2.1) both on the left-hand side of the equation and under the integral sign. It is therefore convenient to start the calculation using an assumed approximate value of $\phi_{\ell, 0}(E)$ in the integral Eq. (2.5), namely,

$$\phi_{\ell, 0}(E) \approx \tilde{\phi}_\ell(E). \quad (2.6)$$

Upon inserting Eq. (2.6) into Eq. (2.5) and taking the incident energy groups \mathcal{E}_g one at a time, it is found that Eq. (2.5) may be viewed as the product of a matrix with a column vector. Here, the column vector has the components $\phi_{\ell, 0}(E'_h)$, and the components of the matrix are given by

$$\mathcal{J}_{g, h, \ell} = \frac{\mathcal{I}_{g, h, \ell}}{\int_{\mathcal{E}_g} dE \tilde{\phi}_\ell(E)}$$

with

$$\mathcal{I}_{g, h, \ell} = \sum_r \int_{\mathcal{E}_g} dE \tilde{\phi}_\ell(E) \int_{\mathcal{E}'_h} dE' \int_{-1}^1 d\mu \mathcal{K}_r(E', \mu | E) P_\ell(\mu).$$

The quantities $\mathcal{J}_{g, h, \ell}$ constitute the entries of the *transfer matrix*.

The above discussion gives one way of defining the transfer matrix, but the **fudge** code has three different representations, depending on whether one wants to conserve the number of particles, the energy, or both. Traditionally, conservation of particle number has been used for neutron transport, conservation of energy for gammas, and conservation of both energy and number for charged particles. These cases are taken up in turn.

2.1 Conservation of particle number

With the approximate flux coefficient $\tilde{\phi}_\ell$ in Eq. (2.6) and the representation Eq. (2.2) of the kernel \mathcal{K}_r , the ℓ -th Legendre coefficient of the contributions of energy groups \mathcal{E}_g and \mathcal{E}'_h to the integral in Eq. (2.1) by reaction r is given by

$$\mathcal{I}_{r,g,h,\ell}^{\text{num}} = \int_{\mathcal{E}_g} dE \sigma_r(E) M_r(E) w_r(E) \tilde{\phi}_\ell(E) \int_{\mathcal{E}'_h} dE' \int_{\mu} d\mu P_\ell(\mu) \pi_r(E', \mu | E). \quad (2.7)$$

For conservation of particle number the elements of the transfer matrix are the sums over all reactions,

$$\mathcal{J}_{g,h,\ell} = \frac{\sum_r \mathcal{I}_{r,g,h,\ell}^{\text{num}}}{\int_{\mathcal{E}_g} dE \tilde{\phi}_\ell(E)}. \quad (2.8)$$

The `merced` code computes the integrals $\mathcal{I}_{r,g,h,\ell}^{\text{num}}$ reaction by reaction, and the operation Eq. (2.8) is performed by `fudge`.

Note that the number-preserving transfer matrices offer a simple check. Because the probability density $\pi_r(E', \mu | E)$ has the normalization

$$\int_0^\infty dE' \int_{-1}^1 d\mu \pi_r(E', \mu | E) = 1,$$

it follows from Eq. (2.7) that

$$\sum_h \mathcal{I}_{r,g,h,0}^{\text{num}} = \int_{\mathcal{E}_g} dE \sigma_r(E) M_r(E) w_r(E) \tilde{\phi}_0(E). \quad (2.9)$$

2.2 Conservation of energy

When conservation of energy is desired, the integral Eq. (2.7) is modified by insertion of E' as a weight factor

$$\mathcal{I}_{r,g,h,\ell}^{\text{en}} = \int_{\mathcal{E}_g} dE \sigma_r(E) M_r(E) w_r(E) \tilde{\phi}_\ell(E) \int_{\mathcal{E}'_h} dE' E' \int_{\mu} d\mu P_\ell(\mu) \pi_r(E', \mu | E). \quad (2.10)$$

With the notation that $\overline{E'_h}$ denotes the midpoint of energy group \mathcal{E}'_h , the elements of the transfer matrix for energy conservation are the sums over all reactions,

$$\hat{\mathcal{J}}_{g,h,\ell} = \frac{\sum_r \mathcal{I}_{r,g,h,\ell}^{\text{en}}}{\overline{E'_h} \int_{\mathcal{E}_g} dE \tilde{\phi}_\ell(E)}. \quad (2.11)$$

The computation of $\hat{\mathcal{J}}_{g,h,\ell}$ in Eq. (2.11) is done by `fudge` using the integrals $\mathcal{I}_{r,g,h,\ell}^{\text{en}}$ calculated by `merced`.

2.3 Conservation of both particles and energy

The **fudge** code also has an option to combine the integrals $\mathcal{I}_{r,g,h,\ell}^{\text{num}}$ in Eq. (2.7) and $\mathcal{I}_{r,g,h,\ell}^{\text{en}}$ in Eq. (2.10) so as to construct a transfer matrix which conserves both energy and particle number. Energy conservation may be violated in the lowest and highest outgoing energy groups, however. The construction is based on the following ideas.

There are two ways to compute the average energy of particles in the outgoing energy group \mathcal{E}'_h . One such average is the midpoint $\overline{E'_h}$ of this group. Preferably, this value should be the same as the average energy derived from the sums over the reactions r of the integrals Eqs. (2.10) and (2.7),

$$\langle E' \rangle_{g,h} = \frac{\sum_r \mathcal{I}_{r,g,h,0}^{\text{en}}}{\sum_r \mathcal{I}_{r,g,h,0}^{\text{num}}}. \quad (2.12)$$

This is accomplished, as much as possible, by properly defining entries of the transfer matrix corresponding to adjacent outgoing energy groups.

For each incident energy group \mathcal{E}_g one iterates through the outgoing energy groups \mathcal{E}'_h . Note that the description of this process in [4] and [5] assumes that the energy group boundaries decrease with increasing index; the energy group boundaries are counted in increasing order here and in **fudge**.

If $\langle E' \rangle_{g,h} < \overline{E'_h}$ and \mathcal{E}'_h is not the lowest energy group, make a fraction of the sum

$$\frac{\sum_r \mathcal{I}_{r,g,h,\ell}^{\text{en}}}{\overline{E'_h} \int_{\mathcal{E}_g} dE \tilde{\phi}_\ell(E)}$$

contribute to the transfer matrix element $\mathcal{J}_{g,h,\ell}$, and make the remainder contribute to $\mathcal{J}_{g,h-1,\ell}$. Specifically, it is desired to find $j_{g,h}$ and $j_{g,h-1}$ which conserve particle number

$$j_{g,h} + j_{g,h-1} = \frac{\sum_r \mathcal{I}_{r,g,h,0}^{\text{num}}}{\int_{\mathcal{E}_g} dE \tilde{\phi}_0(E)}$$

as well as average energy

$$\overline{E'_h} j_{g,h} + \overline{E'_{h-1}} j_{g,h-1} = \sum_r \mathcal{I}_{r,g,h,0}^{\text{en}}.$$

Therefore, set

$$f_{g,h} = \frac{\langle E' \rangle_{g,h} - \overline{E'_{h-1}}}{\overline{E'_h} - \overline{E'_{h-1}}}.$$

For each Legendre coefficient ℓ take as contribution to $\mathcal{J}_{g,h,\ell}$ the quantity

$$j_{g,h} = \frac{f_{g,h} \sum_r \mathcal{I}_{r,g,h,\ell}^{\text{num}}}{\int_{\mathcal{E}_g} dE \tilde{\phi}_\ell(E)},$$

and the contribution to $\mathcal{J}_{g,h-1,\ell}$ is

$$j_{g,h-1} = \frac{(1 - f_{g,h}) \sum_r \mathcal{I}_{r,g,h,\ell}^{\text{num}}}{\int_{\mathcal{E}_g} dE \tilde{\phi}_\ell(E)}.$$

If $\langle E' \rangle_{g,h} < \overline{E'_h}$ and \mathcal{E}'_h is the lowest energy group, the contribution to $\mathcal{J}_{g,h,\ell}$ is simply

$$\frac{\sum_r \mathcal{I}_{r,g,h,\ell}^{\text{num}}}{\int_{\mathcal{E}_g} dE \tilde{\phi}_\ell(E)}.$$

This maintains conservation of particle number.

If $\langle E' \rangle_{g,h} > \overline{E'_h}$ and \mathcal{E}'_h is not the highest energy group, these data are used to calculate contributions to the components $\mathcal{J}_{g,h,\ell}$ and $\mathcal{J}_{g,h+1,\ell}$ of the transfer matrix. Specifically, set

$$f_{g,h} = \frac{\overline{E'_{h+1}} - \langle E' \rangle_{g,h}}{\overline{E'_{h+1}} - \overline{E'_h}}.$$

For each Legendre coefficient ℓ take as contribution to $\mathcal{J}_{g,h,\ell}$ the quantity

$$j_{g,h} = \frac{f_{g,h} \sum_r \mathcal{I}_{r,g,h,\ell}^{\text{num}}}{\int_{\mathcal{E}_g} dE \tilde{\phi}_\ell(E)},$$

and the contribution to $\mathcal{J}_{g,h+1,\ell}$ is

$$j_{g,h+1} = \frac{(1 - f_{g,h}) \sum_r \mathcal{I}_{r,g,h,\ell}^{\text{num}}}{\int_{\mathcal{E}_g} dE \tilde{\phi}_\ell(E)}.$$

If $\langle E' \rangle_{g,h} > \overline{E'_h}$ and \mathcal{E}'_h is the highest energy group, the contribution to $\mathcal{J}_{g,h,\ell}$ is

$$\frac{\sum_r \mathcal{I}_{r,g,h,\ell}^{\text{num}}}{\int_{\mathcal{E}_g} dE \tilde{\phi}_\ell(E)}.$$

The sum of all of these contributions produces the Legendre coefficients $\mathcal{J}_{g,h,\ell}$ of a transfer matrix which conserves particle number as well as usually conserving energy.

2.4 Control of the conservation option

The `merced` code computes the integrals Eq. (2.7) for the number-preserving transfer matrix or the integrals Eq. (2.10) for the energy-preserving transfer matrix or both, depending on the value of the `Conserve` input parameter. See Section 12.4.3. The default mode is to compute both integrals. The actual construction of the transfer matrix is performed by `fudge`.

2.5 Numerical quadrature

The integrals Eqs. (2.7) and (2.10) require some sort of numerical quadrature, and the multiple integrals are computed as a sequence of single integrals. The quadrature method is a modification of an adaptive method proposed by Gander and Gautschi [6]. The main difference is that the Simpson rule used in [6] is replaced by a second-order Gaussian quadrature. The reason for this change is that in the calculations here, one of the limits of integration may be a computed quantity, such as a threshold energy. In such cases, computer arithmetic may give rise to attempts to evaluate $\pi_r(E', \mu \mid E)$ where it makes no sense to do so.

Remark. In the rest of this document the subscript r is omitted from each of the terms in the kernel Eq. (2.2) and from the integrals $\mathcal{I}_{r,g,h,\ell}^{\text{num}}$ and $\mathcal{I}_{r,g,h,\ell}^{\text{en}}$, because from now on the discussion will be about the treatment of the data, reaction by reaction.

3 Interpolation of the data

The data in GND representing the probability density $\pi(E', \mu | E) = \pi_r(E', \mu | E)$ in the integrals (2.7) and (2.10) are given in various forms. In the case of tabulated data, intermediate values must be obtained via some sort of interpolation. Interpolation with respect to one independent variable is described first, followed by a discussion of the 2-dimensional case. In GND full 3-dimensional interpolation of $\pi(E', \mu | E)$ data is reduced to a sequence of 2-dimensional interpolations.

3.1 Interpolation methods for a single variable

For the sake of having a specific application, the discussion here is given in terms of tables of data $\{E_i, f(E_i)\}$, with values E_i of the energy of the outgoing particle as independent variable. These ideas are applicable to one dimension for any tabular data. The types of interpolation method used in GND for such tables are: histogram, linear-linear, log-linear, linear-log, and log-log. The algorithms for interpolation of $F(E)$ on an interval $E_0 < E < E_1$ with given $f(E_0)$ and $f(E_1)$ are as follows. In these definitions it is assumed that the argument of a logarithm is positive.

3.1.1 Histograms

For histogram interpolation set

$$f(E) = f(E_0) \quad \text{for } E_0 \leq E < E_1.$$

3.1.2 Linear-linear

For linear-linear interpolation set

$$\alpha = \frac{E - E_0}{E_1 - E_0} \tag{3.1}$$

and take

$$f(E) = (1 - \alpha)f(E_0) + \alpha f(E_1) \quad \text{for } E_0 \leq E \leq E_1.$$

3.1.3 Log-linear

For log-linear interpolation take α as in Eq. (3.1), and set

$$\log f(E) = (1 - \alpha) \log f(E_0) + \alpha \log f(E_1) \quad \text{for } E_0 \leq E \leq E_1.$$

This relation may also be written as

$$f(E) = f(E_0)^{1-\alpha} f(E_1)^\alpha. \tag{3.2}$$

3.1.4 Linear-log

For linear-log interpolation set

$$\alpha' = \frac{\log(E/E_0)}{\log(E_1/E_0)} \quad (3.3)$$

and take

$$f(E) = (1 - \alpha')f(E_0) + \alpha'f(E_1) \quad \text{for } E_0 \leq E \leq E_1.$$

3.1.5 Log-log

For log-log interpolation take α' as in Eq. (3.3), and set

$$\log f(E) = (1 - \alpha')\log f(E_0) + \alpha'\log f(E_1) \quad \text{for } E_0 \leq E \leq E_1.$$

This is equivalent to

$$f(E) = f(E_0)^{1-\alpha'} f(E_1)^{\alpha'}. \quad (3.4)$$

Remark. With log-linear interpolation written in the form of Eq. (3.2) and log-log interpolation written as Eq. (3.4), it is permitted that $f(E_0) = 0$ or $f(E_1) = 0$. These cases all lead to the result that $f(E) = 0$ for $E_0 < E < E_1$, however.

3.2 Interpolation methods for probability densities

In order to explain the methods for interpolation of probability densities, it suffices to consider a table of values $\pi(E' | E)$

$$\{E'_{j,k}, \pi(E'_{j,k} | E_k)\} \quad \text{for } j = 0, 1, \dots, J_k \quad (3.5)$$

given at values of the incident energy E_k , for $k = 0, 1, \dots, K$. In Eq. (3.5) it is required that the outgoing energies be ordered

$$E'_{0,k} < E'_{1,k} \leq E'_{2,k} \leq \dots \leq E'_{J_k-1,k} < E'_{J_k,k}. \quad (3.6)$$

The condition Eq. (3.6) permits the data of Eq. (3.5) to have equal consecutive intermediate outgoing energies $E'_{j-1,k} = E'_{j,k}$, so that the probability density $\pi(E' | E_k)$ may have a jump discontinuity there. Jump discontinuities are not allowed at the end points $E' = E'_{0,k}$ and $E' = E'_{J_k,k}$. In Eq. (3.5) the possibility of three or more consecutive equal outgoing energies may be ruled out, because all but the first and last would be redundant. The convention adopted here is that the value of $\pi(E' | E_k)$ at a discontinuity is the second data value

$$\pi(E' | E_k) = \pi(E'_{j,k} | E_k) \quad \text{if } E' = E'_{j-1,k} = E'_{j,k}.$$

For fixed incident energy E_k , the rules for interpolation of $\pi(E' | E_k)$ in outgoing energy E' are as given in Section 3.1. The following types of interpolation with respect to E are discussed in subsequent subsections:

1. direct interpolation.

2. unit-base interpolation,
3. interpolation using cumulative points.

The method referred to here as “interpolation by cumulative points” is closely related to “interpolation by corresponding energies” as described in the ENDF/B-VII manual [7]. For a more-detailed discussion of 2-dimensional interpolation methods, see the reference [8].

For a discussion of interpolation of data Eq. (3.5), it suffices to consider interpolation between incident energies E_0 and E_1 . Thus, it is desired to interpolate to incident energy E with $E_0 < E < E_1$ the data

$$\begin{aligned} \{E'_{j,0}, \pi(E'_{j,0} | E_0)\} & \text{ for } j = 0, 1, \dots, J_0, \\ \{E'_{j,1}, \pi(E'_{j,1} | E_1)\} & \text{ for } j = 0, 1, \dots, J_1. \end{aligned} \quad (3.7)$$

The ideas presented apply equally well to interpolation of data in Eq. (3.5) between any consecutive pair of incident energies $E_{k-1} < E_k$.

The methods of 2-dimensional interpolation are described in turn.

3.2.1 Direct interpolation

It is common to do direct interpolation for interpolating tables of angular probability density $\pi(\mu | E)$ with respect to incident energy E , because the range of direction cosines is usually $-1 \leq \mu \leq 1$. For example, in order to determine the value of $\pi(\mu | E)$ for $E_0 < E < E_1$ from data Eq. (3.7), one first interpolates in μ at fixed incident energies to obtain $\pi(\mu | E_0)$ and $\pi(\mu | E_1)$. One then obtains the value of $\pi(\mu | E)$ by interpolating between $\pi(\mu | E_0)$ and $\pi(\mu | E_1)$.

The trouble with the application of direct interpolation to tables of energy distributions is that the range of outgoing energy E' usually depends on the incident energy E . Thus, for the data in Eq. (3.7), the ranges of outgoing energies are given by

$$\begin{aligned} E'_{0,\min} = E'_{0,0} & \text{ and } E'_{0,\max} = E'_{J_0,0} & \text{ for } E = E_0, \\ E'_{1,\min} = E'_{0,1} & \text{ and } E'_{1,\max} = E'_{J_1,1} & \text{ for } E = E_1. \end{aligned} \quad (3.8)$$

Remark. In the definition of the range of outgoing energies Eq. (3.8), it is natural to expect that the data in Eq. (3.7) are such that for each incident energy E_k with $k = 0, 1, \dots, K$, the probability density $\pi(E' | E_k)$ is not equal to zero on the entire lowest outgoing energy range $E'_{0,k} < E' < E'_{1,k}$ or highest outgoing energy range $E'_{J_k-1,k} < E' < E'_{J_k,k}$. That is, Eq. (3.8) ought to give the actual range of outgoing energies. Some nuclear data libraries, e. g., ENDF/B-VII.1 [9], have data of the form Eq. (3.5) which imply that $\pi(E' | E_k) = 0$ on the lowest or highest outgoing energy ranges. The sample input data given in Section 5.3.1 illustrates the problem.

It is convenient to describe the process of direct interpolation using notation of set theory, with the sets

$$\begin{aligned} \mathcal{A}_0 &= \{E' : E'_{0,\min} \leq E' \leq E'_{0,\max}\}, \\ \mathcal{A}_1 &= \{E' : E'_{1,\min} \leq E' \leq E'_{1,\max}\}. \end{aligned} \quad (3.9)$$

The union of these two sets is denoted by

$$\mathcal{A}_X = \mathcal{A}_0 \cup \mathcal{A}_1, \quad (3.10)$$

and the intersection is denoted by

$$\mathcal{A}_T = \mathcal{A}_0 \cap \mathcal{A}_1, \quad (3.11)$$

There are two obvious interpretations of direct interpolation of the data in Eq. (3.7) when the outgoing energy ranges differ, $\mathcal{A}_0 \neq \mathcal{A}_1$. One may do *direct interpolation with extrapolation* or *direct interpolation with truncation*. Linear-linear versions of these methods are described here.

For direct interpolation with extrapolation the probability densities $\pi(E' | E_0)$ and $\pi(E' | E_1)$ constructed from the tables in Eq. (3.7) are extrapolated to

$$\pi_X(E' | E_0) = \begin{cases} \pi(E' | E_0) & \text{for } E' \text{ in } \mathcal{A}_0, \\ 0 & \text{for } E' \text{ in } \mathcal{A}_X \setminus \mathcal{A}_0, \end{cases} \quad (3.12)$$

and

$$\pi_X(E' | E_1) = \begin{cases} \pi(E' | E_1) & \text{for } E' \text{ in } \mathcal{A}_1, \\ 0 & \text{for } E' \text{ in } \mathcal{A}_X \setminus \mathcal{A}_1. \end{cases} \quad (3.13)$$

For direct interpolation to incident energy E with $E_0 < E < E_1$, the proportionality factor q is defined as

$$q = \frac{E - E_0}{E_1 - E_0}. \quad (3.14)$$

In linear-linear direct interpolation with extrapolation, the interpolant is taken to be

$$\pi_X(E' | E) = (1 - q) \pi_X(E' | E_0) + q \pi_X(E' | E_1) \quad (3.15)$$

for E' in the set \mathcal{A}_X .

The method of direct interpolation with truncation differs from that using extrapolation, in that this method uses the truncated probability densities

$$\begin{aligned} \pi_T(E' | E_0) &= C_0 \pi(E' | E_0), \\ \pi_T(E' | E_1) &= C_1 \pi(E' | E_1) \end{aligned} \quad (3.16)$$

for outgoing energy E' in the set \mathcal{A}_T . Here, C_0 and C_1 are normalization constants such that

$$\int_{\mathcal{A}_T} dE' \pi_T(E' | E_0) = 1 \quad \text{and} \quad \int_{\mathcal{A}_T} dE' \pi_T(E' | E_1) = 1.$$

For linear-linear direct interpolation with truncation of the data in Eq. (3.7) to incident energy E with $E_0 < E < E_1$, the factor q is chosen as in Eq. (3.14), and the interpolant is

$$\pi_T(E' | E) = (1 - q) \pi_T(E' | E_0) + q \pi_T(E' | E_1)$$

for E' in the set \mathcal{A}_T .

Remarks. The ENDF/B-VII.1 data [9] contains many instances in which linear-linear direct interpolation is specified, but the ENDF/B-VII manual [7] says nothing about how to deal with differences in range of outgoing energies. Both versions can be expected to produce violation of energy conservation. The `merced` code currently uses direct interpolation with extrapolation.

3.2.2 Unit-base interpolation

Only the linear-linear version of unit-base interpolation is discussed here. The first step in unit-base interpolation is the construction of the range of energies of the outgoing particle. The minimum and maximum outgoing energies for the data in Eq. (3.7) are given by Eq. (3.8). For incident energy E with $E_0 < E < E_1$, the factor q is taken as in Eq. (3.14), and the minimum and maximum outgoing energies are given by

$$\begin{aligned} E'_{\min} &= (1 - q)E'_{0,\min} + qE'_{1,\min}, \\ E'_{\max} &= (1 - q)E'_{0,\max} + qE'_{1,\max}. \end{aligned} \quad (3.17)$$

The interpolated probability density $\pi(E' | E)$ must satisfy the normalization condition

$$\int_{E'_{\min}}^{E'_{\max}} dE' \pi(E' | E) = 1. \quad (3.18)$$

One way to ensure this is to first map the outgoing energy ranges Eq. (3.8) to unit base $0 \leq \hat{E}' \leq 1$ and to scale the probability densities Eq. (3.7) accordingly. Thus, for the data in Eq. (3.7) at incident energy E_0 , set

$$\hat{E}' = \frac{E' - E'_{0,\min}}{E'_{0,\max} - E'_{0,\min}} \quad (3.19)$$

and scale the probability density

$$\hat{\pi}(\hat{E}' | E_0) = (E'_{0,\max} - E'_{0,\min})\pi(E' | E_0). \quad (3.20)$$

For incident energy E_1 , the outgoing energy is scaled as

$$\hat{E}' = \frac{E' - E'_{1,\min}}{E'_{1,\max} - E'_{1,\min}}, \quad (3.21)$$

and the probability density is scaled to define the unit-base probability density

$$\hat{\pi}(\hat{E}' | E_1) = (E'_{1,\max} - E'_{1,\min})\pi(E' | E_1) \quad (3.22)$$

for $0 \leq \hat{E}' \leq 1$.

If linear-linear interpolation with respect to incident energy is desired, the proportionality factor q defined in Eq. (3.14) is used to linearly interpolate between $\hat{\pi}(\hat{E}' | E_0)$ and $\hat{\pi}(\hat{E}' | E_1)$ by setting

$$\hat{\pi}(\hat{E}' | E) = (1 - q)\hat{\pi}(\hat{E}' | E_0) + q\hat{\pi}(\hat{E}' | E_1) \quad (3.23)$$

for $0 \leq \hat{E}' \leq 1$.

Finally, in order to define the interpolated probability density $\pi(E' | E)$, invert the mappings Eq. (3.19) and Eq. (3.20). Specifically, with E'_{\min} and E'_{\max} as in Eq. (3.17), set

$$E' = E'_{\min} + (E'_{\max} - E'_{\min})\hat{E}' \quad (3.24)$$

and take

$$\pi(E' | E) = \frac{\hat{\pi}(\hat{E}' | E)}{E'_{\max} - E'_{\min}}. \quad (3.25)$$

Unit-base interpolation is ordinarily not used with tables of angular probability densities $\pi(\mu | E)$, because the range of direction cosines is usually $-1 \leq \mu \leq 1$. One may want to use it for a table with forward emission given in the laboratory frame, however.

3.2.3 Interpolation by cumulative points

The method of interpolation by cumulative points that is used in the code `merced` is proposed in [8], and it is a modification of interpolation by corresponding energies as described in the ENDF/B-VII manual [7]. Interpolation by corresponding energies requires the selection of N equiprobable energy bins, so the result depends on the value of N . It is shown in [8] that for data Eq. (3.5) which are histogram with respect to outgoing energy E' , interpolation by cumulative points is equivalent to interpolation by corresponding energies with $N = \infty$. The `merced` code therefore uses interpolation by cumulative points whenever the data specify interpolation by corresponding energies.

One objection to unit-base interpolation is that the mapping (3.20) depends only on the range of outgoing energies. One can often get a better approximation to the physics if the interpolation method incorporates knowledge of the local behavior of each $\pi(E' | E_k)$ in Eq. (3.5). One method of doing so is based on the cumulative probability function

$$\Pi(E' | E_k) = \int_{E'_{k,\min}}^{E'} dx \pi(x | E_k) \quad (3.26)$$

for $k = 0, 1, \dots, K$.

Constraint. Interpolation by cumulative points requires that $\Pi(E' | E_k)$ be strictly increasing with respect to E' for $k = 0, 1, \dots, K$. That is, the condition that

$$\Pi(E'_2 | E_k) > \Pi(E'_1 | E_k) \quad (3.27)$$

is imposed for every E'_1 and E'_2 in the outgoing energy range

$$E'_{0,k} \leq E'_1 < E'_2 \leq E'_{J_k,k}.$$

Because the data $\pi(E' | E_k)$ consist of probability densities, it follows that $\pi(E' | E_k) \geq 0$. If the interpolation with respect to outgoing energy E' is log-linear or log-log, the monotonicity condition (3.27) implies that $\pi(E'_{j,k} | E_k) > 0$ for all data points $E'_{j,k}$ in Eq. (3.5), and for histograms only the highest outgoing energies $E'_{k,\max}$ may have zero probability density. For linear-linear and linear-log interpolation, it is permitted that $\pi(E'_{j,k} | E_k) = 0$ at local values of $E'_{j,k}$ but not for two consecutive outgoing energies $E'_{j-1,k}$ and $E'_{j,k}$.

As with unit-base interpolation, it is sufficient to describe interpolation by cumulative points between the incident energies E_0 and E_1 . For incident energy E_0 compute the cumulative probabilities at the data points in Eq. (3.7)

$$y_{j,0} = \Pi(E'_{j,0} | E_0) \quad \text{for } j = 0, 1, \dots, J_0. \quad (3.28)$$

Analogously, for $E = E_1$ determine the cumulative probabilities at the data points in Eq. (3.7)

$$y_{j,1} = \Pi(E'_{j,1} | E_1) \quad \text{for } j = 0, 1, \dots, J_1. \quad (3.29)$$

Form the union of the two sets

$$\{Y_\ell\} = \{y_{j,0}\} \cup \{y_{j,1}\}.$$

The Y_ℓ values are then ordered with removal of duplicates, so that

$$Y_0 = 0 < Y_1 < \dots < Y_{L-1} < Y_L = 1. \quad (3.30)$$

Interpolation by cumulative points consists of a sequence of unit-base interpolations on subintervals. These subintervals are obtained as follows. For incident energy E_0 and each cumulative probability Y_ℓ in Eq. (3.30), the outgoing energies $\tilde{E}'_{\ell,0}$ are computed such that

$$\Pi(\tilde{E}'_{\ell,0} | E_0) = Y_\ell \quad \text{for } \ell = 0, 1, \dots, L.$$

Note that the construction ensures that each of the original data points $E'_{j,0}$ in Eq. (3.7) is one of the $\tilde{E}'_{\ell,0}$ values. The interval $\mathcal{B}_0(\ell)$ is defined as

$$\begin{aligned} \mathcal{B}_0(\ell) &= \{E' : \tilde{E}'_{\ell-1,0} \leq E' < \tilde{E}'_{\ell,0}\} \quad \text{for } \ell = 1, 2, \dots, L-1, \\ \mathcal{B}_0(L) &= \{E' : \tilde{E}'_{L-1,0} \leq E' \leq \tilde{E}'_{L,0}\} \end{aligned} \quad (3.31)$$

The intervals $\mathcal{B}_1(\ell)$ for the data Eq. (3.7) at incident energy E_1 and $\ell = 1, 2, \dots, L$ are defined in a similar manner.

Interpolation by cumulative points is accomplished by doing a sequence of unit-base interpolations between $\pi(E' | E_0)$ on the interval $\mathcal{B}_0(\ell)$ and $\pi(E' | E_1)$ on $\mathcal{B}_1(\ell)$ for $\ell = 1, 2, \dots, L$.

A more detailed discussion of interpolation of probability data by the method of cumulative points may be found in the note [8].

Because interpolation by cumulative points depends on the detailed behavior of the probability densities, the method may also be useful for interpolation of angular probability densities $\pi(\mu | E)$.

3.3 Unscaled interpolation of Kalbach-Mann data

The above discussion pertains to the interpolation of tables of probability densities, for which maintenance of the norm condition Eq. (3.18) is essential. The parameter $r(E'_{\text{cm}}, E)$ in Eq. (10.2) for the Kalbach-Mann model of double-differential data is given as tables depending on the energy E of the incident particle and the energy E'_{cm} of the outgoing particle in the center-of-mass frame, and it has the different constraint,

$$0 \leq r \leq 1. \quad (3.32)$$

Again, it suffices to describe interpolation between Kalbach-Mann r data between tables at incident energies E_0 and E_1 with $E_0 < E_1$. As in Eq. (3.9), consider the sets \mathcal{A}_0

of outgoing energies at $E = E_0$ and \mathcal{A}_1 at $E = E_1$. For unscaled direct interpolation with extrapolation, take $\mathcal{A}_X = \mathcal{A}_0 \cup \mathcal{A}_1$ as in Eq. (3.10), so that the extrapolated r parameter is

$$r_X(E', E_0) = \begin{cases} r(E', E_0) & \text{for } E' \text{ in } \mathcal{A}_0, \\ 0 & \text{for } E' \text{ in } \mathcal{A}_X \setminus \mathcal{A}_0, \end{cases}$$

and

$$r_X(E', E_1) = \begin{cases} r(E', E_1) & \text{for } E' \text{ in } \mathcal{A}_1, \\ 0 & \text{for } E' \text{ in } \mathcal{A}_X \setminus \mathcal{A}_1. \end{cases}$$

Then for $E_0 < E < E_1$, for q as in Eq. (3.14) and for E' in the set \mathcal{A}_X , the linear-linear form of unscaled direct interpolation with extrapolation becomes as in Eq. (3.15),

$$r_X(E', E) = (1 - q) r_X(E', E_0) + q r_X(E', E_1). \quad (3.33)$$

The extrapolation version of direct interpolation of the Kallbach-Mann r parameter as in Eq. (3.33) is implemented in the `merced` code.

For unscaled direct interpolation of the Kalbach-Mann r parameter with truncation, the outgoing energy E' is restricted to the common domain $\mathcal{A}_T = \mathcal{A}_0 \cap \mathcal{A}_1$, and there is no change of scale analogous to that used for probability densities in Eq. (3.16). Thus, the truncated Kalbach-Mann r parameters for incident energies E_0 and E_1 are

$$r_T(E', E_0) = \begin{cases} r(E', E_0) & \text{for } E' \text{ in } \mathcal{A}_T, \\ 0 & \text{for } E' \text{ in } \mathcal{A}_0 \setminus \mathcal{A}_T, \end{cases}$$

and

$$r_T(E', E_1) = \begin{cases} r(E', E_1) & \text{for } E' \text{ in } \mathcal{A}_T, \\ 0 & \text{for } E' \text{ in } \mathcal{A}_1 \setminus \mathcal{A}_T. \end{cases}$$

The linear-linear version of unscaled direct interpolation with truncation is

$$r_T(E', E) = (1 - q) r_T(E', E_0) + q r_T(E', E_1) \quad (3.34)$$

with E' restricted to \mathcal{A}_T . The `merced` code does not currently implement unscaled direct interpolation with truncation of the Kalbach-Mann r parameter given in Eq. (3.34).

There is also an unscaled version of unit-base interpolation with Eqs. (3.20) and (3.22) replaced by

$$\begin{aligned} \hat{r}(\hat{E}', E_0) &= r(E', E_0), \\ \hat{r}(\hat{E}', E_1) &= r(E', E_1), \end{aligned}$$

for $0 \leq \hat{E}' \leq 1$ with \hat{E}' as in Eq. (3.19) for $E = E_0$ and as in Eq. (3.21) for $E = E_1$. For linear-linear unscaled unit-base interpolation to incident energy E with $E_0 < E < E_1$, interpolate the minimal and maximal outgoing energies as in Eq. (3.17), interpolate \hat{r} using

$$\hat{r}(E', E) = (1 - q) \hat{r}(E', E_0) + q \hat{r}(E', E_1),$$

and invert the unit-base map using Eq. (3.24) and

$$r(E', E) = \hat{r}(\hat{E}', E)$$

for $E'_{\min} \leq E' \leq E'_{\max}$.

When the energy probability density $\pi_E(E' | E)$ in Eq. (10.1) is interpolated using the method of cumulative points, the interpolated values of $r(E', E)$ in Eq. (10.2) is obtained using the method of unscaled cumulative points defined as follows. The method uses the outgoing energy ranges $\mathcal{B}_0(\ell)$ given in Eq. (3.31) for $\pi_E(E' | E)$ at $E = E_0$ and the corresponding $\mathcal{B}_1(\ell)$ at $E = E_1$, and it does unscaled unit-base interpolation of $r(E', E)$ between $\mathcal{B}_0(\ell)$ and $\mathcal{B}_1(\ell)$ in sequence for $\ell = 1, 2, \dots, L$.

4 Discrete two-body reactions

This section describes how the contribution to the transfer matrix is calculated for data consisting of probability densities for the cosine of the angle of deflection in discrete 2-body reactions. In this case, the probability densities are always given in the center-of-mass frame. Because the transfer matrices are defined in terms of laboratory coordinates, the computations involve a boost.

For all except very light-weight targets, the mapping from center-of-mass to laboratory coordinates is usually done using Newtonian mechanics. The discussion given here is therefore Newtonian. A relativistic treatment is presented in Appendix A. The choice of Newtonian or relativistic mechanics is determined by the value of the kinetics input parameter to `merced` as explained in Section 12.3.5. Of course, relativistic mechanics must be used if either the incident particle or the outgoing particle is a photon.

For discrete 2-body reactions, the center-of-mass energy of the emitted particle is determined by the energy E of the incident particle. Consequently, the energy-angle probability density $\pi_{\text{cm}}(E'_{\text{cm}}, \mu_{\text{cm}} | E)$ in the center-of-mass frame is given by

$$\pi_{\text{cm}}(E'_{\text{cm}}, \mu_{\text{cm}} | E) = g(\mu_{\text{cm}} | E) \delta(E'_{\text{cm}} - \Psi(E)) \quad (4.1)$$

for the function Ψ given below in Eq. (4.4). From here on, the energy E and direction cosine μ of the outgoing particle will be marked with the subscript “lab” or “cm” to indicate that the variable is in the laboratory or center-of-mass frame.

Because of Eq. (4.1), the data for discrete 2-body reactions consist of angular probability densities $g(\mu_{\text{cm}} | E)$ given in the center-of-mass frame, either as a 2-dimensional table for given incident energy E and direction cosine μ_{cm} or as Legendre coefficients $c_\ell(E)$ for

$$g(\mu_{\text{cm}} | E) = \sum_{\ell} \left(\ell + \frac{1}{2} \right) c_\ell(E) P_\ell(\mu_{\text{cm}}). \quad (4.2)$$

This section begins with an overview of Newtonian mechanics for discrete 2-body problems. In particular, the form of the function Ψ in Eq. (4.1) is derived, as is the boost from the center-of-mass to the laboratory frame. The section closes with an examination of the use of angular probability data $g(\mu_{\text{cm}} | E)$ in the computation of the integrals Eqs. (2.7) and (2.10) used in the calculation of the transfer matrix.

4.1 Newtonian mechanics of discrete 2-body reactions

Only a summary of the results is given here; for more information, see the reference [10]. A relativistic treatment is developed in Appendix A. It is assumed that the target is at rest and that the incident particle has energy E in laboratory coordinates.

The following notations are used for the masses of the particles involved:

- m_{yi} , the mass of the incident particle,
- m_{targ} , the mass of the target,
- m_{yo} , the mass of the emitted particle,
- m_{res} , the mass of the residual.

For the conversion between center-of-mass and laboratory coordinates, define the mass ratios

$$\gamma = \frac{m_{\text{yi}}m_{\text{yo}}}{(m_{\text{yi}} + m_{\text{targ}})^2},$$

$$\beta = \frac{m_{\text{res}}}{m_{\text{yo}} + m_{\text{res}}},$$

and

$$\alpha = \frac{\beta m_{\text{targ}}}{m_{\text{yi}} + m_{\text{targ}}}.$$

Velocity vectors are printed in bold face \mathbf{V} with magnitude (speed) in math italics

$$V = |\mathbf{V}|.$$

For a target at rest and an incident particle with energy E in laboratory coordinates, the center of mass moves in the direction of motion of the incident particle with velocity $\mathbf{V}_{\text{trans}}$ having magnitude squared

$$V_{\text{trans}}^2 = \mathbf{V}_{\text{trans}}^2 = \frac{2m_{\text{yi}}E}{(m_{\text{yi}} + m_{\text{targ}})^2}. \quad (4.3)$$

The reaction may have a nonzero energy value Q , arising for example from the excitation level of the target and/or residual nucleus in inelastic scattering. A nonzero Q value may also arise from the mass difference in a knock-on reaction. It follows from conservation of energy and momentum that in center-of-mass coordinates the energy of the emitted particle is given by

$$E'_{\text{cm}} = \Psi(E) = \alpha E + \beta Q. \quad (4.4)$$

This defines the function Ψ appearing in Eq. (4.1). The speed of the outgoing particle in the center-of-mass frame is

$$V'_{\text{cm}} = |\mathbf{V}'_{\text{cm}}| = \sqrt{\frac{2E'_{\text{cm}}}{m_{\text{yo}}}}. \quad (4.5)$$

It follows from Eq. (4.4) that for an endothermic reaction ($Q < 0$), the threshold is at

$$E = \frac{-\beta Q}{\alpha}.$$

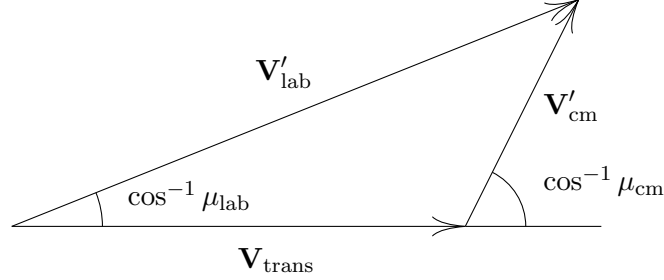


Figure 4.1: Newtonian mapping to laboratory coordinates

4.1.1 The boost to the laboratory frame

As illustrated in Figure 4.1, the boost from center-of-mass to laboratory coordinates is obtained by adding the velocities

$$\mathbf{V}'_{\text{lab}} = \mathbf{V}_{\text{trans}} + \mathbf{V}'_{\text{cm}}. \quad (4.6)$$

Consequently, the energy of the outgoing particle in the laboratory frame is

$$E'_{\text{lab}} = \frac{m_{\text{yo}} \mathbf{V}'_{\text{lab}}{}^2}{2} = \frac{m_{\text{yo}}}{2} (V_{\text{trans}}^2 + V_{\text{cm}}'^2 + 2\mathbf{V}_{\text{trans}} \cdot \mathbf{V}'_{\text{cm}}).$$

In terms of the notation Eq. (4.4) and

$$E'_{\text{trans}} = \frac{m_{\text{yo}} V_{\text{trans}}^2}{2} = \gamma E, \quad (4.7)$$

this equation takes the form

$$E'_{\text{lab}} = E'_{\text{trans}} + E'_{\text{cm}} + 2\mu_{\text{cm}} \sqrt{E'_{\text{trans}} E'_{\text{cm}}}. \quad (4.8)$$

Here, μ_{cm} is the direction cosine defined by the relation

$$\mathbf{V}_{\text{trans}} \cdot \mathbf{V}'_{\text{cm}} = \mu_{\text{cm}} V_{\text{trans}} V'_{\text{cm}}.$$

It is also necessary to determine the direction cosine μ_{lab} in the laboratory frame for

$$\mathbf{V}_{\text{trans}} \cdot \mathbf{V}'_{\text{lab}} = \mu_{\text{lab}} V_{\text{trans}} V'_{\text{lab}}.$$

This is most easily derived from the trigonometry in Figure 4.1

$$\mu_{\text{lab}} V'_{\text{lab}} = V_{\text{trans}} + \mu_{\text{cm}} V'_{\text{cm}}.$$

In terms of the energies defined in Eqs. (4.4), (4.7), and (4.8), this relation takes the form

$$\mu_{\text{lab}} = \frac{\sqrt{E'_{\text{trans}}} + \mu_{\text{cm}} \sqrt{E'_{\text{cm}}}}{\sqrt{E'_{\text{lab}}}} \quad \text{if } E'_{\text{lab}} > 0. \quad (4.9)$$

It is clear from Eq. (4.6) that

$$E'_{\text{lab}} = \frac{m_{\text{yo}} V_{\text{lab}}'^2}{2} = 0,$$

if and only if

$$\mathbf{V}'_{\text{cm}} = -\mathbf{V}_{\text{trans}}.$$

In this case, the value of μ_{lab} is undefined.

4.2 Computation of the transfer matrix from data for discrete 2-body reactions

Consider the use of data $g(\mu_{\text{cm}} | E)$ in Eq. (4.1) in the computation of integrals for the transfer matrix Eqs. (2.7) and (2.10), either as tables or as Legendre coefficients in Eq. (4.2). In these integrals the multiplicity is always $M(E) = 1$ for discrete 2-body reactions. The discussion given here concentrates on the evaluation of the integral in Eq. (2.7). The integral in Eq. (2.10) differs only in that its integrand contains an extra factor E'_{lab} , the energy of the outgoing particle in the laboratory frame.

Because the probability density data $g(\mu_{\text{cm}} | E)$ in Eq. (4.1) is given in center-of-mass coordinates, it is desirable to transform the integrals Eqs. (2.7) to the center-of-mass frame. The center-of-mass form of the integral Eq. (2.7) is

$$\mathcal{I}_{g,h,\ell}^{\text{num}} = \int_{\mathcal{E}_g} dE \sigma(E) w(E) \tilde{\phi}_\ell(E) \int_{\mu_{\text{cm}}} d\mu_{\text{cm}} g(\mu_{\text{cm}} | E) \int_{E'_{\text{cm}}} dE'_{\text{cm}} P_\ell(\mu_{\text{lab}}) \delta(E'_{\text{cm}} - \Psi(E)) \quad (4.10)$$

with $\Psi(E)$ as given by Eq. (4.4). The range of integration over μ_{cm} and E'_{cm} in Eq. (4.10) is such that for fixed incident energy E in \mathcal{E}_g , the energy E'_{lab} of the outgoing particle given by Eq. (4.8) lies in \mathcal{E}'_h .

Integration of Eq. (4.10) with respect to E'_{cm} yields the result that

$$\mathcal{I}_{g,h,\ell}^{\text{num}} = \int_{\mathcal{E}_g} dE \sigma(E) w(E) \tilde{\phi}_\ell(E) \int_{\mu_{\text{cm}}} d\mu_{\text{cm}} P_\ell(\mu_{\text{lab}}) g(\mu_{\text{cm}} | E), \quad (4.11)$$

where it is understood that the direction cosine μ_{lab} in the laboratory frame is calculated from Eq. (4.9) and that the range of integration over μ_{cm} is such that E is in \mathcal{E}'_h .

The `merced` code steps through the data $g(\mu_{\text{cm}} | E)$ to compute contributions to the entries of the transfer matrix in Eq. (4.11). The case of tabular data with direct interpolation (Section 3.2.1) is illustrated in the laboratory frame in Figure 4.2. This figure shows an integration region identified by an incident energy bin \mathcal{E}_g and an outgoing energy bin \mathcal{E}'_h . The data $g(\mu_{\text{cm}} | E)$ are given at incident energies E_{k-1} and E_k , such that the interval $E_{k-1} < E < E_k$ overlaps the energy bin \mathcal{E}_g . Furthermore, it is assumed that data entries $g(\mu_{\text{cm}} | E)$ for $\mu_{\text{cm}} = \mu_{\text{cm},j-1}$ and $\mu_{\text{cm}} = \mu_{\text{cm}}$ are given at $E = E_{k-1}$ or at $E = E_k$ and that the table contains no entries $g(\mu_{\text{cm}} | E_{k-1})$ or $g(\mu_{\text{cm}} | E_k)$ for $\mu_{\text{cm},j-1} < \mu_{\text{cm}} < \mu_{\text{cm}}$. Any missing data values $g(\mu_{\text{cm},j-1} | E_{k-1})$ or $g(\mu_{\text{cm},j} | E_{k-1})$ or

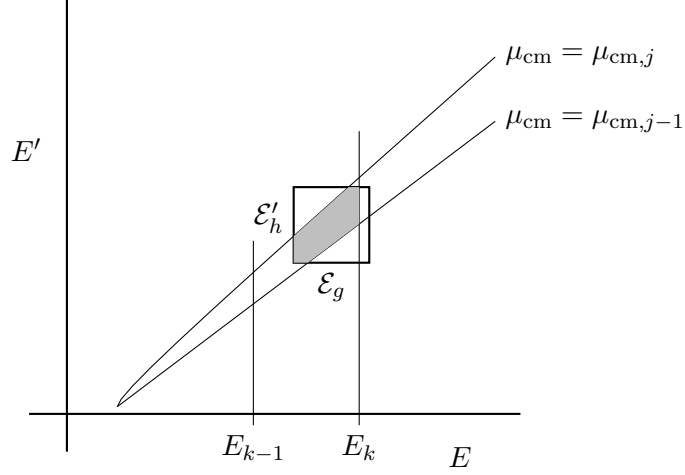


Figure 4.2: Integration region in the incident energy bin \mathcal{E}_g and outgoing bin \mathcal{E}'_h for probability data given at incident energies E_{k-1} and E_k and direction cosines $\mu_{cm,j-1}$ and $\mu_{cm,j}$ shown in the laboratory frame

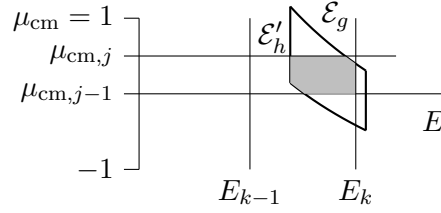


Figure 4.3: Integration region of Fig. 4.2 shown in center-of-mass coordinates

$g(\mu_{cm,j-1} | E_k)$ or $g(\mu_{cm,j} | E_k)$ are computed by interpolation with respect to μ_{cm} . The integration region in the laboratory frame for the contribution of such a set of data to the integral $\mathcal{I}_{g,h,\ell}^{\text{num}}$ in Eq. (4.10) is the shaded area of Figure 4.2. This region is mapped to center-of-mass coordinates in Figure 4.3.

When the tabular data are interpolated by the method of cumulative points of Section 3.2.3, the geometry is complicated by the local unit-base transformations, but the basic ideas are the same. Finally, for probability density data $g(\mu_{cm} | E)$ given as Legendre coefficients in Eq. (4.2), the only significant difference is that the range of direction cosines becomes $-1 \leq \mu_{cm} \leq 1$ with the limitation that the energy E of the outgoing particle lies in the energy bin \mathcal{E}'_h .

4.3 Format of data in the input file

For tabulated probability density data $g(\mu_{\text{cm}} | E)$, the data identifier as in Section 12.3.1, is

```
Process: two body transfer matrix
and for the Legendre coefficients it is
Process: Legendre two body transfer matrix
```

4.3.1 Data for both forms of probability density

Because the boost from the center-of-mass frame to the laboratory frame depends on the rest masses of the particles, these must be included in the input file as described in Section 12.9. The format for doing so is

```
Projectile's mass:  $m_{\text{yi}}$ 
Target's mass:  $m_{\text{targ}}$ 
Product's mass:  $m_{\text{yo}}$ 
Reaction's Q value:  $Q$ 
```

The values of these quantities must be in the same units as the energy bin boundaries.

The code computes the rest mass of the residual from the Q value and the masses of the other particles. If the input file also contains the line

```
Residual's mass:  $m_{\text{res}}$ 
```

the code compares this value with the mass it computed, printing a warning message if they are significantly different.

The code may use either Newtonian or relativistic mechanics in its computations as specified in Section 12.3.5.

The specifications that the energy E of the incident particle is given in the laboratory frame and the direction cosine μ_{cm} in the center-of-mass frame are, Section 12.3.4,

```
Projectile Frame: lab
Product Frame: CenterOfMass
```

4.3.2 Angular probability density tables

The identification line for tabulated angular probability densities is

```
Angular data:  $n = K$ 
```

where K is the number of incident energies E . This is followed by the interpolation rules for probability densities from Section 12.2.3

```
Incident energy interpolation: probability interpolation flag
Outgoing cosine interpolation: list interpolation flag
```

There are then K blocks, one for each incident energy E_k ,

```
Ein:  $E_k$ :  $n = J_k$ 
```

with J_k pairs of values $\mu_{\text{cm},j}$ and $g(\mu_{\text{cm}} | E_k)$. Thus, with incident energy in MeV a table of angular probability densities $g(\mu_{\text{cm}} | E)$ may look like

```
Angular data:  $n = 22$ 
Incident energy interpolation: lin-lin direct
Outgoing cosine interpolation: lin-lin
```

```

Ein:  1.500000000000e-01 :  n = 2
      -1.000000000000e+00  5.000000000000e-01
      1.000000000000e+00  5.000000000000e-01
Ein:  2.000000000000e-01 :  n = 2
      -1.000000000000e+00  4.550000000000e-01
      1.000000000000e+00  5.450000000000e-01
      ...
Ein:  2.000000000000e+01 :  n = 29
      -1.000000000000e+00  3.873180000000e-02
      -9.500000000000e-01  2.943580000000e-02
      -9.000000000000e-01  2.582090000000e-02
      ...
      9.000000000000e-01  2.530490000000e+00
      9.500000000000e-01  3.873180000000e+00
      1.000000000000e+00  8.262750000000e+00

```

4.3.3 Legendre coefficients of angular probability density

Legendre coefficient data of the form Eq. (4.2) for discrete 2-body reactions are given as

Legendre coefficients: $n = K$

where K is the number of incident energies E . This is followed by the interpolation rule for simple lists from Section 12.2.3

Interpolation: list interpolation flag

The file closes with K sets of data

Ein: E_k : $n = L_k$

with L_k Legendre coefficients $c_\ell(E_k)$ for $\ell = 0, 1, \dots, L_k - 1$ in Eq. (4.2). With incident energy in units of MeV, an example of this portion of the input file is

Legendre coefficients: $n = 17$

Interpolation: lin-lin

Ein: 1.843100e+00: $n = 3$

1.000000e+00

0.000000e+00

0.000000e+00

...

Ein: 2.000000e+01: $n = 12$

1.000000e+00

4.640500e-01

2.320700e-01

8.593700e-02

5.338700e-02

2.465600e-02

-1.500600e-03

-1.756300e-02

-1.108000e-02

1.931100e-02
1.150900e-02
5.643500e-03

5 Isotropic energy probability densities in the laboratory frame

The GND library supports several formats for energy probability densities which are isotropic in the laboratory frame. These data are typically used for equilibrium reactions and for fission neutrons. Because the outgoing distribution is isotropic, the probability density $\pi(E'_{\text{lab}}, \mu_{\text{lab}} | E)$ in Eq. (2.2) takes the form

$$\pi(E'_{\text{lab}}, \mu_{\text{lab}} | E) = \pi_0(E'_{\text{lab}} | E). \quad (5.1)$$

Consequently, for the number-conserving matrices only the $\ell = 0$ Legendre order,

$$\mathcal{I}_{g,h,0}^{\text{num}} = \int_{\mathcal{E}_g} dE \sigma(E) M(E) w(E) \tilde{\phi}_0(E) \int_{\mathcal{E}'_h} dE'_{\text{lab}} \pi_0(E'_{\text{lab}} | E) \quad (5.2)$$

needs to be computed, and Eq. (2.10) for the energy-preserving transfer matrix becomes

$$\mathcal{I}_{g,h,0}^{\text{en}} = \int_{\mathcal{E}_g} dE \sigma(E) M(E) w(E) \tilde{\phi}_0(E) \int_{\mathcal{E}'_h} dE'_{\text{lab}} \pi_0(E'_{\text{lab}} | E) E'_{\text{lab}}. \quad (5.3)$$

The data $\pi_0(E'_{\text{lab}} | E)$ may be given in GND either as a table of values or as parameters in a function formula. Because several of the function formulas for isotropic energy probability densities are given in terms of incomplete gamma functions, these are discussed first. This is followed by a presentation of the functional formulas for isotropic probability densities. Then, the treatment of tables of $\pi_0(E'_{\text{lab}} | E)$ for isotropic emission in the laboratory frame is discussed. The section closes with the special treatment of the evaporation of delayed fission neutrons.

5.1 Computational aspects of incomplete gamma functions

Many of the function formulas for $\pi_0(E'_{\text{lab}} | E)$ make use of the lower incomplete gamma function

$$\gamma(\kappa, x) = \int_0^x dt t^{\kappa-1} e^{-t} \quad (5.4)$$

with $\kappa > 0$. The upper incomplete gamma function is

$$\Gamma(\kappa, x) = \int_x^\infty dt t^{\kappa-1} e^{-t}, \quad (5.5)$$

and they are related by

$$\gamma(\kappa, x) + \Gamma(\kappa, x) = \Gamma(\kappa) = \int_0^\infty dt t^{\kappa-1} e^{-t}.$$

In order to reduce the difficulties of computer round-off, the formula

$$\int_a^b dt t^{\kappa-1} e^{-t} = \gamma(\kappa, b) - \gamma(\kappa, a)$$

is used when $0 \leq a < b \leq 1$, and

$$\int_a^b dt t^{\kappa-1} e^{-t} = \Gamma(\kappa, a) - \Gamma(\kappa, b)$$

is used when $1 \leq a < b$. Either form may be used when $a < 1 < b$.

Note that even though it is possible to write down exact formulas for $\gamma(\kappa, x)$ when κ is a positive integer, it is better not to use them in the computations. For example, it is true that

$$\gamma(2, x) = 1 - (1 + x)e^{-x}.$$

For values of x near zero, this formula involves subtracting from 1 a number very close to 1 to get a result close to $x^2/2$. This may lead to bad round-off errors in the computer arithmetic, and it is far better to use the software for $\gamma(2, x)$.

5.2 Functional formulas for isotropic probability densities

The functional formulas used in GND for energy probability densities $\pi_0(E'_{\text{lab}} | E)$ are the evaporation model, the Maxwell model, the Watt model, and the Madland-Nix model. These models are discussed in turn. For all of these models the energy of the outgoing particle is in the laboratory frame.

5.2.1 Evaporation model

For the evaporation model the formula is

$$\pi_0(E'_{\text{lab}} | E) = C E'_{\text{lab}} \exp \left\{ -\frac{E'_{\text{lab}}}{\Theta(E)} \right\} \quad (5.6)$$

with $0 \leq E'_{\text{lab}} \leq E - U$. The value of C in Eq. (5.6) is chosen so that

$$\int_0^{E-U} dE'_{\text{lab}} \pi_0(E'_{\text{lab}} | E) = 1.$$

That is,

$$C = \frac{1}{\Theta^2 \gamma(2, (E - U)/\Theta)}.$$

The data consist of the energy of the reaction U and pairs of values $\{E, \Theta(E)\}$. The 1-dimensional interpolation methods of Section 3.1 are used to determine the value of Θ for intermediate values of the energy E of the incident particle.

According to the comment on incomplete gamma functions above, for the calculation of $\mathcal{I}_{g,h,0}^{\text{num}}$ on an outgoing energy bin, $E_0 \leq E'_{\text{lab}} \leq E_1$ the expression

$$\int_{E_0}^{E_1} dE'_{\text{lab}} \pi_0(E'_{\text{lab}} | E) = C\Theta^2[\gamma(2, E_1/\Theta) - \gamma(2, E_0/\Theta)]$$

is used when $E_0 \leq \Theta$, and

$$\int_{E_0}^{E_1} dE'_{\text{lab}} \pi_0(E'_{\text{lab}} | E) = C\Theta^2[\Gamma(2, E_0/\Theta) - \Gamma(2, E_1/\Theta)]$$

is used when $E_0 > \Theta$. Analogously, for the calculation of $\mathcal{I}_{g,h,0}^{\text{en}}$

$$\int_{E_0}^{E_1} dE'_{\text{lab}} E'_{\text{lab}} \pi_0(E'_{\text{lab}} | E) = C\Theta^3[\gamma(3, E_1/\Theta) - \gamma(3, E_0/\Theta)]$$

is used when $E_0 \leq \Theta$, and

$$\int_{E_0}^{E_1} dE'_{\text{lab}} E'_{\text{lab}} \pi_0(E'_{\text{lab}} | E) = C\Theta^3[\Gamma(3, E_0/\Theta) - \Gamma(3, E_1/\Theta)]$$

is used otherwise.

Input file data for the evaporation model

The process identifier in Section 12.3.1 is

Process: evaporation spectrum

These data are always in the laboratory frame,

Product Frame: lab

One item of model-dependent data in Section 12.9 is the value of U used in defining the range of outgoing energies E in Eq. (5.6), and it is given by

U: U

The other input data are the values of $\Theta(E)$ in Eq. (5.6) depending on the incident energy E . All of these energies, U , E , and $\Theta(E)$, must be in the same units as the energy bins in Sections 12.3.2 and 12.3.3. The format for these data is

Theta: $n = n$

Interpolation: interpolation flag

with n pairs of entries $\{E, \Theta(E)\}$. The interpolation flag is one of those for simple lists as in Section 12.2.3. For example, in units of MeV one may have

U: 11.6890

Theta: $n = 2$

Interpolation: lin-lin

12.0 1.04135

20.0 1.04135

5.2.2 Maxwell model

The formula for the Maxwell is

$$\pi_0(E'_{\text{lab}} | E) = C \sqrt{E'_{\text{lab}}} \exp \left\{ -\frac{E'_{\text{lab}}}{\Theta(E)} \right\} \quad (5.7)$$

for $0 \leq E'_{\text{lab}} \leq E - U$. This model is often used for fission neutrons. The value of C in Eq. (5.7) is given by

$$C = \frac{1}{\Theta^{3/2} \gamma(3/2, (E - U)/\Theta)}.$$

Because of round-off problems with small values of x , it is unwise to use the mathematically equivalent formula

$$\gamma(3/2, x) = \frac{\sqrt{\pi}}{2} \operatorname{erf} \{ \sqrt{x} \} - \sqrt{x} e^{-x}.$$

The data consist of the energy of the reaction U and pairs of values $\{E, \Theta(E)\}$. The parameter Θ is interpolated by the methods of Section 3.1 to obtain intermediate values.

Depending on the value of E_0/Θ , the calculation of $\mathcal{I}_{g,h,0}^{\text{num}}$ on an outgoing energy bin $E_0 \leq E'_{\text{lab}} \leq E_1$ uses the expression

$$\int_{E_0}^{E_1} dE'_{\text{lab}} \pi_0(E'_{\text{lab}} | E) = C \Theta^{3/2} [\gamma(3/2, E_1/\Theta) - \gamma(3/2, E_0/\Theta)]$$

or

$$\int_{E_0}^{E_1} dE'_{\text{lab}} \pi_0(E'_{\text{lab}} | E) = C \Theta^{3/2} [\Gamma(3/2, E_0/\Theta) - \Gamma(3/2, E_1/\Theta)].$$

Analogously, the calculation of $\mathcal{I}_{g,h,0}^{\text{en}}$ uses either

$$\int_{E_0}^{E_1} dE'_{\text{lab}} E'_{\text{lab}} \pi_0(E'_{\text{lab}} | E) = C \Theta^{5/2} [\gamma(5/2, E_1/\Theta) - \gamma(5/2, E_0/\Theta)]$$

or

$$\int_{E_0}^{E_1} dE'_{\text{lab}} E'_{\text{lab}} \pi_0(E'_{\text{lab}} | E) = C \Theta^{5/2} [\Gamma(5/2, E_0/\Theta) - \Gamma(5/2, E_1/\Theta)].$$

Input file data for the Maxwell model

The process identifier in Section 12.3.1 is

Process: Maxwell spectrum

Again, this data is in the laboratory frame,

Product Frame: lab

One item of model-dependent data in Section 12.9 is the value of U used in defining the range of outgoing energies E in Eq. (5.7), and it is given by

U: U

The other input data are the values of $\Theta(E)$ in Eq. (5.7) depending on the incident energy E . These energies, U , E , and $\Theta(E)$, must all be in the same units as the energy

bins in Sections 12.3.2 and 12.3.3. The format for such data is

Theta: `n = n`

Interpolation: interpolation flag

with n pairs of entries $\{E, \Theta(E)\}$. The interpolation flag is one of those for simple lists as in Section 12.2.3. For example, in units of MeV one may have

U: `-20`

Theta: `n = 2`

Interpolation: `lin-lin`

`1.0e-11 1.28`

`20.0 1.28`

5.2.3 Watt model

Another model sometimes used for fission neutrons in GND is the Watt formula

$$\pi_0(E'_{\text{lab}} | E) = C \sinh \sqrt{bE'_{\text{lab}}} \exp \left\{ -\frac{E'_{\text{lab}}}{a} \right\} \quad (5.8)$$

for $0 \leq E'_{\text{lab}} \leq E - U$. The value of C in Eq. (5.8) is given by

$$\frac{1}{C} = \frac{az\sqrt{\pi}}{2} \exp \{z^2\} (\text{erf} \{y - z\} - \text{erf} \{y + z\}) - a \exp \{-y^2\} \sinh \sqrt{b(E - U)}$$

with $y = \sqrt{(E - U)/a}$ and $z = \sqrt{ab/4}$. The data consist of the energy of the reaction U and pairs of values $\{E, a(E)\}$ and $\{E, b(E)\}$. For intermediate incident energies E , the parameters b and a are interpolated by the methods of Section 3.1.

Input file data for the Watt model

The process identifier in Section 12.3.1 is

Process: `Watt spectrum`

This data is in the laboratory frame,

Product Frame: `lab`

One item of model-dependent data in Section 12.9 is the value of U used in defining the range of outgoing energies E in Eq. (5.8), and it is given by

U: `U`

The other input data are the values of $a(E)$ and $b(E)$ in Eq. (5.8). The energies, U , E , and $a(E)$, must be in the same units as the energy bins in Sections 12.3.2 and 12.3.3, and the units for $b(E)$ are the reciprocal of these units. The format for these data is

a: `n = n`

Interpolation: interpolation flag

with n pairs of entries $\{E, a(E)\}$ and

b: `n = n`

Interpolation: interpolation flag

with n pairs of entries $\{E, b(E)\}$. The interpolation flags for a and b are those for simple lists as in Section 12.2.3. For example, with energies in MeV one may have

```

U: -10
a:  n = 11
Interpolation:  lin-lin
1.000000e-11  9.770000e-01
1.500000e+00  9.770000e-01
...
3.000000e+01  1.060000e+00
b:  n = 11
Interpolation:  lin-lin
1.000000e-11  2.546000e+00
1.500000e+00  2.546000e+00
...
3.000000e+01  2.620000e+00

```

5.2.4 Madland-Nix model

The Madland-Nix model [11] for prompt fission neutrons uses the formula

$$\pi_0(E'_{\text{lab}} | E) = \frac{C}{2} [g(E'_{\text{lab}}, E_{FL}) + g(E'_{\text{lab}}, E_{FH})] \quad (5.9)$$

for

$$0 \leq E'_{\text{lab}} \leq \text{maxEout}, \quad (5.10)$$

where **maxEout** is one of the input parameters. Note that the range of outgoing energies Eq. (5.10) is independent of the incident energy. In fact, the ENDF/B-VII manual [7] gives no way for the data to specify the maximum outgoing energy for the Madland-Nix model.

In Eq. (5.9) E_{FL} is the average kinetic energy of the light fission fragments, and E_{FH} is the average kinetic energy of the heavy fission fragments. The function $g(E'_{\text{lab}}, E_F)$ in Eq. (5.9) is given in terms of the parameters T_m and

$$u_1 = \frac{(\sqrt{E'_{\text{lab}}} - \sqrt{E_F})^2}{T_m}, \quad u_2 = \frac{(\sqrt{E'_{\text{lab}}} + \sqrt{E_F})^2}{T_m} \quad (5.11)$$

by the formula

$$g(E'_{\text{lab}}, E_F) = \frac{1}{3\sqrt{E_F T_m}} \left[u_2^{3/2} E_1(u_2) - u_1^{3/2} E_1(u_1) - \Gamma(3/2, u_2) + \Gamma(3/2, u_1) \right], \quad (5.12)$$

where E_1 denotes the exponential integral

$$E_1(x) = \int_x^\infty dt \frac{1}{t} e^{-t}.$$

It is clear from the definitions that

$$E_1(x) = \Gamma(0, x),$$

but software to compute $\Gamma(\kappa, x)$ generally requires that κ be positive. The data for the Madland-Nix model contains the average energies E_{FL} and E_{FH} as well as pairs of values $\{E, T_m(E)\}$. The interpolation rule for T_m is also given.

If the range of outgoing energies is taken to be $0 \leq E'_{\text{lab}} < \infty$ in Eq. (5.9), then $C = 1$. For other ranges of E'_{lab} and for computation of $\mathcal{T}_{g,h,0}^{\text{num}}$, it follows from Eq. (5.12) that it is necessary to compute integrals

$$\mathcal{G}_i(a, b) = \int_a^b dE'_{\text{lab}} u_i^{3/2} E_1(u_i) \quad (5.13)$$

and

$$\mathcal{H}_i(a, b) = \int_a^b dE'_{\text{lab}} \Gamma(3/2, u_i) \quad (5.14)$$

with $i = 1, 2$.

The values of the integrals Eqs. (5.13) and (5.14) are conveniently expressed in terms of the parameters

$$\alpha = \sqrt{T_m}, \quad \beta = \sqrt{E_F}, \quad (5.15)$$

$$A = \frac{(\sqrt{a} + \beta)^2}{\alpha^2}, \quad B = \frac{(\sqrt{b} + \beta)^2}{\alpha^2}, \quad (5.16)$$

and

$$A' = \frac{(\beta - \sqrt{a})^2}{\alpha^2}, \quad B' = \frac{(\sqrt{b} - \beta)^2}{\alpha^2}. \quad (5.17)$$

One might think it sufficient to calculate

$$\mathcal{G}_i(0, b) \quad \text{and} \quad \mathcal{H}_i(0, b)$$

in Eqs. (5.13) and (5.14) and to use

$$\mathcal{G}_i(a, b) = \mathcal{G}_i(0, b) - \mathcal{G}_i(0, a),$$

$$\mathcal{H}_i(a, b) = \mathcal{H}_i(0, b) - \mathcal{H}_i(0, a)$$

for $i = 1, 2$. In fact, this approach is suitable only for $i = 2$. The reason for the difficulty is seen from Eqs. (5.11) and (5.15), in that

$$u_1^{3/2} = \begin{cases} (\beta - \sqrt{E'_{\text{lab}}})^3 / \alpha^3 & \text{for } 0 \leq E'_{\text{lab}} \leq \beta^2, \\ (\sqrt{E'_{\text{lab}}} - \beta)^3 / \alpha^3 & \text{for } E'_{\text{lab}} > \beta^2. \end{cases} \quad (5.18)$$

Consequently, the integrals used to compute $\mathcal{G}_i(a, b)$ and $\mathcal{H}_i(a, b)$ in Eqs. (5.13) and (5.14) are evaluated as

$$\mathcal{G}_1(a, \beta^2) = \frac{\alpha\beta}{2} \gamma(2, A') - \frac{2\alpha^2}{5} \gamma\left(\frac{5}{2}, A'\right) + \left[\frac{2\alpha\sqrt{A'}}{5} - \frac{\beta}{2} \right] \alpha A'^2 E_1(A') \quad \text{for } 0 \leq a < \beta^2, \quad (5.19)$$

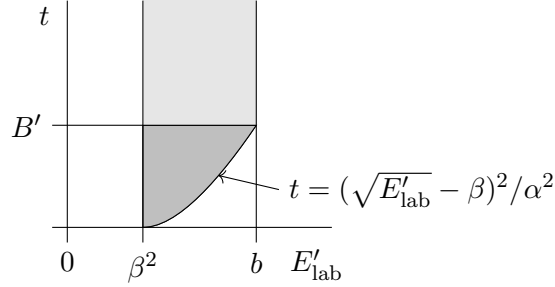


Figure 5.1: Domain of integration for $\mathcal{G}_1(\beta^2, b)$ with $b > \beta^2$ in the Madland-Nix model

$$\mathcal{G}_1(\beta^2, b) = \frac{\alpha\beta}{2} \gamma(2, B') + \frac{2\alpha^2}{5} \gamma\left(\frac{5}{2}, B'\right) + \left[\frac{\beta}{2} + \frac{2\alpha\sqrt{B'}}{5}\right] \alpha B'^2 E_1(B') \quad \text{for } b > \beta^2, \quad (5.20)$$

$$\begin{aligned} \mathcal{G}_2(0, b) = & \frac{2\alpha^2}{5} \gamma\left(\frac{5}{2}, B\right) - \frac{\alpha\beta}{2} \gamma(2, B) - \frac{\beta^5}{10\alpha^3} e^{-B} + \\ & \left[\frac{2\alpha^2}{5} B^{5/2} - \frac{\alpha\beta}{2} B^2 + \frac{\beta^5}{10\alpha^3}\right] E_1(B) - C_1 \quad \text{for } b \geq 0, \end{aligned} \quad (5.21)$$

$$\mathcal{H}_1(a, \beta^2) = 2\alpha\beta \gamma(2, A') - \alpha^2 \gamma\left(\frac{5}{2}, A'\right) + (\beta^2 - a) \Gamma\left(\frac{3}{2}, A'\right) \quad \text{for } 0 \leq a < \beta^2, \quad (5.22)$$

$$\mathcal{H}_1(\beta^2, b) = 2\alpha\beta \gamma(2, B') + \alpha^2 \gamma\left(\frac{5}{2}, B'\right) + (b - \beta^2) \Gamma\left(\frac{3}{2}, B'\right) \quad \text{for } b \geq \beta^2, \quad (5.23)$$

and

$$\mathcal{H}_2(0, b) = \alpha^2 \gamma\left(\frac{5}{2}, B\right) - 2\alpha\beta \gamma(2, B) + \beta^2 \gamma\left(\frac{3}{2}, B\right) + b \Gamma\left(\frac{3}{2}, B\right) - C_2 \quad \text{for } b > 0. \quad (5.24)$$

In the relations for $\mathcal{G}_2(0, b)$ and $\mathcal{H}_2(0, b)$ above, C_1 and C_2 are constants of integration.

In order to illustrate how the above integration formulas may be derived, consider the case of Eq. (5.20) for $\mathcal{G}_1(\beta^2, b)$ defined in Eq. (5.13) with u_1 as in Eq. (5.18) and with $b > \beta^2$. Substitution of the definition of the exponential integral E_1 gives the double integral

$$\mathcal{G}_1(\beta^2, b) = \int_{\beta^2}^b dE'_{\text{lab}} u_1^{3/2} \int_{u_1}^{\infty} dt \frac{1}{t} e^{-t}.$$

The region of integration for this integral is the union of the two shaded domains in Figure 5.1. The integral over the darker shaded region of Figure 5.1 is

$$J_{11} = \int_{\beta^2}^b dE'_{\text{lab}} u_1^{3/2} \int_{u_1}^{B'} dt \frac{e^{-t}}{t}.$$

Reversal of the order of integration transforms this integral to

$$J_{11} = \int_0^{B'} dt \frac{1}{t} e^{-t} \int_{\beta^2}^{(\alpha\sqrt{t}+\beta)^2} dE'_{\text{lab}} u_1^{3/2}.$$

Under the substitution

$$E'_{\text{lab}} = (\alpha\sqrt{u_1} + \beta)^2,$$

the inner integral takes the form

$$\int_{\beta^2}^{(\alpha\sqrt{t}+\beta)^2} dE'_{\text{lab}} u_1^{3/2} = \int_0^t du_1 u_1^{3/2} \left(\alpha^2 + \frac{\alpha\beta}{\sqrt{u_1}} \right) = \frac{2\alpha^2}{5} t^{5/2} + \frac{\alpha\beta}{2} t^2.$$

Thus, it follows that the integral over the dark shaded region in Figure 5.1 is

$$J_{11} = \frac{2\alpha^2}{5} \gamma(5/2, B') + \frac{\alpha\beta}{2} \gamma(2, B').$$

This relation gives the first two terms on the right-hand side of Eq. (5.20).

The other terms on the right-hand side of Eq. (5.20) result from evaluation of the integral over the light shaded region in Figure 5.1,

$$J_{12} = \int_{\beta^2}^b dE'_{\text{lab}} u_1^{3/2} \int_{B'}^{\infty} dt \frac{e^{-t}}{t} = \int_{B'}^{\infty} dt \frac{1}{t} e^{-t} \int_{\beta^2}^b dE'_{\text{lab}} u_1^{3/2}.$$

Input file data for the Madland-Nix model

The process identifier in Section 12.3.1 is

Process: Madland-Nix spectrum

This data is in the laboratory frame,

Product Frame: lab

The model-dependent data in Section 12.9 contains values of E_{FL} , the average kinetic energy of the light fission fragment and E_{FH} , the average kinetic energy of the heavy fission fragment. These parameters are given by

EFL: E_{FL}

EFH: E_{FH}

The user must also specify a maximum outgoing energy **maxEout** for use in Eq. (5.10).

The other input data are the values of T_m as a function of incident energy in Eq. (5.9). The format for these data is

TM: **n** = n

Interpolation: interpolation flag

with n pairs of entries $\{E, T_m(E)\}$. The interpolation flag is one of those for simple lists as in Section 12.2.3. The energies, E_{FL} , E_{FH} , E , and $T_m(E)$, must be in the same units as the energy bins in Sections 12.3.2 and 12.3.3. For example, in MeV units one may have

EFL: 1.029979

EFH: 0.5467297

maxEout: 60

TM: **n** = 38

Interpolation: lin-lin

1.0000000e-11 1.0920640e+00

5.0000010e-01 1.1014830e+00

...

2.0000000e+01 1.1292690e+00

5.3 Energy probability density tables

Another form of isotropic probability density data $\pi_0(E'_{\text{lab}} | E)$ Eq. (5.1) in GND is in the form of tables. The computation of transfer matrices for such data given in the laboratory frame is discussed here. For data in the center-of-mass frame, this is a special case of Legendre expansions discussed in Section 8 with Legendre order zero. For given incident energies E_i , the data consist of pairs $\{E'_{k,j}, \pi_0(E'_{k,j} | E_k)\}$ as in Eq. (3.5). For such tabular data, computation of the integrals $\mathcal{I}_{g,h,0}^{\text{num}}$ in Eq. (5.2) and $\mathcal{I}_{g,h,0}^{\text{en}}$ in Eq. (5.3) depends on the type of interpolation used between different incident energies. The effects of the unit-base map Eq. (3.19) are discussed here. The considerations are the same, whether the unit-base map is used alone or as a component of interpolation by cumulative points.

After the unit-base transformation Eq. (3.19) the integrals Eqs. (5.2) and (5.3) take the form

$$\mathcal{I}_{g,h,0}^{\text{num}} = \int_{\mathcal{E}_g} dE \sigma(E) M(E) w(E) \tilde{\phi}_0(E) \int_{\hat{\mathcal{E}}'_h} d\hat{E}'_{\text{lab}} \hat{\pi}_0(\hat{E}'_{\text{lab}} | E) \quad (5.25)$$

and

$$\mathcal{I}_{g,h,0}^{\text{en}} = \int_{\mathcal{E}_g} dE \sigma(E) M(E) w(E) \tilde{\phi}_0(E) \int_{\hat{\mathcal{E}}'_h} d\hat{E}'_{\text{lab}} \hat{\pi}_0(\hat{E}'_{\text{lab}} | E) E'_{\text{lab}}. \quad (5.26)$$

In these integrals $\hat{\mathcal{E}}'_h$ denotes result of mapping the outgoing energy bin \mathcal{E}'_h with the transformation Eq. (3.19). Furthermore, E'_{lab} in Eq. (5.26) is to be obtained from \hat{E}'_{lab} using the inverse unit-base mapping Eq. (3.25).

Figure 5.2 illustrates the effect of the unit-base map Eq. (3.19). For incident energies $E = E_{k-1}$ and $E = E_k$, 1-dimensional interpolation is used to produce data at a common set of unit-base outgoing energies $\{\hat{E}'_j\}$. In the left-hand portion of Figure 5.2, suppose that probability densities $\pi_0(E'_{\text{lab}} | E)$ are given at incident energies $E = E_{k-1}$ and $E = E_k$ and at unit-base outgoing energies \hat{E}'_{j-1} and \hat{E}'_j . Then for this set of data, the range of integration over E in Eqs. (5.25) or (5.26) requires both that $E_{k-1} < E < E_k$ and that E be in the bin \mathcal{E}_g . The outgoing energy E'_{lab} is required to be in the bin \mathcal{E}'_h and to satisfy the constraint $\hat{E}'_{j-1} < \hat{E}'_{\text{lab}} < \hat{E}'_j$.

The right-hand portion of Figure 5.2 shows a rectangle with vertices at $E = E_{k-1}$ and $E = E_k$ and at $\hat{E}'_{\text{lab}} = \hat{E}'_{j-1}$ and $\hat{E}'_{\text{lab}} = \hat{E}'_j$, and data values $\hat{\pi}_\ell(\hat{E}'_{\text{lab}} | E)$ are given at these corners after any required interpolation in outgoing energy. The values of $\hat{\pi}_\ell(\hat{E}'_{\text{lab}} | E)$ interior to this rectangle are determined by interpolation. The contribution of this portion of the data to the transfer matrix is obtained by integrating Eqs. (5.25) or (5.26) over the shaded region in Figure 5.2.

5.3.1 Input of isotropic energy probability tables

The process identifier in Section 12.3.1 is

Process: isotropic energy probability table

This option permits either the center-of-mass or the laboratory frame. For data in the laboratory frame, the command in Section 12.3.4 is

Product Frame: lab

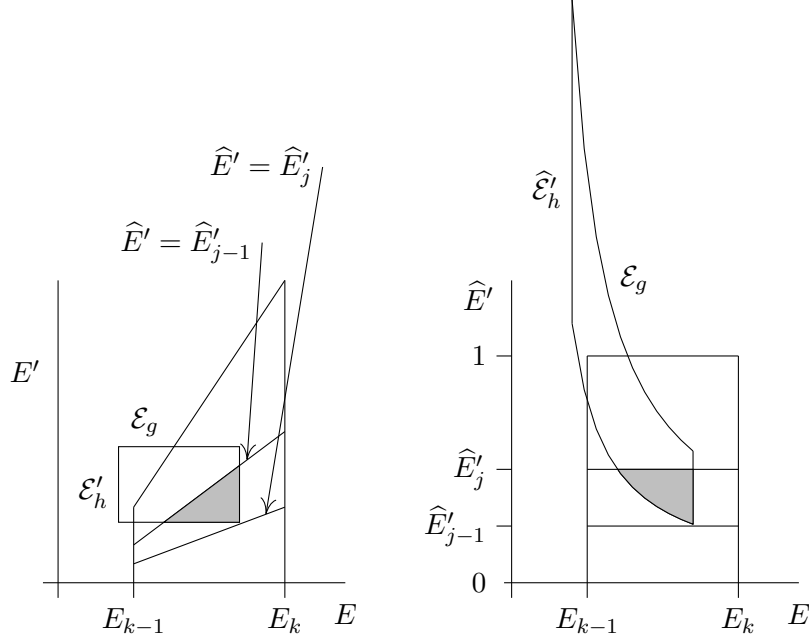


Figure 5.2: Domains of integration for tabulated probability densities, laboratory frame on the left and unit base on the right

The data as in Section 12.9 for tables of isotropic energy probability densities is entered in the format

```
EEpPData:  n = K
Incident energy interpolation: probability interpolation flag
Outgoing energy interpolation: list interpolation flag
```

The interpolation flag for incident energy is one those used for probability density tables in Section 12.2.3, and that for outgoing energy is one for simple lists. This information is followed by K sections of the form

```
Ein:  E: n = J
```

with J pairs of values of E'_{lab} and $\pi_E(E'_{\text{lab}} | E)$.

An example with energies in eV of the model-dependent section of the input file for isotropic energy probability density tables is

```
EEpPData:  n = 4
Incident energy interpolation:  lin-lin unitbase
Outgoing energy interpolation:  flat
Ein:  1.722580000000e+07 :  n = 34
      0.000000000000e+00 0.000000000000e+00
      1.000000000000e-08 0.000000000000e+00
      1.778280000000e-08 2.766140000000e-07
      3.162280000000e-08 4.918960000000e-07
      ...
```

```

5.623410000000e-01 8.396540000000e-01
1.000000000000e+00 0.000000000000e+00
...
Ein: 2.000000000000e+07 : n = 38
0.000000000000e+00 0.000000000000e+00
7.500000000000e-03 0.000000000000e+00
1.333710000000e-02 4.877750000000e-14
2.371710000000e-02 8.674000000000e-14
...
2.250000000000e+06 4.413810000000e-08
2.750000000000e+06 0.000000000000e+00

```

Note that for these data it is not clear what should be used as the minimum outgoing energy. In particular for incident energy $E_0 = 1.72258 \times 10^7$ eV, it is not clear whether it is more reasonable to set $E'_{0,\min} = 0$ or $E'_{0,\min} = 1.77828 \times 10^{-8}$ eV in the unit-base interpolation. The `merced` code uses $E'_{0,\min} = 0$, to be consistent with Eq. (3.8).

5.4 General evaporation of delayed fission neutrons

For some fissionable targets, the energy spectra data for delayed fission neutrons is represented in GND in the form

$$\pi_0(E'_{\text{lab}} | E) = g \left(\frac{E'_{\text{lab}}}{\Theta(E)} \right). \quad (5.27)$$

For this model, values of Θ are given as a function of E , and values of g as a function of $x = E'_{\text{lab}}/\Theta(E)$. In fact, all of the general evaporation data in GND have Θ constant, and the `merced` code requires that Θ be constant. The isotropic probability density $\pi_0(E'_{\text{lab}} | E)$ in Eq. (5.27) is then independent of E . In this case, the integrals $\mathcal{I}_{g,h,0}^{\text{num}}$ in Eq. (5.2) and $\mathcal{I}_{g,h,0}^{\text{en}}$ in Eq. (5.3) needed for the transfer matrix become simply products of 1-dimensional integrals

$$\mathcal{I}_{g,h,0}^{\text{num}} = \int_{\mathcal{E}_g} dE \sigma(E) M(E) w(E) \tilde{\phi}_0(E) \int_{\mathcal{E}'_h} dE'_{\text{lab}} g(E'_{\text{lab}}/\Theta)$$

and

$$\mathcal{I}_{g,h,0}^{\text{en}} = \int_{\mathcal{E}_g} dE \sigma(E) M(E) w(E) \tilde{\phi}_0(E) \int_{\mathcal{E}'_h} dE'_{\text{lab}} g(E'_{\text{lab}}/\Theta) E'_{\text{lab}}.$$

5.4.1 Input of data for the general evaporation model

For the general evaporation model, the process identifier in Section 12.3.1 is

Process: general evaporation

This data is in the laboratory frame,

Product Frame: lab

The model-dependent data in Section 12.9 consist of pairs $\{E, \Theta(E)\}$ and of pairs $\{x, g(x)\}$ with $x = E'_{\text{lab}}/\Theta$. The format for these data is

Theta: n = n

Interpolation: interpolation flag

with n pairs of entries $\{E, \Theta(E)\}$ and

```
g:  n = n
```

```
Interpolation: interpolation flag
```

with n pairs of entries $\{x, g(x)\}$. In both cases, the interpolation flag is one of those for simple lists as in Section 12.2.3. The Θ parameter is dimensionless, and the units for E and x must be the same as those for the energy bins. For example, in MeV one may have

```
Theta:  n = 2
```

```
Interpolation:  lin-lin
```

```
1.0e-11 1.0
```

```
20.0 1.0
```

```
g:  n = 185
```

```
Interpolation:  lin-lin
```

```
0.0000000e+00 3.1433980e-01
```

```
1.0000000e-02 2.8124280e+00
```

```
2.0000000e-02 3.1373560e+00
```

```
...
```

```
1.8400000e+00 0.0000000e+00
```

6 Uncorrelated energy-angle probability densities

The simplest form of joint energy-angle probability density data in GND is as tables of uncorrelated dependence on outgoing energy E'_{lab} and direction cosine μ_{lab} ,

$$\pi(E'_{\text{lab}}, \mu_{\text{lab}} | E) = \pi_{\mu}(\mu_{\text{lab}} | E) \pi_E(E'_{\text{lab}} | E). \quad (6.1)$$

The case of data given in the laboratory coordinate system is discussed here. Data of the form

$$\pi(E'_{\text{cm}}, \mu_{\text{cm}} | E) = \pi_{\mu}(\mu_{\text{cm}} | E) \pi_E(E'_{\text{cm}} | E)$$

in the center-of-mass frame with $\pi_{\mu}(\mu_{\text{cm}} | E)$ represented as Legendre coefficients are converted into Legendre expansions Eq. (8.1) and are processed as described in Section 8.

The tables for Eq. (6.1) are given as pairs $\{E'_{i,j}, \pi_E(E'_{i,j} | E_i)\}$ for the energy probability and pairs $\{\mu_{i,j}, \pi_{\mu}(\mu_{i,j} | E_i)\}$ for the angular probability. The incident energies E_i need not be the same for the two data sets, but the ranges of incident energy must agree.

For uncorrelated energy-angle probability densities Eq. (6.1) the number-preserving integral Eq. (2.7) becomes

$$\mathcal{I}_{gh,\ell}^{\text{num}} = \int_{\mathcal{E}_g} dE \sigma(E) M(E) w(E) \tilde{\phi}_{\ell}(E) \int_{\mathcal{E}'_h} dE'_{\text{lab}} \pi_E(E'_{\text{lab}} | E) \int_{\mu_{\text{lab}}} d\mu_{\text{lab}} P_{\ell}(\mu_{\text{lab}}) \pi_{\mu}(\mu_{\text{lab}} | E), \quad (6.2)$$

and the energy-preserving integral Eq. (2.10) takes the form

$$\mathcal{I}_{gh,\ell}^{\text{en}} = \int_{\mathcal{E}_g} dE \sigma(E) M(E) w(E) \tilde{\phi}_{\ell}(E) \int_{\mathcal{E}'_h} dE'_{\text{lab}} \pi_E(E'_{\text{lab}} | E) E'_{\text{lab}} \int_{\mu_{\text{lab}}} d\mu_{\text{lab}} P_{\ell}(\mu_{\text{lab}}) \pi_{\mu}(\mu_{\text{lab}} | E). \quad (6.3)$$

It is clear from Eqs. (6.2) and (6.3) that one should first evaluate the integrals

$$\mathcal{U}_{\ell}(E) = \int_{\mu_{\text{lab}}} d\mu_{\text{lab}} P_{\ell}(\mu_{\text{lab}}) \pi_{\mu}(\mu_{\text{lab}} | E) \quad (6.4)$$

for the Legendre orders ℓ required. When interpolation of $\pi_{\mu}(\mu_{\text{lab}} | E)$ in μ_{lab} is piecewise linear or histogram, the integrand in Eq. (6.4) is a piecewise polynomial and the integrals are evaluated exactly using Gaussian quadrature. Currently, the code handles Legendre

order $\ell \leq 18$ in this way. Integrals with higher Legendre order are evaluated using adaptive quadrature.

For the integrals

$$\mathcal{V}_n(E) = \int_{\mathcal{E}'_h} dE'_{\text{lab}} \pi_E(E'_{\text{lab}} | E)$$

and

$$\mathcal{V}_E(E) = \int_{\mathcal{E}'_h} dE'_{\text{lab}} \pi_E(E'_{\text{lab}} | E) E'_{\text{lab}}$$

the same geometric considerations apply as for the integrals Eqs. (5.2) and (5.3) of tabular isotropic data $\pi_0(E'_{\text{lab}} | E)$ as discussed in Section 5.3. That is, if unit-base interpolation Eq. (3.20) is being used, then the integral $\mathcal{V}_n(E)$ takes the form

$$\mathcal{V}_n(E) = \int_{\hat{\mathcal{E}}'_h} d\hat{E}'_{\text{lab}} \pi_E(\hat{E}'_{\text{lab}} | E),$$

and the range of integration is determined by the geometry of the shaded region in Figure 5.2.

6.1 Input of data for uncorrelated energy-angle probability densities

The process identifier in Section 12.3.1 is

Process: Uncorrelated energy-angle data transfer matrix

These data are in the laboratory frame, Section 12.3.4,

Product Frame: lab

The model-dependent data in Section 12.9 consists of tables of values of the angular probability density $\pi_\mu(\mu_{\text{lab}} | E)$ and energy probability density $\pi_E(E'_{\text{lab}} | E)$ in Eq. (6.1). All energies must be in the same units as those used for the energy groups.

The angular probability density table is of the form

Angular data: $\mathbf{n} = K$

Incident energy interpolation: probability interpolation flag

Outgoing cosine interpolation: list interpolation flag

The interpolation flag for incident energy is one of those used for probability density tables in Section 12.2.3, while that for the cosine is for simple lists. This information is followed by K sections of the form

Ein: $E: \mathbf{n} = J$

with J pairs of values of μ_{lab} and $\pi_\mu(\mu_{\text{lab}} | E)$.

The energy probability density table is of the form

EEpPData: $\mathbf{n} = K$

Incident energy interpolation: probability interpolation flag

Outgoing energy interpolation: list interpolation flag

The interpolation flags are those used for probability density tables in Section 12.2.3. This information is followed by K sections of the form

Ein: E : $n = J$
with J pairs of values of E'_{lab} and $\pi_E(E'_{\text{lab}} | E)$.
An example with energies in MeV of the model-dependent section of the input file for uncorrelated energy-angle probability densities is

```
Angular data:  n = 10
Incident energy interpolation:  lin-lin direct
Outgoing cosine interpolation:  lin-lin
Ein:  2.8260000e+00 :  n = 2
      -1 0.5
      1 0.5
...
Ein:  2.0000000e+01:  n = 10
      -1.0000000e+00 2.86849000e-01
      -9.0000000e-01 2.98228000e-01
      -6.0000000e-01 3.48724000e-01
      -3.0000000e-01 4.08451000e-01
      -1.0000000e-01 4.54198000e-01
      1.0000000e-01 5.05334000e-01
      3.0000000e-01 5.62452000e-01
      7.0000000e-01 6.93910000e-01
      9.0000000e-01 7.47781000e-01
      1.0000000e+00 7.65990000e-01
EEpPData:  n = 10
Incident energy interpolation:  lin-lin unitbase
Outgoing energy interpolation:  lin-lin
Ein:  2.826000e+00:  n = 3
      1.000000e-03 0.000000e+00
      2.000000e-03 1.000000e+03
      3.000000e-03 0.000000e+00
...
Ein:  2.000000e+01:  n = 33
      0.000000e+00 0.000000e+00
      1.000000e-01 1.678010e-02
      2.000000e-01 2.383160e-02
      ...
      1.530000e+01 1.150130e-02
      1.560000e+01 9.260950e-03
```

7 Legendre expansions of energy-angle probability densities in the laboratory frame

Another representation of joint energy-angle probability densities $\pi(E', \mu | E)$ in GND is as a table of the Legendre coefficients $\pi_\ell(E' | E)$ in the expansion

$$\pi(E', \mu | E) = \sum_{\ell} \left(\ell + \frac{1}{2} \right) \pi_\ell(E' | E) P_\ell(\mu). \quad (7.1)$$

Here, E denotes the energy of the incident particle in the laboratory frame. For the outgoing particle, the energy E' and direction cosine μ may be given in either center-of-mass or laboratory coordinates. The treatment of laboratory-frame data is discussed in this section, center-of-mass data in the next. Data given in the laboratory frame is much easier to deal with because no boost is involved.

This type of data is ordered according to

$$\{E, \{E', \{\pi_\ell(E' | E)\}\}\}. \quad (7.2)$$

All of the data for the lowest incident energy E is given first, ordered according to outgoing energy E' . For given values of E and E' , the data consist of Legendre coefficients $\pi_\ell(E', | E)$. Note that for this data format, the number of Legendre coefficients may vary, depending on the energies E and E' .

The `merced` code also handles data for Legendre expansions of energy-angle probability densities in the ENDL format [4],

$$\{\ell, \{E, \{E', \pi_\ell(E', | E)\}\}\}. \quad (7.3)$$

That is, the $\ell = 0$ data are given first, ordered according to incident energy E . The data then consist of pairs $\{E', \pi_\ell(E', | E)\}$ for given ℓ and E .

7.1 Computation of the transfer matrices for data in the laboratory frame

The calculation of the transfer matrices for laboratory-frame data proceeds as follows. In terms of $\pi_\ell(E'_{\text{lab}} | E)$, the integral Eq. (2.7) for the number-preserving transfer matrix takes the form

$$\mathcal{I}_{g,h,\ell}^{\text{num}} = \int_{\mathcal{E}_g} dE \sigma(E) M(E) w(E) \tilde{\phi}_\ell(E) \int_{\mathcal{E}'_h} dE'_{\text{lab}} \pi_\ell(E'_{\text{lab}} | E), \quad (7.4)$$

and Eq. (2.10) for the energy-preserving transfer matrix becomes

$$\mathcal{I}_{g,h,\ell}^{\text{en}} = \int_{\mathcal{E}_g} dE \sigma(E) M(E) w(E) \tilde{\phi}_\ell(E) \int_{\mathcal{E}'_h} dE'_{\text{lab}} \pi_\ell(E'_{\text{lab}} | E) E'_{\text{lab}}. \quad (7.5)$$

Computation of the integrals Eqs. (7.4) and (7.5) depends on the type of interpolation used with respect to the energy E of the incident particle, and the procedures are exactly the same as for integration in Eqs. (5.2) and (5.3) of the isotropic energy probability densities $\pi_0(E'_{\text{lab}} | E)$. Thus, if unit-base interpolation is to be used for $\pi_\ell(E'_{\text{lab}} | E)$, then the map Eq. (3.20) converts the integrals Eqs. (7.4) and (7.5) to the form

$$\mathcal{I}_{g,h,\ell}^{\text{num}} = \int_{\mathcal{E}_g} dE \sigma(E) M(E) w(E) \tilde{\phi}_\ell(E) \int_{\hat{\mathcal{E}}'_h} d\hat{E}'_{\text{lab}} \hat{\pi}_\ell(\hat{E}'_{\text{lab}} | E) \quad (7.6)$$

and

$$\mathcal{I}_{g,h,\ell}^{\text{en}} = \int_{\mathcal{E}_g} dE \sigma(E) M(E) w(E) \tilde{\phi}_\ell(E) \int_{\hat{\mathcal{E}}'_h} d\hat{E}'_{\text{lab}} \hat{\pi}_\ell(\hat{E}'_{\text{lab}} | E) E'_{\text{lab}}. \quad (7.7)$$

In these intergrals $\hat{\mathcal{E}}'_h$ denotes result of mapping the outgoing energy bin \mathcal{E}'_h with the transformation Eq. (3.20). Furthermore, E'_{lab} in Eq. (7.7) is to be obtained from \hat{E}'_{lab} using the inverse unit-base mapping Eq. (3.25).

The geometrical considerations involved in integrating Eqs. (7.6) and (7.7) over the incident energy bin \mathcal{E}_g and the mapped outgoing energy bin $\hat{\mathcal{E}}'_h$ are illustrated in Figure 5.2.

7.2 Form of the input file for Legendre coefficient data in the laboratory frame

These data may be input in either of two forms, the format in Eq. (7.2) from ENDF/B-VII with all Legendre coefficients given together at each incident energy E and outgoing energy E' or that in Eq. (7.3) with one Legendre order at a time. For both formats, all energies must be in the same units as the energy groups.

7.2.1 Input of all Legendre coefficients together

For energy-angle tables in the standard format of Eq. (7.2), the Section 12.3.1 line in the input file to identify the data is

Process: Legendre energy-angle data

and the model-dependent data in Section 12.9 consists of the Legendre coefficients $\pi_\ell(E' | E)$ in Eq. (7.2) at incident energies E and outgoing energies E' .

The format for the Legendre coefficient data in Section 12.9 given at K values of E is

Product Frame: lab

Legendre data by incident energy: $n = K$

Incident energy interpolation: probability interpolation flag

Outgoing energy interpolation: list interpolation flag

where the interpolation flag for incident energy is one for probability density tables as in

Section 12.2.3, and that for outgoing energy is for a simple list. These lines are followed by K sections of the form

```
Ein:  E: n =  $J_k$ 
for  $J_k$  outgoing energies  $E$ . For each value of  $E$  there is data
Eout:   $E'$ : n =  $L$ 
with Legendre coefficients  $\pi_\ell(E' | E)$  for  $\ell = 0, 1, \dots, L - 1$ .
```

An example of these data with energies in MeV is

```
Legendre data by incident energy:  n = 26
Incident energy interpolation:  lin-lin cumulativepoints
Outgoing energy interpolation:  flat
Ein:  1.140200e+01:  n = 2
Eout:  0.000000e+00:  n = 5
      1.000000e+11
      0.000000e+00
      0.000000e+00
      0.000000e+00
      0.000000e+00
Eout:  1.000000e-11:  n = 5
      0.000000e+00
      0.000000e+00
      0.000000e+00
      0.000000e+00
      0.000000e+00
...
Ein:  2.000000e+01:  n = 27
Eout:  0.000000e+00:  n = 5
      4.179200e-02
      0.000000e+00
      4.179200e-06
      0.000000e+00
      3.395500e-07
      etc.
```

7.2.2 Input of one Legendre coefficient at a time

For data given one Legendre coefficient at a time as in Eq. (7.3), the line in Section 12.3.1 of the input file identifying the data is

```
Process:  Legendre EEpP data transfer matrix
```

The first lines in the data for Section 12.9 are

```
Product Frame:  lab
LEEpPData:  n =  $L$ 
```

where L is the number of Legendre coefficients, one greater than the order of the Legendre expansion. The interpolation flags as in Section 12.2.3 are

```
Incident energy interpolation:  probability interpolation flag
```

Outgoing energy interpolation: list interpolation flag

The interpolation flag for incident energy is one for probability density tables as in Section 12.2.3, and that for outgoing energy is for a simple list.

The data are then given in L sections, each of the form

order: $l = \ell$: $n = K$

where K is the number of incident energies. For each incident energy E' there is a block of data

Ein: E : $n = J_k$

for J_k pairs of values of outgoing energy E' and Legendre coefficient $\pi_\ell(E' | E)$. For energies measured in MeV, these data may look like

```
LEEpPData:  n = 4
Incident energy interpolation:  lin-lin unitbase
Outgoing energy interpolation:  lin-lin
order:  l = 0:  n = 10
Ein:  3.350000000000e+00 :  n = 3
      3.716500000000e-01 0.000000000000e+00
      3.716800000000e-01 2.857140000000e+04
      3.717200000000e-01 0.000000000000e+00
Ein:  4.460200000000e+00 :  n = 2
      1.238900000000e-01 1.008970000000e+00
      1.115000000000e+00 1.008970000000e+00
...
Ein:  2.000000000000e+01 :  n = 2
      1.699600000000e-02 1.232820000000e-01
      8.128500000000e+00 1.232820000000e-01
order:  l = 1:  n = 10
Ein:  3.350000000000e+00 :  n = 3
      3.716500000000e-01 0.000000000000e+00
      3.716800000000e-01 2.690500000000e+04
      3.717200000000e-01 0.000000000000e+00
...
order:l = 3:  n = 10
Ein:  3.350000000000e+00 :  n = 3
      3.716500000000e-01 0.000000000000e+00
      3.716800000000e-01 2.690500000000e+04
      3.717200000000e-01 0.000000000000e+00
...
Ein:  2.000000000000e+01 :  n = 28
      1.699600000000e-02 1.172400000000e-01
      3.283800000000e-02 -8.646000000000e-03
      4.868100000000e-02 -3.589400000000e-02
      6.452400000000e-02 -4.528500000000e-02
      8.036700000000e-02 -4.921500000000e-02
      1.120500000000e-01 -5.186400000000e-02
```

...
7.082900000000e+00 7.783200000000e-02
8.128500000000e+00 1.172400000000e-01

8 Legendre expansions of energy-angle probability densities in the center-of-mass frame

Energy-angle probability density data in GND may also be given as Legendre coefficients for the expansion Eq. (7.1) with outgoing energy E and direction cosine μ in the center-of-mass frame. In this case, the data consists of tables of coefficients $\pi_\ell(E'_{\text{cm}} | E)$ for the sum

$$\pi(E'_{\text{cm}}, \mu_{\text{cm}} | E) = \sum_{\ell} \left(\ell + \frac{1}{2} \right) \pi_\ell(E'_{\text{cm}} | E) P_\ell(\mu_{\text{cm}}) \quad (8.1)$$

for a set of outgoing energies E'_{cm} at incident energies E . The number of terms in the sum in Eq. (8.1) is determined by the data.

The analysis given in this section is also applicable to the case of isotropic energy probability densities given in the center-of-mass frame. The data then consist only of values of the $\pi_0(E'_{\text{cm}} | E)$ term in Eq. (8.1).

For incident energies E between the tabulated values, the coefficients $\pi_\ell(E'_{\text{cm}} | E)$ are obtained by one of the interpolation methods discussed in Section 3.2.

For the probability density $\pi(E'_{\text{cm}}, \mu_{\text{cm}} | E)$ in Eq. (8.1), the integral Eq. (2.7) for computing the number-preserving transfer matrix becomes

$$\mathcal{I}_{gh,\ell}^{\text{num}} = \int_{\mathcal{E}_g} dE \sigma(E) M(E) w(E) \tilde{\phi}_\ell(E) \int_{\mathcal{D}_{h,\text{cm}}} dE'_{\text{cm}} d\mu_{\text{cm}} P_\ell(\mu_{\text{lab}}) \pi(E'_{\text{cm}}, \mu_{\text{cm}} | E), \quad (8.2)$$

where $\mathcal{D}_{h,\text{cm}}$ is the set of outgoing energies E'_{cm} and direction cosines μ_{cm} which are mapped into \mathcal{E}'_h under the boost to the laboratory frame for incident particles with energy E .

Figure 8.1 illustrates the portion of the region $\mathcal{D}_{h,\text{cm}}$ for one incident energy generated by a range of outgoing energies corresponding to the data

$$E'_{\text{cm},j-1} \leq E'_{\text{cm}} \leq E'_{\text{cm},j}. \quad (8.3)$$

In this figure the outgoing energy bin \mathcal{E}'_h in the laboratory frame is a half annulus centered at the origin with radii corresponding to the upper and lower boundaries of the energy bin. The vector $\mathbf{V}_{\text{trans}}$ is the velocity of the center of mass with magnitude V_{trans} as in Eq. (4.3). The range of outgoing center-of-mass energies in Eq. (8.3) produces the second half annulus in Figure 8-1, and its contribution to the set $\mathcal{D}_{h,\text{cm}}$ is the intersection of these two half annuli and is shaded dark gray. This dark gray set displays the outgoing energies E'_{cm} in the center-of-mass frame which satisfy Eq. (8.3) and the direction cosines μ_{cm} such that the energy E of the outgoing particle in the laboratory frame is in the bin \mathcal{E}'_h . In this figure, the upper limit of \mathcal{E}'_h is indicated by the arc $E'_{\text{lab}} = E'_{\text{bin}}$.

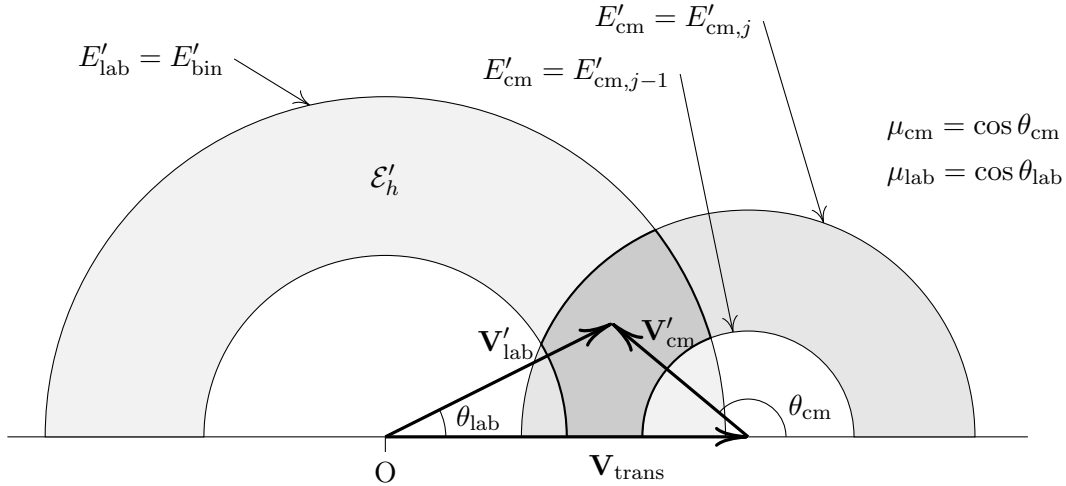


Figure 8.1: Integration region over E'_{cm} and μ_{cm} for the outgoing energy bin \mathcal{E}'_h at a fixed incident energy for data given at energies $E'_{\text{cm},j-1} \leq E'_{\text{cm}} \leq E'_{\text{cm},j}$ in the center-of-mass frame

8.1 Geometrical considerations

The first question in the analysis of the integral in Eq. (8.2) is the determination of the set $\mathcal{D}_{h,\text{cm}}$. This requires knowing whether or not the arc for a bin boundary $E'_{\text{lab}} = E'_{\text{bin}}$ intersects an arc $E'_{\text{cm}} = E'_{\text{cm},j}$ derived from a data point. For a boost to the laboratory frame using Newtonian mechanics as in Eq. (4.8), this identification is achieved by the function

$$G_0(E'_{\text{bin}}, E'_{\text{cm}}, E) = 2E'_{\text{bin}}(E'_{\text{trans}} + E'_{\text{cm}}) - (E'_{\text{trans}} - E'_{\text{cm}})^2 - E'_{\text{bin}}{}^2. \quad (8.4)$$

Note that in G_0 the dependence on the energy E of the incident particle typically enters in two ways. For one thing, E'_{trans} depends on E as in Eq. (4.7). On the other hand, if the interpolation with respect to incident energy is unit-base or by cumulative points, then the inversion of the unit-base map Eq. (3.24) takes the form

$$E'_{\text{cm}} = E'_{\text{cm},\text{min}} + (E'_{\text{cm},\text{max}} - E'_{\text{cm},\text{min}})\hat{E}'_{\text{cm}}. \quad (8.5)$$

In linear-linear unit-base interpolation, \hat{E}'_{cm} is fixed in the interval $0 \leq \hat{E}'_{\text{cm}} \leq 1$, while $E'_{\text{cm},\text{min}}$ and $E'_{\text{cm},\text{max}}$ depend on E according to Eq. (3.17) with q given by Eq. (3.14).

The utility of the function G_0 in Eq. (8.5) depends on the following result.

8.1.1 Assertion

In Figure 8.1 under a Newtonian boost at fixed incident energy E , an arc $E'_{\text{lab}} = E'_{\text{bin}}$ representing an edge of an energy bin in the laboratory frame intersects an arc $E'_{\text{cm}} = \text{const}$

generated by data in the center-of-mass frame if and only if

$$G_0(E'_{\text{bin}}, E'_{\text{cm}}, E) \geq 0. \quad (8.6)$$

This assertion is proved in Appendix B.

One application of Assertion 8.1.1 is that of finding the incident energies E in \mathcal{E}_g in the integral Eq. (8.2) such that the set $\mathcal{D}_{h,\text{cm}}$ is non-empty. This may be done by locating the zeros of $G_0(E'_{\text{bin}}, E'_{\text{cm}}, E)$ as a function of E with the edges of the bin \mathcal{E}'_h as values of E'_{bin} and with E'_{cm} as in Eq. (8.5) for

$$\hat{E}'_{\text{cm}} = \hat{E}'_{\text{cm},j-1} \quad \text{and} \quad \hat{E}'_{\text{cm}} = \hat{E}'_{\text{cm},j},$$

according to the data.

8.2 Input of Legendre coefficients of energy-angle probability densities in the center-of-mass frame

The format for input of the coefficients $\pi_\ell(E'_{\text{cm}} | E)$ in Eq. (8.1) is that of Section 7.2.1 with some obvious modifications. For one thing, the data are in the center-of-mass frame

Product Frame: CenterOfMass

The other difference is that information on particle masses is required by the boost to the laboratory frame

Projectile's mass: m_{yi}

Target's mass: m_{targ}

Product's mass: m_{yo}

Reaction's Q value: Q

The values of these quantities must be in the same units as the energy bin boundaries.

The code computes the mass of the residual from the Q value and the masses of the other particles. If the input file also contains the line

Residual's mass: m_{res}

the code compares this value with the mass it computed, printing a warning message if they are significantly different.

Currently, the boost for this type of data is only implemented using Newtonian mechanics.

8.3 Input of isotropic energy probability densities in the center-of-mass frame

The format for isotropic energy probability density data given in the center-of-mass frame is the same as that for laboratory-frame data in Section 5.3.1, except that the line

Product Frame: lab

is replaced by

Product Frame: CenterOfMass

9 Joint energy-angle probability density tables

It is also possible to give energy-angle probability densities as tables in GND. These probability tables must be in the laboratory coordinate system. The ENDL [4] and ENDF/B-VII [7] forms of these tables differ slightly, and `merced` supports both formats. The ENDF/B-VII format is described first.

One format for tables of values of $\pi(E'_{\text{lab}}, \mu_{\text{lab}} | E)$ is as arrays

$$\{E, \{\mu_{\text{lab}}, \{E'_{\text{lab}}, \pi(E'_{\text{lab}}, \mu_{\text{lab}} | E)\}\}\}. \quad (9.1)$$

The data for the lowest incident energy E are given first, and data for a given incident energy are ordered by increasing direction cosine μ_{lab} . For fixed E and μ_{lab} , the data consist of pairs $\{E'_{\text{lab}}, \pi(E'_{\text{lab}}, \mu_{\text{lab}} | E)\}$ for values of the energy E'_{lab} of the outgoing particle. The normalization of the data $\pi(E'_{\text{lab}}, \mu_{\text{lab}} | E)$ is such that for each incident energy E the total probability is

$$\int_0^\infty dE'_{\text{lab}} \int_{-1}^1 d\mu_{\text{lab}} \pi(E'_{\text{lab}}, \mu_{\text{lab}} | E) = 1.$$

The ENDL energy-angle probability density data tables are given in the form of the product

$$\pi(E'_{\text{lab}}, \mu_{\text{lab}} | E) = \pi_\mu(\mu_{\text{lab}} | E) \pi_E(E'_{\text{lab}} | E, \mu_{\text{lab}}), \quad (9.2)$$

in which $\pi_E(E'_{\text{lab}} | E, \mu_{\text{lab}})$ is normalized so that

$$\int_0^\infty dE'_{\text{lab}} \pi_E(E'_{\text{lab}} | E, \mu_{\text{lab}}) = 1$$

for each of the tabulated values of E and μ_{lab} .

In the `merced` code energy-angle probability density tables in the format of Eq. (9.1) are converted to the format of Eq. (9.2) via the formulas

$$\pi_\mu(\mu_{\text{lab}} | E) = \int_0^\infty dE'_{\text{lab}} \pi(E'_{\text{lab}}, \mu_{\text{lab}} | E)$$

and

$$\pi_E(E'_{\text{lab}} | E, \mu_{\text{lab}}) = \frac{\pi(E'_{\text{lab}}, \mu_{\text{lab}} | E)}{\pi_\mu(\mu_{\text{lab}} | E)}.$$

The rest of the discussion of energy-angle probability density tables is therefore in terms of the form of the data in Eq. (9.2). Thus, the discussion is in terms of the angular probability density $\pi_\mu(\mu_{\text{lab}} | E)$ and the outgoing energy conditional probability density $\pi_E(E'_{\text{lab}} | E, \mu_{\text{lab}})$.

With the correlated energy-angle probability density (9.2) the number-preserving integral (2.7) is

$$\mathcal{I}_{gh,\ell}^{\text{num}} = \int_{\mathcal{E}_g} dE \sigma(E) M(E) w(E) \tilde{\phi}_\ell(E) \int_{\mathcal{E}'_h} dE'_{\text{lab}} \int_{\mu_{\text{lab}}} d\mu_{\text{lab}} P_\ell(\mu_{\text{lab}}) \pi_\mu(\mu_{\text{lab}} | E) \pi_E(E'_{\text{lab}} | E, \mu_{\text{lab}}), \quad (9.3)$$

and the energy-preserving integral (2.10) becomes

$$\mathcal{I}_{gh,\ell}^{\text{en}} = \int_{\mathcal{E}_g} dE \sigma(E) M(E) w(E) \tilde{\phi}_\ell(E) \int_{\mathcal{E}'_h} dE'_{\text{lab}} E'_{\text{lab}} \int_{\mu_{\text{lab}}} d\mu_{\text{lab}} P_\ell(\mu_{\text{lab}}) \pi_\mu(\mu_{\text{lab}} | E) \pi_E(E'_{\text{lab}} | E, \mu_{\text{lab}}). \quad (9.4)$$

The method used by **merced** to evaluate the integrals (9.3) and (9.4) is to first compute the Legendre coefficients

$$\pi_\ell(E'_{\text{lab}} | E) = \int_{-1}^1 d\mu_{\text{lab}} P_\ell(\mu_{\text{lab}}) \pi_\mu(\mu_{\text{lab}} | E) \pi_E(E'_{\text{lab}} | E, \mu_{\text{lab}}). \quad (9.5)$$

The coding for the integration of (7.4) and (7.5) is then applied to obtain the transfer matrix.

9.1 Input of $\pi(E'_{\text{lab}}, \mu_{\text{lab}} | E)$ the form of a table, Eq. (9.1)

For tables of the energy-angle probability density $\pi(E'_{\text{lab}}, \mu_{\text{lab}} | E)$ in the format Eq. (9.1), the identification line in Section 12.9 is

Process: ENDF Double differential EMuEpP data

These data are always in the laboratory frame,

Product Frame: lab

The first lines in the data for Section 12.9 give the number K of incident energies along with the interpolation rules

EMuEpPData: $n = K$

Incident energy interpolation: probability interpolation flag

Outgoing cosine interpolation: probability interpolation flag

Outgoing energy interpolation: list interpolation flag

The flags for interpolation with respect to incident energy E and direction cosine μ_{lab} are those for probability density tables in Section 12.2.3, and that for outgoing energy E' is one for simple lists.

For each incident energy E there is a data section of the form

Ein: E : **n** = N

indicating that data are given for N values of μ_{lab} . The block of data corresponding to a value of μ_{lab} is of the form

mu: μ_{lab} : n = J
followed by J pairs of values of outgoing energy E'_{lab} and probability density $\pi(E'_{\text{lab}}, \mu_{\text{lab}} | E)$.

An example of such data with energy in MeV is

```
EMuEpPData:  n = 18
Incident energy interpolation:  lin-lin unitbase
Outgoing cosine interpolation:  lin-lin unibase
Outgoing energy interpolation:  lin-lin
Ein:  1.748830e+00:  n = 21
mu:   -1.000000e+00:  n = 15
      1.092990e-03  0.000000e+00
      1.093000e-03  7.406740e-01
      3.278900e-03  1.166140e+00
      7.650800e-03  1.466540e+00
      1.202300e-02  1.585880e+00
      2.076600e-02  1.610940e+00
      2.951000e-02  1.546240e+00
      5.574100e-02  1.071950e+00
      7.104300e-02  7.097100e-01
      8.197300e-02  4.021720e-01
      9.071600e-02  1.795810e-01
      9.508800e-02  9.526480e-02
      9.946000e-02  2.867760e-02
      1.016500e-01  4.692750e-03
      1.016510e-01  0.000000e+00
      ...
Ein:  2.000000e+01:  n = 21
mu:   -1.000000e+00:  n = 76
      4.606790e-02  0.000000e+00
      4.606800e-02  3.837140e-02
      9.213400e-02  4.393050e-02
      1.842700e-01  4.977660e-02
      2.764100e-01  4.806820e-02
      3.685400e-01  4.385540e-02
      6.449500e-01  2.695920e-02
      7.370900e-01  2.255450e-02
      etc.
```

9.2 Input of $\pi(E'_{\text{lab}}, \mu_{\text{lab}} | E)$ as a product, Eq. (9.2)

For tables of the energy-angle probability density $\pi(E'_{\text{lab}}, \mu_{\text{lab}} | E)$ given as the product in Eq. (9.2), the identification line in Section 12.9 is

```
Process: Double differential EMuEpP data transfer matrix
```

These data are always in the laboratory frame,

Product Frame: lab

The model-dependent portion of the input file in Section 12.9 contains a section for the angular probability density $\pi_\mu(\mu_{\text{lab}} | E)$ and another for the conditional probability density $\pi_E(E'_{\text{lab}} | E, \mu_{\text{lab}})$.

The section for angular probability density starts with the lines

Angular data: $n = K$

Incident energy interpolation: probability interpolation flag

Outgoing cosine interpolation: list interpolation flag

where K is the number of incident energies E . The flag for interpolation with respect to incident energy is one of those for probability density tables in Section 12.2.3, and that for the direction cosine μ_{lab} is one of those for simple lists. There follows K blocks of data, one for each incident energy

Ein: E : $n = N$

indicating that data are given for N pairs of values of μ_{lab} and $\pi_\mu(\mu_{\text{lab}} | E)$.

The section for conditional probability density of outgoing energy $\pi_E(E'_{\text{lab}} | E, \mu_{\text{lab}})$ gives the number K of incident energies along with the interpolation rules

EMuEpPData: $n = K$

Incident energy interpolation: probability interpolation flag

Outgoing cosine interpolation: probability interpolation flag

Outgoing energy interpolation: list interpolation flag

The flags for interpolation with respect to incident energy E and direction cosine μ_{lab} are those for probability density tables in Section 12.2.3, and that for outgoing energy E is one of those for simple lists.

For each incident energy E there is a data section of the form

Ein: E : $n = N$

indicating that data are given for N values of μ_{lab} . The block of data corresponding to a value of μ_{lab} is of the form

mu: μ_{lab} : $n = J$

followed by J pairs of values of outgoing energy E and probability density $\pi_E(E'_{\text{lab}} | E, \mu_{\text{lab}})$.

An example of this type of data with energy in MeV is given by

Angular data: $n = 13$

Incident energy interpolation: lin-lin unitbase

Outgoing cosine interpolation: lin-lin

Ein: 7.78148000e+00: $n = 5$

9.99788143e-01 5.88016882e+01

9.99841107e-01 1.03998708e+03

9.99894071e-01 1.70086214e+03

9.99947036e-01 2.60922780e+03

1.00000000e+00 2.70023193e+04

...

Ein: 2.00000000e+02: $n = 5$

-1.00000000e+00 3.26136085e-01

```

-5.00000000e-01 3.82892835e-01
0.00000000e+00 4.64096868e-01
5.00000000e-01 5.89499334e-01
1.00000000e+00 8.00885838e-01
EMuEpPData:  n = 13
Incident energy interpolation:  lin-lin unitbase
Outgoing cosine interpolation:  lin-lin unitbase
Outgoing energy interpolation:  lin-lin
Ein:  7.78148000e+00:  n = 5
mu:   9.99788143e-01:  n = 4
      2.35390141e-03 1.62759930e+05
      2.35697064e-03 1.62877493e+05
      2.35697074e-03 1.62877496e+05
      2.36004196e-03 1.62892892e+05
mu:   9.99841107e-01:  n = 16
      2.30884914e-03 9.56657064e+03
      2.32094195e-03 9.99310479e+03
      etc.
Ein:   2.00000000e+02:  n = 5
mu:   -1.00000000e+00:  n = 501
      1.00000000e-18 5.38736174e-10
      1.00563208e-17 1.70842412e-09
      1.91126417e-17 2.35524717e-09
      2.81689625e-17 2.85931206e-09
      3.72252834e-17 3.28696542e-09
...
mu:   1.00000000e+00:  n = 993
      1.00000000e-18 2.19383712e-10
      7.55831305e-18 6.03138181e-10
      ...
      1.32751551e+01 1.88436981e-03
      1.38015128e+01 1.90038969e-03

```

10 Formulas for double-differential energy-angle data

This section explains the coding used to treat two representations by formula for double-differential energy-angle data in the GND library, the Kalbach-Mann formula and the phase-space model. The Kalbach-Mann model is described first, because it is used so often in GND.

10.1 The Kalbach-Mann model for double-differential data

In the Kalbach-Mann representation [12] the double differential probability density is of the form

$$\pi(E'_{\text{cm}}, \mu_{\text{cm}} | E) = \pi_E(E'_{\text{cm}} | E) \pi_\mu(\mu_{\text{cm}} | E'_{\text{cm}}, E), \quad (10.1)$$

where E is the energy of the incident particle in laboratory coordinates and E'_{cm} and μ_{cm} are the energy and cosine of the outgoing particle in center-of-mass coordinates. The values of the probability density $\pi_E(E'_{\text{cm}} | E)$ for outgoing energy E'_{cm} are given as a table with normalization

$$\int_0^\infty dE'_{\text{cm}} \pi_E(E'_{\text{cm}} | E) = 1.$$

In Eq. (10.1) the function $\pi_\mu(\mu_{\text{cm}} | E'_{\text{cm}}, E)$ is an exponential in μ_{cm} depending on parameters a and r [12],

$$\pi_\mu(\mu_{\text{cm}} | E'_{\text{cm}}, E) = \frac{1}{C} [\cosh(a\mu_{\text{cm}}) + r \sinh(a\mu_{\text{cm}})]. \quad (10.2)$$

The value of r in Eq. (10.2) depends on the incident and outgoing energies E and E'_{cm} and is given in a data table. The formula Eq. (10.2) represents a pre-equilibrium model, with $r = 0$ representing complete equilibrium and $r = 1$ no equilibrium at all. It is therefore always true that

$$0 \leq r \leq 1.$$

The value of C in Eq. (10.2) is chosen to ensure the normalization

$$\int_{-1}^1 d\mu_{\text{cm}} \pi_\mu(\mu_{\text{cm}} | E'_{\text{cm}}, E) = 1.$$

That is, take

$$C = \frac{2 \sinh a}{a}.$$

10.1.1 The Kalbach-Mann a parameter

The values of the parameter a in Eq. (10.2) may be given as a table depending on the incident energy E and on E'_{cm} , the center-of-mass kinetic energy of the outgoing particle. It is more common, however, to use the formula for a as a function of E as found in the references [12] and [7]. The details are repeated here for the sake of completeness.

Some special notation is used in this subsection. The reaction is of the form

$$A + a \rightarrow C \rightarrow B + b, \quad (10.3)$$

where

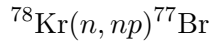
- A : the target with mass m_{targ} , assumed to be at rest in the laboratory frame,
- a : the incident particle with mass m_{yi} ,
- C : the compound nucleus,
- B : the residual nucleus with mass m_{res} ,
- b : the emitted particle with mass m_{yo} .

Several energies are needed, all measured in MeV,

- $E_{a,\text{lab}}$: energy of the incident particle in the laboratory frame,
- $E_{a,\text{cm}}$: energy of the incident particle in the center-of-mass frame,
- $E_{A,\text{cm}}$: energy of the target in the center-of-mass frame,
- $E_{aA,\text{cm}}$: $E_{a,\text{cm}} + E_{A,\text{cm}} = m_{\text{targ}} E_{a,\text{lab}} / (m_{\text{targ}} + m_{\text{yi}})$,
- $E_{b,\text{cm}}$: energy of the outgoing particle in the center-of-mass frame,
- $E_{bB,\text{cm}}$: $(m_{\text{res}} + m_{\text{yo}}) E_{b,\text{cm}} / m_{\text{yo}}$.

Note that the quantity $E_{bB,\text{cm}}$ is the total kinetic energy of B and b if the breakup of C is a discrete 2-body reaction with the excitation level of B unspecified.

For a reaction with several outgoing particles, b in Eq. (10.3) is the particle corresponding to the current data, and B is the residual following the emission of b from the compound nucleus C . Thus, for the



reaction, one uses

$$B = ^{78}\text{Kr}$$

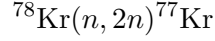
in the computation of $a(E, E_{b,\text{cm}})$ with Kalbach-Mann data for the outgoing neutron, while

$$B = ^{78}\text{Br}$$

with outgoing proton data. Analogously, use

$$B = ^{78}\text{Kr}$$

in the computation of $a(E, E_{b,\text{cm}})$ with Kalbach-Mann neutron data for the



reaction.

For massive incident particles, the value of $a(E, E_{b,\text{cm}})$ is given by the expression

$$a(E, E_{b,\text{cm}}) = C_1 X_1 + C_2 X_1^3 + C_3 M_a m_b X_3^4 \quad (10.4)$$

with terms explained below.

The coefficients in Eq. (10.4) are

$$C_1 = 0.04 \text{ MeV}^{-1}, \quad C_2 = 1.8 \times 10^{-6} \text{ MeV}^{-3}, \quad C_3 = 6.7 \times 10^{-7} \text{ MeV}^{-4}.$$

The values of X_1 and X_3 in Eq. (10.4) depend on the energies S_a and S_b of the capture and breakup reactions in Eq. (10.3). For the target define

$$\begin{aligned} Z_A &: \text{ number of protons in the target nucleus,} \\ N_A &: \text{ number of neutrons in the target nucleus,} \\ A_A &: Z_A + N_A. \end{aligned}$$

Corresponding Z_C , N_C , and A_C are defined for the compound nucleus C and Z_B , N_B , and A_B for the residual nucleus B . For the capture reaction, S_a is taken as

$$\begin{aligned} S_a = & 15.68(A_C - A_A) - 28.07 \left(\frac{(N_C - Z_C)^2}{A_C} - \frac{(N_A - Z_A)^2}{A_A} \right) - \\ & 18.56(A_C^{2/3} - A_A^{2/3}) + 33.22 \left(\frac{(N_C - Z_C)^2}{A_C^{4/3}} - \frac{(N_A - Z_A)^2}{A_A^{4/3}} \right) - \\ & 0.717 \left(\frac{Z_C^2}{A_C^{1/3}} - \frac{Z_A^2}{A_A^{1/3}} \right) + 1.211 \left(\frac{Z_C^2}{A_C} - \frac{Z_A^2}{A_A} \right) - I_a. \end{aligned} \quad (10.5)$$

Here, I_a is the breakup energy for the incident particle as given in Table 10.1. The energy S_b corresponding to the second reaction in Eq. (10.3) is obtained from Eq. (10.5) with Z_A , N_A , A_A , and I_a replaced, respectively by Z_B , N_B , A_B , and I_b .

The quantities X_1 and X_3 in Eq. (10.4) are obtained by setting

$$\begin{aligned} \mathbf{E}_a &= E_{aA,\text{cm}} + S_a, & \mathbf{E}_b &= E_{bB,\text{cm}} + S_b, \\ E_{t1} &= 130 \text{ MeV}, & E_{t3} &= 41 \text{ MeV}, \\ R_1 &= \min(\mathbf{E}_a, E_{t1}), & R_3 &= \min(\mathbf{E}_a, E_{t3}), \\ X_1 &= R_1 \mathbf{E}_b / \mathbf{E}_a, & X_3 &= R_3 \mathbf{E}_b / \mathbf{E}_a. \end{aligned}$$

Finally the values M_a for the incident particle and m_b for the outgoing particle in the last term of Eq. (10.4) are given in Table 10.2. Note that M_a is not defined for incident tritons or for incident helium-3 nuclei, so that the Kalbach-Mann model is not applicable when the incident energy of such particles is so large that $\mathbf{E}_a > E_{t3}$.

Table 10.1: Breakup energies for incident and outgoing particles in MeV

particle	I_a or I_b
n	0
p	0
d	2.22
t	8.48
${}^3\text{He}$	7.72
α	28.3

Table 10.2: Values of M_a and m_b in Eq. (10.4)

particle	M_a	m_b
n	1	1/2
p	1	1
d	1	1
t	—	1
${}^3\text{He}$	—	1
α	0	2

10.1.2 Photo-nuclear reactions

When Kalbach-Mann data are given for photo-nuclear reactions, the parameter $a(E, E_{b,\text{cm}})$ in Eq. (10.4) and the angular probability density $\pi_\mu(\mu_{\text{cm}} \mid E'_{\text{cm}}, E)$ in Eq. (10.2) are modified as in the paper [13].

One begins by computing $a_n(E, E_{b,\text{cm}})$ in Eq. (10.4) using a neutron as incident particle. Then, for the incident photon one takes

$$a(E, E_{b,\text{cm}}) = a_n(E, E_{b,\text{cm}}) \sqrt{\frac{E}{2m_n}} \min \left(4, \max \left(1, \frac{9.3}{\sqrt{E_{b,\text{cm}}}} \right) \right). \quad (10.6)$$

Here, m_n is the mass of the neutron in MeV.

For incident photons the angular probability density takes the form

$$\pi_\mu(\mu_{\text{cm}} \mid E'_{\text{cm}}, E) = \frac{1}{2} \left[(1 - r) + \left(\frac{ar}{\sinh(a)} \right) \exp \{a\mu_{\text{cm}}\} \right].$$

10.1.3 Interpolation of Kalbach-Mann data

In the GND library, the Kalbach-Mann data are given as a table of the probability density $\pi_E(E'_{\text{cm}} \mid E)$ of outgoing energy E'_{cm} for an incident particle with energy E , along with a table of values of the parameter r in Eq. (10.2) as a function of E and E'_{cm} . It is also

permitted to include a table of values $a(E, E_{b,\text{cm}})$ to be used in place of the expression in Eq. (10.4).

Because $\pi_E(E'_{\text{cm}} | E)$ is a probability density, it is to be interpolated with respect to E by one of the methods of Section 3.2. The interpolated values of r , however, must maintain the physical constraints that $0 \leq r \leq 1$, so the Kalbach-Mann r parameter is interpolated by the unscaled methods of Section 3.3. If the values of a are also given as a table, they are also interpolated as in Section 3.3.

For unit-base interpolation the method is as follows. The energy probability density $\pi_E(E'_{\text{cm}} | E)$ is first mapped to unit base as defined in equations Eqs. (3.19) and (3.20), so that

$$\hat{\pi}_E(\hat{E}'_{\text{cm}} | E) = (E'_{\text{cm,max}} - E'_{\text{cm,min}})\pi_E(E'_{\text{cm}} | E) \quad (10.7)$$

for $0 \leq \hat{E}'_{\text{cm}} \leq 1$. The scale factor in Eq. (10.7) is chosen so as to normalize the function $\hat{\pi}_E(\hat{E}'_{\text{cm}} | E)$,

$$\int_0^1 d\hat{E}'_{\text{cm}} \hat{\pi}_E(\hat{E}'_{\text{cm}} | E) = 1.$$

The values of $\hat{\pi}_E(\hat{E}'_{\text{cm}} | E)$ are interpolated linearly with respect to E .

For the values of the parameter r , the energy of the outgoing particle to is mapped $0 \leq \hat{E}'_{\text{cm}} \leq 1$ using Eq. (8.5) in the form of

$$\hat{E}'_{\text{cm}} = \frac{E'_{\text{cm}} - E'_{\text{cm,min}}}{E'_{\text{cm,max}} - E'_{\text{cm,min}}}.$$

Because of the restriction that $0 \leq r \leq 1$, the parameter r is mapped according to

$$\tilde{r}(\hat{E}'_{\text{cm}}, E) = r(E'_{\text{cm}}, E). \quad (10.8)$$

With these transformations, the number-preserving integral Eq. (2.7) takes the form

$$\mathcal{I}_{gh,\ell}^{\text{num}} = \int_{\mathcal{E}_g} dE \sigma(E) M(E) w(E) \tilde{\phi}_\ell(E) \int_{\hat{E}'_{\text{cm}}} d\hat{E}'_{\text{cm}} \hat{\pi}_E(\hat{E}'_{\text{cm}} | E) \int_{\mu_{\text{cm}}} d\mu_{\text{cm}} P_\ell(\mu_{\text{lab}}) \pi_\mu(\mu_{\text{cm}} | E'_{\text{cm}}, E), \quad (10.9)$$

and the energy-preserving integral Eq. (2.10) becomes

$$\mathcal{I}_{gh,\ell}^{\text{en}} = \int_{\mathcal{E}_g} dE \sigma(E) M(E) w(E) \tilde{\phi}_\ell(E) \int_{\hat{E}'_{\text{cm}}} d\hat{E}'_{\text{cm}} \hat{\pi}_E(\hat{E}'_{\text{cm}} | E) \int_{\mu_{\text{cm}}} d\mu_{\text{cm}} P_\ell(\mu_{\text{lab}}) \pi_\mu(\mu_{\text{cm}} | E'_{\text{cm}}, E) E'_{\text{lab}}. \quad (10.10)$$

The subscripts on μ serve to emphasize the facts that the argument μ_{lab} of the Legendre polynomial $P_\ell(\mu_{\text{lab}})$ in Eqs. (10.9) and (10.10) is the direction cosine of the outgoing particle in laboratory coordinates, while the integration variable μ_{cm} is the direction cosine in

center-of-mass coordinates. Specifically, E'_{lab} depends on E and μ_{cm} according to equation Eq. (4.8), and μ_{lab} is given by Eq. (4.9).

Because the energy probability density $\pi_E(E'_{\text{cm}} | E)$ data are given in the center-of-mass frame, the identification of the region of integration over \hat{E}'_{cm} and μ_{cm} in Eqs. (10.9) and (10.10) involves the geometric considerations presented for tabular center-of-mass data in Section 8.1. For a given incident energy E in bin \mathcal{E}_g , the regions of integration over \hat{E}'_{cm} and μ_{cm} in Eqs. (10.9) and (10.10) depend on how the domains for data interpolation $\hat{E}'_{\text{cm},j-1} \leq \hat{E}'_{\text{cm}} \leq \hat{E}'_{\text{cm},j}$ intersect the \mathcal{E}'_h outgoing laboratory energy bin. The situation for a fixed incident energy E is illustrated in Figure 8.1. The half annulus

$$E'_{\text{cm},j-1} \leq E'_{\text{cm}} \leq E'_{\text{cm},j}$$

is derived from the Kalbach-Mann data. The region of integration over μ_{cm} and E'_{cm} for fixed incident energy E is the intersection of these two half annuli, and it is shaded dark gray in Figure 8.1.

10.1.4 The input file for the Kalbach-Mann model

The data identifier in Section 12.3.1 for the Kalbach-Mann model is

Process: Kalbach spectrum

and the data are always in the center-of-mass frame

Product Frame: CenterOfMass

Currently, only a Newtonian boost to the laboratory frame is implemented.

The masses of the particles a , A , C , b , and B in the reaction Eq. (10.3) are input in Section 12.9 of the input file

Projectile's mass: m_{yi}

Target's mass: m_{targ}

Compound's mass: m_C

Product's mass: m_{yo}

Residual's mass: m_{res}

The units used for these masses are arbitrary, but they must be the same for all particles.

The number of protons Z_A and the atomic number A_A of the target are needed for the computation of S_a in Eq. (10.5). This information is entered into the input file as

$$\text{ZA}_A = 1000Z_A + A_A,$$

from which A_A , Z_A , and the number of neutrons $N_A = A_A - Z_A$ are easily computed. Corresponding numbers ZA_a for the projectile and ZA_b for the emitted particle are also given. The numbers ZA_C for the compound nucleus and ZA_B for the residual may be calculated using

$$\text{ZA}_C = \text{ZA}_A + \text{ZA}_a,$$

$$\text{ZA}_B = \text{ZA}_C - \text{ZA}_b.$$

This section of the input file is therefore

Projectile's ZA: ZA_a

Target's ZA: ZA_A

Product's ZA: ZA_b

The remainder of the input file consists of tables of $\pi_E(E'_{\text{cm}} | E)$ and the parameter r in Eq. (10.2) as functions of E and E'_{cm} . There may also be a table of values of a to be used in place of the expression Eq. (10.4).

The format for the probability density $\pi_E(E'_{\text{cm}} | E)$ is

Kalbach probabilities: $n = K$

Incident energy interpolation: probability interpolation flag

Outgoing energy interpolation: list interpolation flag

followed by K blocks of the form

Ein: E : $n = J$

with J pairs of values of E'_{cm} and $\pi_E(E'_{\text{cm}} | E)$. The flag for interpolation with respect to incident energy E is one of those for probability densities in Section 12.2.3, while that for the outgoing energy is one for simple lists.

The table for the r parameter is of the form

Kalbach r parameter: $n = K$

Incident energy interpolation: unscaled interpolation flag

Outgoing energy interpolation: list interpolation flag

followed by K blocks of the form

Ein: E : $n = J$

with J pairs of values of E'_{cm} and $r(E'_{\text{cm}}, E)$. The flag for interpolation with respect to incident energy E is one of those for unscaled Kalbach-Mann data in Section 12.2.3, while that for the outgoing energy is one for simple lists.

The format for the Kalbach-Mann a parameter is the same as that for r , with “ r ” replaced by “ a ”. *The tables for $\pi_E(E'_{\text{cm}} | E)$, r , and a must be given at the same incident energies, and at each incident energy E , the ranges of outgoing energies E' must also agree.*

An example of the content of Section 12.9 of the input file for Kalbach-Mann data is as follows. All energies are in MeV.

Product Frame: centerOfMass

masses

Projectile's mass: 1.008665

Target's mass: 56.935394

Compound's mass: 57.933276

Product's mass: 1.008665

Residual's mass: 56.935394

ZA numbers

Projectile's ZA: 1

Target's ZA: 26057

Product's ZA: 1

Kalbach-Mann probability data

Kalbach probabilities: $n = 12$

Incident energy interpolation: lin-lin unitbase

Outgoing energy interpolation: flat

```

Ein: 7.781480e+00: n = 2
    0.000000e+00 1.000000e+06
    1.000000e-06 0.000000e+00
Ein: 7.800000e+00: n = 7
    0.000000e+00 7.375605e+00
    1.473426e-03 1.472617e+01
    3.437994e-03 3.676034e+01
    7.367130e-03 5.717426e+01
    1.473426e-02 8.186549e+00
    3.437994e-02 5.948511e+00
    7.367130e-02 1.000000e-30
...
Ein: 2.000000e+01: n = 53
    0.000000e+00 2.063824e-03
    1.473426e-03 3.887721e-03
    3.437994e-03 9.245874e-03
    7.367130e-03 1.805939e-02
    1.473426e-02 3.554576e-02
    3.437994e-02 8.408804e-02
    7.367130e-02 1.261293e-01
    ...
    1.154184e+01 1.604784e-03
    1.203298e+01 1.000000e-30
# Kalbach-Mann r data
Kalbach r parameter: n = 12
Incident energy interpolation: lin-lin unscaledunitbase
Outgoing energy interpolation: flat
Ein: 7.781480e+00: n = 2
    0.000000e+00 0.000000e+00
    1.000000e-06 0.000000e+00
Ein: 7.800000e+00: n = 7
    0.000000e+00 4.272290e-02
    1.473426e-03 2.992310e-02
    3.437994e-03 1.833870e-02
    7.367130e-03 1.427320e-02
    1.473426e-02 1.829320e-02
    3.437994e-02 1.611740e-02
    7.367130e-02 1.590910e-02
...
Ein: 2.000000e+01: n = 53
    0.000000e+00 7.037570e-02
    1.473426e-03 4.957320e-02
    3.437994e-03 3.056740e-02
    7.367130e-03 2.555550e-02

```

```

1.473426e-02 1.908500e-02
...
1.154184e+01 9.548000e-01
1.203298e+01 9.656400e-01

```

10.2 The n -body phase space model

The n -body phase space model gives the probability density for the energy of an outgoing particle in center-of-mass coordinates. The formula is derived from the volume in phase space occupied by the particles, subject to the constraints of conservation of energy and momentum. The model uses Newtonian mechanics.

In the ENDF/B-VII manual [7] there are two scenarios for this model: (1) inelastic collision followed by break-up of the excited residual, and (2) break-up induced by the collision. In the first case, the n -body phase space model treats only the particles emitted in the break-up of the excited residual, not the one from the initial collision. The total kinetic energy E^* of the outgoing particles treated by the model therefore depends on the scenario.

In the case of break-up following an inelastic collision, the analysis is in the frame in which the residual from the inelastic collision is stationary. The total kinetic energy of the outgoing particles involved is then

$$E^* = Q_{\text{res}},$$

where Q_{res} is the energy of the break-up of the excited residual. In this case, the reference frame for the model is that in which the residual nucleus is stationary after the initial inelastic collision. The `merced` code currently does not implement this scenario, because this is a 2-step reaction.

For the break-up of a compound nucleus following the collision of a projectile with a stationary target in the laboratory frame, the total kinetic energy E^* of the outgoing particles in the center-of-mass frame is the sum of two components, the Q of the reaction plus the energy of the initial collision in the center-of-mass frame. For an incident particle of mass m_i and energy E in the laboratory frame hitting a stationary target of mass m_{targ} , this collision energy in the center-of-mass frame is

$$\frac{m_{\text{targ}}E}{m_{\text{yi}} + m_{\text{targ}}}.$$

Consequently, in this scenario the total center-of-mass kinetic energy for all outgoing particles is

$$E^* = Q + \frac{m_{\text{targ}}E}{m_{\text{yi}} + m_{\text{targ}}}. \quad (10.11)$$

The details of the n -body phase space model are as follows. Consider a particular outgoing particle, and suppose that its mass is m_{yo} . Then conservation of energy and momentum implies that the maximum kinetic energy of this particle in the center-of-mass frame is given by

$$E_{\text{max}} = \frac{(M_t - m_{\text{yo}})E^*}{M_t}, \quad (10.12)$$

where M_t is the total mass of the outgoing particles covered by the n -body phase space model.

Suppose that n is the number of particles resulting from the break-up reaction. For an outgoing particle with mass m_{yo} , let E_{\max} be as in Eq. (10.12). Then in the n -body phase space model, the energy probability density that this outgoing particle will have energy E'_{cm} with $0 \leq E'_{\text{cm}} \leq E_{\max}$ is given by

$$\pi_{\text{cm}}(E'_{\text{cm}} | E) = C_n \sqrt{E'_{\text{cm}}} (E_{\max} - E'_{\text{cm}})^{(3n-8)/2}. \quad (10.13)$$

Note that this probability density is isotropic in the center-of-mass frame. Furthermore, the relation Eq. (10.13) was derived using Newtonian mechanics.

The normalization constant C_n in Eq. (10.13) is best represented in terms of the beta function

$$B(\alpha, \beta) = \int_0^1 dt t^{\alpha-1} (1-t)^{\beta-1} = \frac{\Gamma(\alpha)\Gamma(\beta)}{\Gamma(\alpha+\beta)}. \quad (10.14)$$

With this notation, it is seen that

$$\frac{1}{C_n} = B\left(\frac{3}{2}, \frac{3n-6}{2}\right) E_{\max}^{(3n-5)/2}. \quad (10.15)$$

10.2.1 Geometry of the n -body phase space model

The construction of Figure 8.1 made use of the fact that the tabular data required the consideration of ranges of energy E'_{cm} of the outgoing particle between the tabulated values,

$$E'_{\text{cm},j-1} \leq E'_{\text{cm}} \leq E'_{\text{cm},j}. \quad (10.16)$$

Here, the limiting values $E'_{\text{cm},j-1}$ and $E'_{\text{cm},j}$ depend on the energy E of the incident particle according to the principles of unit-base interpolation in Eq. (8.5).

For the n -body phase space model, however, the range of center-of-mass energies of the outgoing particle is

$$0 \leq E'_{\text{cm}} \leq E_{\max}, \quad (10.17)$$

where E_{\max} is as in Eq. (10.12). That is, for the n -body phase space the annular ring Eq. (10.16) in Figure 8.1 is replaced by the interior of the semicircle Eq. (10.17).

10.2.2 Input file for the n -body phase space model

The data identifier in Section 12.3.1 for the n -body phase space model is

Process: phase space spectrum

and the data are always in the center-of-mass frame

Product Frame: CenterOfMass

Currently, only a Newtonian boost to the laboratory frame is implemented.

In the model-dependent Section 12.9 of the input file, the computation of E^* in Eq. (10.11) requires the reaction's Q value, as well as the masses m_{yi} of the projectile and m_{targ} of the target. The units used for the masses are arbitrary, but the same units

must be used for all particles. The Q value must be in the same units as the energy bins. This information is input using the commands

```
Q value:  $Q$ 
Projectile's mass:  $m_{yi}$ 
Target's mass:  $m_{targ}$ 
```

For the calculation of E_{\max} in Eq. (10.12), the mass m_{yo} is needed, along with the total mass M_t of the outgoing particles covered by the n -body phase space model. This information is input using

```
Product's mass:  $m_{yo}$ 
Total mass:  $M_t$ 
```

The units used for these masses must be the same as is used for the other particles.

Finally, the probability density in Eq. (10.13) requires the number of particles n in the model, and this is given by

```
Number of particles:  $n$ 
```

A sample Section 12.9 of the input file for the n -body phase space model is

```
Product Frame: CenterOfMass
Q value: -2.225002
Projectile's mass: 1.008665
Target's mass: 2.014102
Product's mass: 1.008665
Total mass: 3.0246030
Number of particles: 3
```

11 Data for incident gammas

The `merced` code calculates cross sections and the integrals in Eqs. (2.7) and (2.10) for computation of the transfer matrix for coherent scattering and Compton scattering. Photoemission, pair production, and triplet production are handled by `fudge`.

11.1 Coherent scattering

This reaction is the result of interaction of the incident photon with all of the electrons in the target atom and sometimes called whole-atom scattering. There is essentially no change in energy between the outgoing and incident photons. In `GND` instead of the energy E of the incident photon, the data are given in terms of x , where x is

$$x = \frac{1}{\lambda} \sin\left(\frac{\theta}{2}\right) = \frac{1}{\lambda} \sqrt{\frac{1 - \mu_{\text{lab}}}{2}}. \quad (11.1)$$

In Eq. (11.1) λ is the wave length of the incident photon given in Å. Thus, in terms of the incident energy E , the value of x is

$$x = \frac{E}{ch} \sqrt{\frac{1 - \mu_{\text{lab}}}{2}}. \quad (11.2)$$

In `merced` the values of x are scaled by ch , to convert to units of energy.

The angular differential cross section $\sigma_C(\mu_{\text{lab}} | E)$ takes the form

$$\sigma_C(\mu_{\text{lab}} | E) = \frac{3\sigma_T}{8} (1 + \mu_{\text{lab}}^2) \{ [F_F(x) + F_R(x)]^2 + F_I(x)^2 \}. \quad (11.3)$$

where the parameter σ_T is the classical Thompson scattering cross section. In Eq. (11.3) $F_F(x)$ is the coherent form factor, and it is a function of x in Eq. (11.1) The real anomalous form factor $F_R(E)$, and the imaginary anomalous form factor $F_I(E)$ are given in terms of the incident energy E . The units of $\sigma_C(\mu_{\text{lab}} | E)$ are barns per cosine. See the reference [7] for more information.

The reaction cross section is computed using

$$\sigma(E) = \int_{-1}^1 d\mu_{\text{lab}} \sigma_C(\mu_{\text{lab}} | E). \quad (11.4)$$

Because the energy is assumed to be unchanged, $E'_{\text{lab}} = E$, and because the gamma multiplicity is 1, the formula Eq. (2.2) for the kernel $K(E'_{\text{lab}}, \mu_{\text{lab}} | E)$ for coherent scattering becomes

$$K(E'_{\text{lab}}, \mu_{\text{lab}} | E) = \sigma_C(\mu_{\text{lab}} | E) w(E) \delta(E'_{\text{lab}} - E). \quad (11.5)$$

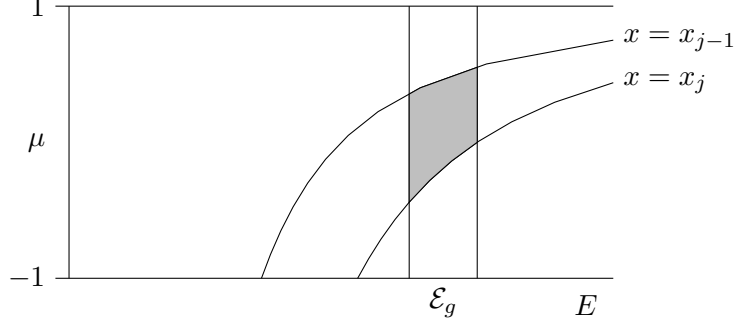


Figure 11.1: Domain of integration for whole-atom scattering

For photons it is customary to use the energy-preserving transfer matrices Eq. (2.11) derived from the integrals Eq. (2.10), so details are given only for the evaluation of Eq. (2.10). From Eq. (11.5) it is seen that

$$\mathcal{I}_{gh,\ell}^{\text{en}} = \int_{\mathcal{E}_g} dE w(E) \tilde{\phi}_\ell(E) \int_{\mathcal{E}'_h} dE'_{\text{lab}} \int_{\mu_{\text{lab}}} d\mu_{\text{lab}} P_\ell(\mu_{\text{lab}}) \sigma_C(\mu_{\text{lab}} | E) \delta(E'_{\text{lab}} - E) E'_{\text{lab}}. \quad (11.6)$$

Because both the incident particles and the outgoing particles are photons, the outgoing energy groups \mathcal{E}'_h are the same as the incident energy groups \mathcal{E}_g . Therefore, an integration over E'_{lab} in Eq. (11.6) gives the result that

$$\mathcal{I}_{gh,\ell}^{\text{en}} = 0 \quad \text{for } h \neq g$$

and

$$\mathcal{I}_{gg,\ell}^{\text{en}} = \int_{\mathcal{E}_g} dE w(E) \tilde{\phi}_\ell(E) E \int_{\mu_{\text{lab}}} d\mu_{\text{lab}} P_\ell(\mu_{\text{lab}}) \sigma_C(\mu_{\text{lab}} | E). \quad (11.7)$$

The domain of integration for Eq. (11.7) is shown in Figure 11.1. The curves for $x = x_{j-1}$ and $x = x_j$ are obtained from Eq. (11.2), and for $x_{j-1} \leq x \leq x_j$ the region of integration is bounded by these two curves and lies within the \mathcal{E}_g energy bin. This region is shaded gray in Figure 11.1.

11.1.1 A programming detail

Because of the $\sqrt{1 - \mu_{\text{lab}}}$ singularity in Eq. (11.2), the default method for evaluating integrals with respect to μ_{lab} in this section is adaptive quadrature based on first-order Gaussian quadrature for

$$\int_a^b d\mu_{\text{lab}} F(\mu_{\text{lab}}) \sqrt{1 - \mu_{\text{lab}}}. \quad (11.8)$$

This method is used for integration over μ_{lab} in Eqs. (11.4) and (11.7).

The default method for integration over incident energy E in Eq. (11.7) is second-order adaptive Gaussian quadrature.

11.1.2 The input file for coherent scattering

For coherent scattering, the reaction identifier in Section 12.3.1 is

```
Process: coherent scattering
```

and the data are always in the laboratory frame

```
Product Frame: lab
```

The quadrature methods with respect to μ_{lab} and E in Eq. (11.7) may be set independently using the commands of Section 12.5. The defaults are

```
mu quadrature method: square root
```

```
Ein quadrature method: adaptive
```

The quadrature method specified for μ_{lab} also applies to the computation of the cross section in Eq. (11.4).

In GND the values of x in Eq. (11.1) are given in units of \AA^{-1} , and the `merced` code converts x to energy using the factor `ch`. This conversion must be to the units used for the energy bin boundaries in Sections 12.3.2 and 12.3.3. The conversion factor from \AA^{-1} to energy is set as described in Section 12.7.1.

The value of the Thompson scattering cross section σ_T in Eq. (11.3) specified as discussed in Section 12.7.2.

Section 12.9 of the input file contains the information required for calculation of the differential cross section in Eq. (11.3). The values of the coherent form factor $F_F(x)$ are input using

```
Form factor: n = n
```

```
Interpolation: list interpolation flag
```

followed by n pairs of values of x and $F_F(x)$. The interpolation flag is one for simple lists as in Section 12.2.3.

The real anomalous form factor $F_R(E)$ and imaginary anomalous form factor $F_I(E)$ are input analogously

```
anomalous real form factor: n = n
```

```
Interpolation: list interpolation flag
```

followed by n pairs of values of E and $F_R(E)$, and

```
anomalous imaginary form factor: n = n
```

```
Interpolation: list interpolation flag
```

followed by n pairs of values of E and $F_I(E)$.

An input file for coherent scattering with x values to be converted from \AA^{-1} to eV is as follows.

```
Process: coherent scattering
```

```
Product Frame: lab
```

```
inverseWavelengthToEnergyFactor: 12398.4190576
```

```
ThompsonScattering: 0.6652448
```

```
# Data section
```

```
Form factor: n = 1272
```

```
Interpolation: lin-lin
```

```
0.000000000000e+00 8.000000000000e+00
```

```
1.000000000000e-03 8.000000000000e+00
```

```

5.000000000000e-03 7.997400000000e+00
6.250000000000e-03 7.995640000000e+00
7.187500000000e-03 7.994550000000e+00
...
1.000000000000e+09 7.999700000000e-29
Anomalous real form factor:  n = 253
Interpolation:  lin-lin
1.000000000000e+00 -8.001506000000e+00
3.000000000000e+00 -8.012308000000e+00
8.367019000000e+00 -7.916407000000e+00
9.300337000000e+00 -7.564924000000e+00
9.624912000000e+00 -7.096145000000e+00
...
1.000000000000e+07 -4.100212000000e-03
Anomalous imaginary form factor:  n = 255
Interpolation:  lin-lin
1.000000000000e+00 0.000000000000e+00
3.000000000000e+00 0.000000000000e+00
9.030040000000e+00 0.000000000000e+00
9.871915000000e+00 0.000000000000e+00
9.913590000000e+00 3.647675000000e-01
9.920512000000e+00 4.548976000000e-01
...
1.000000000000e+07 3.311053000000e-07

```

11.2 Compton scattering

This reaction is also called incoherent scattering, and it is the scattering of a photon by an individual bound electron. See the reference [7]. The data in **GND** give the values of the scattering factor $S_F(x)$ for discrete values of the parameter x , defined in Eq. (11.1) or, equivalently, in Eq. (11.2).

The angular differential cross section for Compton scattering, $\sigma_I(\mu_{\text{lab}} | E)$, depends on the ratio, κ , of the energy, E , of the incident photon to the rest mass, m_e , of the electron,

$$\kappa = \frac{E}{m_e}. \quad (11.9)$$

In terms of κ and x , the Compton differential cross section is

$$\sigma_I(\mu_{\text{lab}} | E) = \frac{3\sigma_T S_F(x)}{8[1 + \kappa(1 - \mu_{\text{lab}})]^2} \left[1 + \mu_{\text{lab}}^2 + \frac{\kappa^2(1 - \mu_{\text{lab}})^2}{1 + \kappa(1 - \mu_{\text{lab}})} \right]. \quad (11.10)$$

Here, σ_T is again the Thompson scattering coefficient, and the units of $\sigma_I(\mu_{\text{lab}} | E)$ are barns per unit cosine. In Eq. (11.10) the scattering factor $S_F(x)$ accounts for the deviation

from the Klein-Nishina formula due to the fact that the electrons are bound. Just as for coherent scattering, the cross section for Compton scattering is given by

$$\sigma(E) = \int_{-1}^1 d\mu_{\text{lab}} \sigma_I(\mu_{\text{lab}} | E). \quad (11.11)$$

The calculation in `merced` of the energy E'_{lab} of the outgoing photon from Compton scattering is actually inconsistent. On the one hand, the formula Eq. (11.10) for the differential cross section takes into account the fact that the scattering is from bound electrons. For the computation of E'_{lab} , however, the approximation is made that the electron is initially free and stationary. This is a discrete two-body reaction, and conservation of energy and momentum yields the result that

$$E'_{\text{lab}} = \frac{E}{1 + \kappa(1 - \mu_{\text{lab}})}. \quad (11.12)$$

Therefore, for Compton scattering the kernel $K(E'_{\text{lab}}, \mu_{\text{lab}} | E)$ in Eq. (2.2) takes the form

$$K(E'_{\text{lab}}, \mu_{\text{lab}} | E) = w(E) \sigma_I(\mu_{\text{lab}} | E) \delta \left(E'_{\text{lab}} - \frac{E}{1 + \kappa(1 - \mu_{\text{lab}})} \right). \quad (11.13)$$

Upon inserting the kernel Eq. (11.13) into Eq. (2.10), the computation of energy-preserving transfer matrices for Compton scattering requires evaluation of the integrals

$$\begin{aligned} \mathcal{I}_{gh,\ell}^{\text{en}} = \int_{\mathcal{E}_g} dE w(E) \int_{\mathcal{E}'_h} dE'_{\text{lab}} \int_{\mu_{\text{lab}}} d\mu_{\text{lab}} P_\ell(\mu_{\text{lab}}) \sigma_I(\mu_{\text{lab}} | E) \tilde{\phi}_\ell(E) \\ \delta \left(E'_{\text{lab}} - \frac{E}{1 + \kappa(1 - \mu_{\text{lab}})} \right) E'_{\text{lab}}. \end{aligned} \quad (11.14)$$

After integrating over E'_{lab} , it is found that

$$\mathcal{I}_{gh,\ell}^{\text{en}} = \int_{\mathcal{E}_g} dE E w(E) \tilde{\phi}_\ell(E) \int_{\mu_{\text{lab}}} d\mu_{\text{lab}} \frac{P_\ell(\mu_{\text{lab}}) \sigma_I(\mu_{\text{lab}} | E)}{1 + \kappa(1 - \mu_{\text{lab}})}. \quad (11.15)$$

As in coherent scattering, the default quadrature method for integration with respect to μ_{lab} in Eqs. (11.11) and (11.15) is first-order Gaussian quadrature for the weighted integral Eq. (11.8).

Because of the relation Eq. (11.12) between the energies of the incident and outgoing photons, the range of integration in Eq. (11.15) has an extra degree of complexity in comparison with Eq. (11.7). In particular, the presence of the δ -function in Eq. (11.14) constrains E and μ_{lab} so that E'_{lab} is in the \mathcal{E}'_h energy bin. Figure 11.2 shows the geometry in the case of down-scattering by one energy group, $\mathcal{E}'_h = \mathcal{E}'_{g-1}$. In Figure 11.2 the curves delimiting the \mathcal{E}'_h were obtained by rewriting the energy condition Eq. (11.12) in the form

$$E = \frac{E'_{\text{lab}}}{1 - (1 - \mu_{\text{lab}})E'_{\text{lab}}/m_e}$$

and taking the top and bottom of the \mathcal{E}'_h energy bin as values of E'_{lab} . The range of integration in Eq. (11.15) is the overlap of the three regions (1) that determined by the interval $x_i \leq x \leq x_{i+1}$ of scattering factor data values, (2) the incident energy bin E in \mathcal{E}_g , and (3) the outgoing energy bin E'_{lab} in \mathcal{E}'_h .

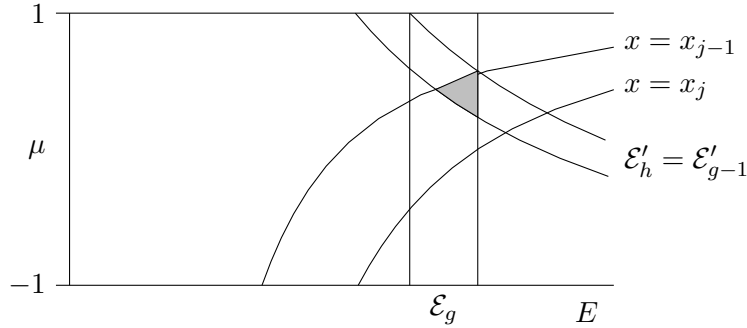


Figure 11.2: Domain of integration for Compton scattering

11.2.1 The input file for Compton scattering

The reaction identifier in Section 12.3.1 for Compton scattering is

Process: Compton scattering

and the data is always in the laboratory frame

Product Frame: lab

This default quadrature methods with respect to μ_{lab} and E in Eq. (11.15) are

mu quadrature method: square root

Ein quadrature method: adaptive

The quadrature method specified for μ_{lab} also applies to the computation of the cross section in Eq. (11.11). It is possible to override these choices as explained in Section 12.5.

As in coherent scattering, the values of x used for Compton scattering in GND are in units of \AA^{-1} , so these are converted to energy units as in Section 12.7.1. This conversion must be to the units used for the energy bin boundaries in Sections 12.3.2 and 12.3.3.

Specification of the Thompson scattering cross section σ_T in Eq. (11.10) is as in Section 12.7.2. The value m_e of the rest mass of the electron used in Eq. (11.9) is set as in Section 12.7.3, and it must be given in the units used for the energy bin boundaries.

Section 12.9 of the input file contains the value of the scattering factor $S_F(x)$ for various values of x . The format is

ScatteringFactorData: n = n

Interpolation: list interpolation flag

followed by n pairs of values of x and $S_F(x)$. The interpolation flag is one for simple lists as in Section 12.2.3.

An input file for Compton scattering with units of x to be converted from \AA^{-1} to eV is as follows.

Process: Compton scattering

Product Frame: lab

inverseWavelengthToEnergyFactor: 12398.4190576

ThompsonScattering: 0.6652448

Electron mass: 511000

```

ScatteringFactorData:  n = 453
Interpolation:  lin-lin
    0.000000000000e+00  0.000000000000e+00
    1.000000000000e-07  1.100000000000e-12
    1.059602649007e-07  1.235033551160e-12
    1.126760563380e-07  1.396548303908e-12
    1.163636363636e-07  1.489454545455e-12
    ...
    1.000000000000e+09  8.000000000000e+00

```

12 Usage of merced

The command to run `merced` is

```
merced [-inputOption] InputFile
```

The input options are described in Section 12.4 below. Most of them may be specified either in the input file or on the command line, and command line options override those given in the input file. For example, to get output with 9 significant figures, the command line could be

```
getTransferMatrix -datafield_precision 9 InputFile
```

Alternatively, one may insert the line

```
datafield_precision: 9
```

into the input file. Note the presence of the colon in this line. The format for identification of data in the input file is

```
data identifier: value
```

For most types of data, the units of energy are arbitrary, but they must be consistent. In particular, rest masses of particles must be in the same units as the energy bins. As mentioned in the individual sections on the data, some models require that energies be given in MeV.

12.1 Output file

The default name of the output file is `utfil`. It may be changed on the command line with

```
-output OutputFile
```

It may also be changed with the line

```
output: OutputFile
```

in the input file.

12.2 Form of the input file

The first line of the input file must be

```
xndfgenTransferMatrix: version 1.0
```

This line is followed by information common to all data models. The file closes with data specific to the particular data model. Blank lines are ignored.

12.2.1 Comments

Comments may be included in the input file in either of two forms.

```
Comment: This comment is printed to the output file.
```

On a line, anything after a pound sign is ignored.

For example, the input file usually contains a comment identifying the particles involved in the reaction, e.g.,

```
Comment:  n1 + C12 --> n1 + C12 outgoing data for n1
```

12.2.2 Parallel computing

The `merced` code may be compiled to run in parallel if `OpenMP` is available on your computer. In fact, the default `Makefile` uses `OpenMP`. Compile with `Makefile_serial` to obtain serial code.

For the parallel code, the number of threads is set to n by the line

```
num_threads: n
```

in the input file. The default is $n = 0$, which causes the computer to choose the number of threads. If the specified n is larger than the number of available threads, then the code runs on the threads available.

The parallel code may be forced to run in serial mode by the command line option

```
-num_threads 1
```

or by inclusion of

```
num_threads: 1
```

in the input file.

12.2.3 Interpolation flags

The identifiers for the standard interpolation methods given in Section 3.1 are

```
flat for histograms  
lin-lin for linear-linear  
lin-log for linear-log  
log-lin for log-linear  
log-log for log-log
```

The identifiers are incorporated in different ways into the interpolation flags for simple lists such as reaction cross sections, for probability densities, and for the Kalbach-Mann r and a parameters. The complete identifiers for the interpolation of the various types of tabulated data are as follows.

Interpolation flags for simple lists

For simple lists of data such as $\{E, M\}$ for particle multiplicity M at incident energy E , the interpolation flags are

```
Interpolation: identifier
```

with one of the identifiers above. For example, the command

```
Interpolation: lin-lin
```

specifies linear-linear interpolation.

Interpolation flags for probability densities

For probability density tables

$$\{x, y, \pi(y | x)\}, \quad (12.1)$$

the interpolation method with respect to x as discussed in Section 3.2 is identified by

`x interpolation: identifier interpolation-flag`

where the identifier is one of those for simple lists and the interpolation flag here is one of

`direct` for direct interpolation with extrapolation

`unitbase` for unit-base interpolation

`cumulativepoints` for interpolation by cumulative points

Thus, a table of probability densities of outgoing energies $\pi(E' | E)$ may be marked

`Incident energy interpolation: lin-lin cumulativepoints`

to indicate that interpolation with respect to incident energy E is to be done using linear-linear cumulative points as in Section 3.2.3.

The method for interpolation of the data in Eq. (12.1) with respect to y is specified by

`y interpolation: identifier`

with an identifier as in a simple list. For example, the command

`Outgoing energy interpolation: flat`

specifies histogram interpolation with respect to the energy of the outgoing particle.

Interpolation flags for unscaled interpolation of Kalbach-Mann data

The methods of interpolation of tables for the Kalbach-Mann parameters $r(E', E)$ and $a(E', E)$ with respect to the energy E of the incident particle are discussed in Section 3.3. The options for interpolation flags are

`Incident energy interpolation: identifier unscaleddirect`

`Incident energy interpolation: identifier unscaledunitbase`

`Incident energy interpolation: identifier unscaledcumulativepoints`

where the identifier is one of those for simple lists. For example, the command denoting linear-linear unscaled unit-base interpolation with respect to incident energy is

`Incident energy interpolation: lin-lin unscaledunitbase`

The method for interpolation of tables of Kalbach-Mann r and a parameters with respect to outgoing energy E is specified by

`Outgoing energy interpolation: identifier`

with an identifier as in a simple list. For example, the comand

`Outgoing energy interpolation: flat`

specifies histogram interpolation with respect to the energy of the outgoing particle.

12.3 Information used by all data models

The following information is required, but the order is arbitrary.

12.3.1 The data model

Identification of the data model.

Process: Identifier of the type of data

These identifiers are specified in the previous sections.

12.3.2 Incident energy groups

The boundaries of the incident energy groups.

Projectile's group boundaries: $n = n$

This is followed by the n values the incident energy bin boundaries. Thus, in units of eV this section may take the form

Projectile's group boundaries: $n = 88$

```
1.306800000000e-03 2.090800000000e-02 1.306800000000e-01
3.345300000000e-01 1.176100000000e+00 2.090800000000e+00
...
2.000000000000e+07
```

12.3.3 Outgoing energy groups

The boundaries of the outgoing energy groups.

Product's group boundaries: $n = n$

This is followed by the n values the outgoing energy bin boundaries. The units must be the same as for the incident energy groups. A sample input given in eV is

Product's group boundaries: $n = 88$

```
1.306800000000e-03 2.090800000000e-02 1.306800000000e-01
3.345300000000e-01 1.176100000000e+00 2.090800000000e+00
...
2.000000000000e+07
```

12.3.4 Frames of reference

The energy E of the incident particle must be given in the laboratory frame, as indicated by the command

Projectile Frame: `lab`

For the outgoing particle, the energy E' and direction cosine μ may be given in the laboratory frame with

Product Frame: `lab`

or the center-of-mass frame as

Product Frame: `CenterOfMass`

12.3.5 Relativistic kinetics

For discrete 2-body reactions, the code may use either Newtonian or relativistic mechanics in its computations. The command to control this option is

kinetics: `Newtonian`

or

kinetics: relativistic

The default is **Newtonian** except when the emitted particle is a gamma.

12.3.6 Approximate flux

The Legendre coefficients $\tilde{\phi}_\ell(E)$ used as weights in the integrals Eqs. (2.7) and (2.10).

Fluxes: n = n

Interpolation: interpolation flag

Here, n is the number of incident energies E , and the interpolation flag is one of those for simple lists, Section 12.2.3. Note that because of the scaling performed in Eqs. (2.8) and (2.11), the units of $\tilde{\phi}_\ell(E)$ are arbitrary, but barns are most common. The computed transfer matrix is unchanged if $\tilde{\phi}_\ell(E)$ is multiplied by a constant.

For each incident energy, the input file has a block specifying the Legendre coefficients given as

Ein: E: n = n

and $\tilde{\phi}_\ell(E)$ for $n = 0, 1, \dots, n-1$. The incident energy E must be in the same units as the energy groups. The number of Legendre coefficients given here need not be consistent with the Legendre order L of the computed transfer matrix as specified in Section 12.4.1. If $n-1 < L$, then the **merced** code sets

$$\tilde{\phi}_\ell(E) = \tilde{\phi}_{n-1}(E) \quad \text{for } \ell = n, n+1, \dots, L.$$

A sample input with E in eV and with all Legendre coefficients the same is

Fluxes: n = 2

Interpolation: lin-lin

Ein: 0: n = 1

8.500000000000e+01

Ein: 2.100000000000e+07: n = 1

8.500000000000e+01

12.3.7 Reaction cross section

As explained in Section 11, the cross sections for coherent photon scattering and Compton scattering are computed from the data. Reaction cross sections are required for all other data models.

Cross section: n = n

Interpolation: interpolation flag

Here, n is the number of pairs $\{E, \sigma(E)\}$, and the interpolation flag is one of those for simple lists, Section 12.2.3. This is followed by n pairs of incident energy E and reaction cross section $\sigma(E)$.

A sample of such data with energies in MeV is given by

Cross section: n = 22

Interpolation: lin-lin

7.78148000e+00 0.00000000e+00

```

7.80000000e+00 4.40157000e-04
8.00000000e+00 1.13781000e-02
8.50000000e+00 6.96097100e-02
...
2.00000000e+01 9.17094100e-01

```

12.3.8 Multiplicity

The multiplicity of the outgoing particle must be given if it is different from 1. The format is

```

Multiplicity:  n = n
Interpolation: interpolation flag

```

followed by n pairs $\{E, M(E)\}$. The interpolation flag is one of those for simple lists, Section 12.2.3. The units of incident energy E must be the same as for the energy groups. For example, with E in MeV, an $(n, 2n)$ reaction would typically have

```

Multiplicity:  n = 2
Interpolation: flat
0.0 2.0
20.0 2.0

```

12.3.9 Model weight

The model weight $w_r(E)$ is used in the formation of the reaction kernel $\mathcal{K}_r(E', \mu | E)$ in Eq. (2.2) and is discussed in Section 2. Its value is usually 1 over the entire range of incident energies in the cross section data. If this is not the case, then the model weight is input as

```

Weight:  n = n
Interpolation: flat

```

followed by n pairs $\{E, w(E)\}$. For example, the weight

$$w(E) = \begin{cases} 0 & \text{for } 0 \leq E < 6, \\ 1 & \text{for } 6 \leq E \leq 20, \end{cases}$$

may be specified using the input

```

Weight:  n = 3
Interpolation: flat
0.0 0.0
6.0 1.0
20.0 1.0

```

12.4 Optional flags, output information

The following options control the output of `merced`. All of them may also be input as command line options.

12.4.1 Legendre order of the output

The Legendre order of the matrices Eqs. (2.7) and (2.10) computed by `merced` is set by the command

```
outputLegendreOrder:  n = L
```

The default is $L = 3$.

12.4.2 Numerical precision of the output

The number of significant figures for the output data is set by

```
datafield_precision:  n = n
```

The default is $n = 8$.

12.4.3 Conservation flag

This flag determines whether the `merced` code computes integrals Eq. (2.7) for the number-conserving transfer matrix, integrals Eq. (2.10) for the energy-conserving matrix, or both. The options are

```
Conserve:  number
```

for the integrals Eq. (2.7)

```
Conserve:  energy
```

for the integrals Eq. (2.10)

```
Conserve:  both
```

for the both integrals. The default is `both` for most types of data.

12.4.4 Consistency check

If the integrals Eq. (2.7) for the number-preserving transfer matrix are computed, it is possible to check the consistency as in Eq. (2.9). With the option

```
check_row_sum:  true
```

both sides of Eq. (2.9) are printed, along with their differences and relative differences. This information is not printed if the option is `false`. The default is `false`.

To scale the integrals Eq. (2.7) so as to enforce the identity Eq. (2.9), use the option

```
scale_rows:  true
```

In this case, the integrals Eq. (2.10) are also scaled. The default is `true`, scale the integrals.

12.5 Optional inputs, quadrature methods

For the integrals Eqs. (2.7) and (2.10) and their equivalents in the center-of-mass frame, the quadrature methods may be set by commands of the form

```
Variable quadrature method: Method
```

The ‘Variable’ in this line is any of the following.

`Ein` for integrals with respect to incident energy E ,

`Eout` for integrals with respect to outgoing energy E'_{lab} or E'_{cm} ,

`mu` for integrals with respect to direction cosine μ_{lab} or μ_{cm} .

- Omission of this parameter gives the same quadrature method for all integrals. The options for the ‘Method’ in the command to set the quadrature method are

- adaptive** for adaptive 2nd-order Gaussian quadrature,
- square root** for adaptive 1st-order Gaussian quadrature with weight $\sqrt{1-\mu}$,
- Gauss2** for non-adaptive 2nd-order Gaussian quadrature,
- Gauss4** for non-adaptive 4th-order Gaussian quadrature,
- Gauss6** for non-adaptive 6th-order Gaussian quadrature.

The default for most data models is

```
quadrature method: adaptive
```

to use adaptive 2nd-order Gaussian quadrature for all integrals. The exceptions are

```
mu quadrature method: square root
```

for the integrals over direction cosine μ_{lab} with data for coherent scattering and Compton scattering. The non-adaptive options are primarily used in debugging.

12.6 Optional inputs, numerical tolerances

The user may reset the tolerances for convergence of the adaptive quadrature and for determination of the equality of two floating-point numbers.

12.6.1 Convergence of adaptive quadrature

The adaptive quadrature routine produces an estimate \mathcal{I} of the integral, along with an estimate $e_{\mathcal{I}}$ of the error. The process of successive subdivision stops when

$$|e_{\mathcal{I}}| < \epsilon_a + \epsilon_r |\mathcal{I}|.$$

The absolute quadrature tolerance is set by the command

```
abs_quad_tol:  $\epsilon_a$ 
```

The default is $\epsilon_a = 1.0\text{e-}8$. To set the relative quadrature tolerance, use

```
quad_tol:  $\epsilon_r$ 
```

The default is $\epsilon_r = 1.0\text{e-}4$.

There is also a limit on the total number of intervals used in adaptive quadrature

```
max_divisions: n = n
```

If this limit is exceeded, the adaptive quadrature routine returns the current estimate and prints a warning that this result may be inaccurate.

12.6.2 Near equality of floating-point numbers

In comparisons of floating-point numbers x_1 and x_2 , the code treats them as essentially equal if

$$|x_1 - x_2| \leq \delta_a + \delta_r \min(|x_1|, |x_2|).$$

Here, the absolute tolerance δ_a is set by

```
abs_tol:  $\delta_a$ 
```

The default value is $\delta_a = 2.0\text{e-}14$ and is appropriate when energies are measured in MeV.

It should be scaled accordingly, when other energy units are used. The relative tolerance δ_r is set using

`E_tol: δ_r`

The default value is $\delta_r = 1.0\text{e-}9$.

12.7 Physical constants

The coding for coherent photon scattering and Compton scattering discussed in Section 11 requires the values of several physical constants. These are input as follows.

12.7.1 Conversion from \AA^{-1} to energy

In order to convert the energy of photons from inverse wavelength to energy, multiply by ch . This parameter is set by the command

`inverseWaveLengthToEnergyFactor: ch` .

12.7.2 Thompson scattering cross section

The Thompson scattering cross section σ_T in Eqs. (11.3) and (11.10) is set by

`ThompsonScattering: σ_T`

The default value is $\sigma_T = 0.6652448$ barns.

12.7.3 Electron rest mass

The rest mass m_e of the electron in Eq. (11.9) is set by the command

`electron mass: m_e` .

12.7.4 Neutron rest mass

The rest mass of the neutron m_n is used in Eq. (10.6) by the Kalbach-Mann model of photo-nuclear reactions. Its units are MeV, and its value is set by the command

`m_neutron: m_n`

Its default value is $m_n = 939.565653471$ MeV.

12.8 Errors and warning messages

These options control the printing of informational messages, warnings, and fatal errors. To set which messages are printed, use the command

`message_level: $n = n$`

The effect of this option is:

$$\text{message_level} = \begin{cases} 0 & \text{print all messages,} \\ 1 & \text{print only warnings and errors,} \\ 2 & \text{print only severe errors; these cause exits anyway.} \end{cases}$$

The default value is 0, print all messages.

It is also possible to turn off all messages with the command

`skip_logging: true`

The default value is `false`.

12.9 Model-dependent information

The remainder of the input file consists of data required by the model.

A Relativistic 2-body problems

In this appendix, relativistic 2-body mechanics is examined from the point of view of computational physics. That is, the subtraction nearly equal numbers is avoided as much as is possible. The analysis starts with a collision of an incident particle with a stationary target. This determines the mapping between the laboratory frame and the center-of-mass frame. The appendix closes with a discussion of emission after the reaction.

As is customary in discussions of relativity, the units are such that the speed of light has the value $c = 1$.

A.1 Initial collision

For this appendix, E is the total energy of a system and p its total momentum. Thus, for a particle with rest mass m_0 and kinetic energy T , it follows that $E = m_0 + T$. *The convention $c = 1$ implies that the data must be such that particle rest masses and kinetic energies must be given in the same units.* The analysis makes repeated use of the invariance under Lorentz transformations of the quantity

$$S_0 = E^2 - p^2. \quad (\text{A.1})$$

If the system is a single particle in a frame in which the particle is stationary, then $S_0 = m_0^2$. Consequently, for a single particle in any frame Eq. (A.1) takes the form

$$m_0^2 = (m_0 + T)^2 - p^2, \quad (\text{A.2})$$

or

$$p^2 = 2m_0T + T^2. \quad (\text{A.3})$$

When it is desired to solve Eq. (A.3) for T corresponding to a known value of p^2 , it is recommended to use the formula

$$T = \frac{p^2}{m_0 + \sqrt{m_0^2 + p^2}}. \quad (\text{A.4})$$

The relation Eq. (A.4) is computationally more reliable than the more obvious solution of the quadratic equation Eq. (A.3)

$$T = -m_0 + \sqrt{m_0^2 + p^2}.$$

Consider the application of Eq. (A.1) to the system consisting of a moving incident particle and a target at rest in the laboratory frame. Suppose that the incident particle

has rest mass m_i and kinetic energy $T_{i,\text{lab}}$, and let m_t be the rest mass of the target. Then it follows from Eq. (A.3) that the initial laboratory-frame momentum is given by

$$p_{i,\text{lab}}^2 = 2m_i T_{i,\text{lab}} + T_{i,\text{lab}}^2. \quad (\text{A.5})$$

Consequently, for the system of consisting of the two particles in the laboratory frame, the energy-momentum invariant is

$$S = (m_t + m_i + T_{i,\text{lab}})^2 - (2m_i T_{i,\text{lab}} + T_{i,\text{lab}}^2),$$

This expression simplifies to

$$S = (m_i + m_t)^2 + 2m_t T_{i,\text{lab}}. \quad (\text{A.6})$$

The value of S must be the same when this system of two particles is considered in the center-of-mass frame. Denote the center-of-mass kinetic energy of the incident particle by $T_{i,\text{cm}}$ and its momentum by $p_{i,\text{cm}}$. Similarly, let the target have center-of-mass kinetic energy $T_{t,\text{cm}}$, and its momentum is $-p_{i,\text{cm}}$. The energy-momentum invariant for the system is therefore

$$S = (m_i + T_{i,\text{cm}} + m_t + T_{t,\text{cm}})^2, \quad (\text{A.7})$$

the square of the total energy of the system in the center-of-mass frame. By using Eq. (A.2) on each of the particles, it is possible to rewrite this as

$$S = \left(\sqrt{m_i^2 + p_{i,\text{cm}}^2} + \sqrt{m_t^2 + p_{i,\text{cm}}^2} \right)^2.$$

Upon solving this equation for $p_{i,\text{cm}}^2$, it is found that

$$p_{i,\text{cm}}^2 = \frac{[S - (m_i^2 + m_t^2)]^2 - 4m_i^2 m_t^2}{4S}. \quad (\text{A.8})$$

An expression for $p_{i,\text{cm}}^2$ in terms of the laboratory incident kinetic energy $T_{i,\text{lab}}$ is obtained by substituting in Eq. (A.8) the value of S given by Eq. (A.6),

$$p_{i,\text{cm}}^2 = \frac{m_t^2 (2m_i T_{i,\text{lab}} + T_{i,\text{lab}}^2)}{(m_t + m_i)^2 + 2m_t T_{i,\text{lab}}}. \quad (\text{A.9})$$

It follows from Eq. (A.3) that this equation may also be written as

$$p_{i,\text{cm}}^2 = \frac{m_t^2 p_{i,\text{lab}}^2}{(m_t + m_i)^2 + 2m_t T_{i,\text{lab}}}.$$

A.2 Mapping between frames

Consider a coordinate system in which the momentum $p_{i,\text{lab}}$ of the incident particle is in the direction of the first spatial axis. The boost from the laboratory to the center-of-mass frame then takes the form

$$(E_{\text{cm}}, p_{\text{cm}})^T = R(E_{\text{lab}}, p_{\text{lab}})^T$$

with the matrix

$$R = \begin{bmatrix} \cosh \chi & -\sinh \chi & 0 & 0 \\ -\sinh \chi & \cosh \chi & 0 & 0 \\ 0 & 0 & 1 & 0 \\ 0 & 0 & 0 & 1 \end{bmatrix}. \quad (\text{A.10})$$

Upon applying the rotation Eq. (A.10) to the target, it is found that

$$\begin{bmatrix} m_t + T_{t,\text{cm}} \\ -|p_{i,\text{cm}}| \\ 0 \\ 0 \end{bmatrix} = R \begin{bmatrix} m_t \\ 0 \\ 0 \\ 0 \end{bmatrix}.$$

It follows that

$$\sinh \chi = \frac{|p_{i,\text{cm}}|}{m_t}. \quad (\text{A.11})$$

By using Eq. (A.9), one may conclude that

$$\sinh \chi = \frac{\sqrt{2m_i T_{i,\text{lab}} + T_{i,\text{lab}}^2}}{\sqrt{(m_t + m_i)^2 + 2m_t T_{i,\text{lab}}}}. \quad (\text{A.12})$$

Note that except for incident gammas, $T_{i,\text{lab}}$ is much smaller than the rest mass m_i , so that χ is a small, positive number.

In the next section of this appendix, for 2-body problems the center-of-mass energy and momentum of the emitted particle and residual are determined. In order to boost these 4-vectors to the laboratory frame, one may use the inverse of the matrix R in Eq. (A.10), so that

$$(E_{\text{lab}}, p_{\text{lab}})^T = R^{-1}(E_{\text{cm}}, p_{\text{cm}})^T \quad (\text{A.13})$$

with

$$R^{-1} = \begin{bmatrix} \cosh \chi & \sinh \chi & 0 & 0 \\ \sinh \chi & \cosh \chi & 0 & 0 \\ 0 & 0 & 1 & 0 \\ 0 & 0 & 0 & 1 \end{bmatrix}. \quad (\text{A.14})$$

A.2.1 Incident photons

When the incident particle is a photon, the boost from the center-of-mass frame to the laboratory frame must be determined relativistically, because the mass of the incident particle is zero but its momentum is nonzero.

In this case, Eq. (A.5) simplifies to

$$|p_{i,\text{lab}}| = T_{i,\text{lab}},$$

and Eq. (A.12) becomes

$$\sinh \chi = \frac{T_{i,\text{lab}}}{\sqrt{m_t^2 + 2m_t T_{i,\text{lab}}}}.$$

It follows that

$$\cosh \chi = \frac{m_t + T_{i,\text{lab}}}{\sqrt{m_t^2 + 2m_t T_{i,\text{lab}}}}.$$

A.3 Outgoing particles

Denote by m_e the rest mass of the emitted particle and $T_{e,\text{cm}}$ its kinetic energy in the center-of-mass frame. The convention in GND is that the energy Q of the reaction is specified by the data, and the rest mass m_R of the residual is calculated from

$$m_R = m_t + (m_i - m_e) - Q. \quad (\text{A.15})$$

Let $T_{R,\text{cm}}$ be the kinetic energy of the residual in the center-of-mass frame. In terms of these variables, the energy-momentum invariant for the system is the square of the total energy

$$S = (m_e + T_{e,\text{cm}} + m_R + T_{R,\text{cm}})^2,$$

with the same value of S as in Eq. (A.7). The argument leading to Eq. (A.8) shows that the momentum $p_{e,\text{cm}}$ of the emitted particle in the center-of-mass frame has magnitude given by

$$p_{e,\text{cm}}^2 = \frac{[S - (m_R^2 + m_e^2)]^2 - 4m_R^2 m_e^2}{4S}. \quad (\text{A.16})$$

It is not a good idea to use Eq. (A.16) in a computation, because of its subtraction of nearly equal numbers. It is therefore desirable to do some algebraic manipulation in order to mitigate this problem as much as possible. As a first step, Eq. (A.16) is rewritten in the form

$$4Sp_{e,\text{cm}}^2 = [S - (m_R + m_e)^2] [S - (m_R - m_e)^2]. \quad (\text{A.17})$$

In this expression, the subtraction of nearly equal numbers is confined to the first factor on the right-hand side. For photon emission the two factors are identical. An analysis of photon emission later, because it offers some simplifications.

By using the expression for S in Eq. (A.6), one obtains the relation

$$S - (m_R + m_e)^2 = (m_t + m_i)^2 - (m_R + m_e)^2 + 2m_t T_{i,\text{lab}}.$$

In terms of the energy Q of the discrete 2-body reaction and the parameter

$$M_T = m_t + m_R + m_i + m_e, \quad (\text{A.18})$$

it follows that

$$S - (m_R + m_e)^2 = M_T Q + 2m_t T_{i,\text{lab}}.$$

Consequently, it is seen that Eq. (A.16) may be replaced by

$$p_{e,\text{cm}}^2 = \frac{(M_T Q + 2m_t T_{i,\text{lab}})(M_T Q + 2m_t T_{i,\text{lab}} + 4m_R m_e)}{4S}. \quad (\text{A.19})$$

Remark. It is clear from Eq. (A.19) that for endothermic reactions ($Q < 0$), the threshold occurs when the incident particle has kinetic energy

$$T_{i,\text{lab}} = \frac{-M_T Q}{2m_t}.$$

In Eq. (A.19) there is subtraction of nearly equal numbers when the kinetic energy $T_{i,\text{lab}}$ of the incident particle is just above the threshold in endothermic reactions. That operation is unavoidable in the analysis of nuclear reactions.

Now that $p_{e,\text{cm}}^2$ has been obtained in Eq. (A.19), one may use Eq. (A.4) to determine the kinetic energy of the emitted particle in the center-of-mass frame as

$$T_{e,\text{cm}} = \frac{p_{e,\text{cm}}^2}{m_e + \sqrt{m_e^2 + p_{e,\text{cm}}^2}}. \quad (\text{A.20})$$

A.3.1 The boost to the laboratory frame

It is often desired to determine the kinetic energy $T_{e,\text{lab}}$ and momentum $p_{e,\text{lab}}$ of the emitted particle in the laboratory frame for given direction cosine μ_{cm} in the center-of-mass frame. It is possible to use the boost Eq. (A.13) to determine $p_{e,\text{lab}}$ as follows. Recall that the form of Eq. (A.13) is determined by the requirement that the first axis of the coordinate system was chosen parallel to $p_{i,\text{lab}}$. Consequently, one has

$$p_{e1,\text{cm}} = \mu_{\text{cm}} |p_{e,\text{cm}}|.$$

If the orientation of the coordinate system is such that

$$p_{e3,\text{cm}} = 0 \quad \text{and} \quad p_{e2,\text{cm}} \geq 0,$$

then

$$p_{e2,\text{cm}} = |p_{e,\text{cm}}| \sqrt{1 - \mu_{\text{cm}}^2}.$$

The momentum components of the boost Eq. (A.13) then take the form

$$\begin{aligned} p_{e1,\text{lab}} &= (m_e + T_{e,\text{cm}}) \sinh \chi + \mu_{\text{cm}} |p_{e,\text{cm}}| \cosh \chi, \\ p_{e2,\text{lab}} &= |p_{e,\text{cm}}| \sqrt{1 - \mu_{\text{cm}}^2}, \\ p_{e3,\text{lab}} &= 0. \end{aligned}$$

The magnitude of the momentum in the laboratory frame is

$$|p_{e,\text{lab}}| = \sqrt{p_{e1,\text{lab}}^2 + p_{e2,\text{lab}}^2 + p_{e3,\text{lab}}^2}.$$

If $|p_{e,\text{lab}}| = 0$, the direction cosine μ_{lab} in the laboratory frame is undetermined. Otherwise, it is given by

$$\mu_{\text{lab}} = \frac{p_{e1,\text{lab}}}{|p_{e,\text{lab}}|}.$$

The kinetic energy $T_{e,\text{lab}}$ is calculated from $|p_{e,\text{lab}}|$ by using Eq. (A.4).

A.3.2 Photon emission

When the emitted particle is a photon, because $m_e = 0$, Eqs. (A.19) and (A.20) take the simpler form

$$E_{e,\text{cm}} = T_{e,\text{cm}} = |p_{e,\text{cm}}| = \frac{M_T Q + 2m_t T_{i,\text{lab}}}{2\sqrt{S}}.$$

For given direction cosine μ_{cm} in the center-of-mass frame, the energy component of the boost Eq. (A.13) gives the Doppler shift

$$E_{e,\text{lab}} = E_{e,\text{cm}} (\cosh \chi + \mu_{\text{cm}} \sinh \chi).$$

The first component of the momentum of the photon in the laboratory frame is

$$p_{e1,\text{lab}} = E_{e,\text{cm}} (\sinh \chi + \mu_{\text{cm}} \cosh \chi),$$

so the direction cosine is

$$\mu_{\text{lab}} = \frac{\sinh \chi + \mu_{\text{cm}} \cosh \chi}{\cosh \chi + \mu_{\text{cm}} \sinh \chi}.$$

B Proof of Assertion 8.1.1

It is proved in this appendix that for a Newtonian boost, for the function G_0 defined in Eq. (8.4), it is true that arcs $E'_{\text{lab}} = E_{\text{bin}}$ and $E'_{\text{cm}} = \text{const}$ in Figure 8.1 intersect if and only if $G_0(E_{\text{bin}}, E'_{\text{cm}}, E) \geq 0$.

The clearest way to prove this assertion is to argue four cases directly:

$$G_0(E'_{\text{bin}}, E'_{\text{cm}}, E) \geq 0 \quad \text{and} \quad E'_{\text{trans}} + E'_{\text{cm}} \geq E'_{\text{bin}}, \quad (\text{B.1})$$

$$G_0(E'_{\text{bin}}, E'_{\text{cm}}, E) \geq 0 \quad \text{and} \quad E'_{\text{trans}} + E'_{\text{cm}} < E'_{\text{bin}}, \quad (\text{B.2})$$

$$G_0(E'_{\text{bin}}, E'_{\text{cm}}, E) < 0 \quad \text{and} \quad E'_{\text{trans}} + E'_{\text{cm}} \geq E'_{\text{bin}}, \quad (\text{B.3})$$

$$G_0(E'_{\text{bin}}, E'_{\text{cm}}, E) < 0 \quad \text{and} \quad E'_{\text{trans}} + E'_{\text{cm}} < E'_{\text{bin}}. \quad (\text{B.4})$$

In these inequalities E'_{trans} is as defined in Eq. (4.7).

A geometric condition for the intersection of the two arcs is presented first. It is then shown that this geometric condition is equivalent to the non-negativity of G_0 .

B.1 An equivalent geometric condition

The geometric condition is that for given values of E'_{bin} , E'_{cm} and E , the arcs $E'_{\text{lab}} = E'_{\text{bin}}$ and $E'_{\text{cm}} = \text{const}$ in Figure 8.1 intersect if and only if

$$\left(\sqrt{E'_{\text{trans}}} - \sqrt{E'_{\text{cm}}} \right)^2 \leq E'_{\text{bin}} \leq \left(\sqrt{E'_{\text{trans}}} + \sqrt{E'_{\text{cm}}} \right)^2. \quad (\text{B.5})$$

For the purposes of this argument, it is convenient to use units of mass such that the mass of the outgoing particle is $m_{y0} = 2$. Thus, its speed in the center-of-mass frame is $V'_{\text{cm}} = \sqrt{E'_{\text{cm}}}$. The arcs in Figure 8.1 may be viewed either as curves of constant energy or constant speed. For given energy E of the incident particle, the speed $V_{\text{trans}} = \sqrt{E'_{\text{trans}}}$ of the center of mass is determined. In terms of the speeds with $V'_{\text{bin}} = \sqrt{E'_{\text{bin}}}$, the condition Eq. (B.5) is equivalent to

$$V_{\text{trans}}^2 + V_{\text{cm}}'^2 - 2V_{\text{trans}}V_{\text{cm}}' \leq V_{\text{bin}}'^2 \leq V_{\text{trans}}^2 + V_{\text{cm}}'^2 + 2V_{\text{trans}}V_{\text{cm}}'. \quad (\text{B.6})$$

For emission in the forward direction, the speed of the outgoing particle in the laboratory frame is

$$V'_{\text{lab}} = V_{\text{trans}} + V'_{\text{cm}},$$

so that its energy in the laboratory frame is

$$V_{\text{lab}}'^2 = V_{\text{trans}}^2 + V_{\text{cm}}'^2 + 2V_{\text{trans}}V_{\text{cm}}'.$$

In backward emission, the speed of the outgoing particle in the laboratory frame is

$$V'_{\text{lab}} = |V_{\text{trans}} - V'_{\text{cm}}|,$$

and its energy in the laboratory frame is

$$V'^2_{\text{lab}} = V^2_{\text{trans}} + V'^2_{\text{cm}} - 2V_{\text{trans}}V'_{\text{cm}}.$$

It follows that if condition Eq. (B.6) is true, then there exists a center-of-mass direction cosine μ_{cm} with $-1 \leq \mu_{\text{cm}} \leq 1$ for which the emitted particle has the desired laboratory energy

$$V'^2_{\text{bin}} = V^2_{\text{trans}} + V'^2_{\text{cm}} + 2\mu_{\text{cm}}V_{\text{trans}}V'_{\text{cm}}.$$

The two arcs $E'_{\text{lab}} = E'_{\text{bin}}$ and $E'_{\text{cm}} = \text{const}$ intersect at this value of μ_{cm} . It is seen that if the geometric condition Eq. (B.5) is satisfied, then the arcs $E'_{\text{lab}} = E'_{\text{bin}}$ and $E'_{\text{cm}} = \text{const}$ do intersect.

It is now shown that if Eq. (B.6) is false, then the arcs $E'_{\text{lab}} = E'_{\text{bin}}$ and $E'_{\text{cm}} = \text{const}$ do not intersect. One way for Eq. (B.6) to be false is that

$$V'_{\text{bin}} > V_{\text{trans}} + V'_{\text{cm}}. \quad (\text{B.7})$$

In this case, forward emission has insufficient energy in the laboratory frame, and the arc $E'_{\text{cm}} = \text{const}$ in Figure 8.1 is entirely enclosed within the arc $E'_{\text{lab}} = E'_{\text{bin}}$.

If

$$V'_{\text{bin}} < |V_{\text{trans}} - V'_{\text{cm}}|, \quad (\text{B.8})$$

there are two more ways for Eq. (B.6) to be false, depending on whether

$$V'_{\text{cm}} < V_{\text{trans}} \quad (\text{B.9})$$

or

$$V'_{\text{cm}} > V_{\text{trans}}. \quad (\text{B.10})$$

Under the conditions in Eq. (B.9), backward emission in the center-of-mass frame boosts to forward emission in the laboratory frame. The condition Eq. (B.8) implies that

$$V'_{\text{bin}} < V_{\text{trans}} - V'_{\text{cm}},$$

so that the arc $E'_{\text{lab}} = E'_{\text{bin}}$ is completely to the left of the arc $E'_{\text{cm}} = \text{const}$ in Figure 8.1. (In fact, one pair of such arcs is shown in Figure 8.1.)

The final way for Eq. (B.6) to be false is that conditions Eqs. (B.8) and (B.10) be valid. In this case, backward emission in the center-of-mass frame produces backward emission in the laboratory frame with

$$V'_{\text{bin}} < V'_{\text{cm}} - V_{\text{trans}}.$$

In this case, the arc $E'_{\text{lab}} = E'_{\text{bin}}$ is completely contained within the arc $E'_{\text{cm}} = \text{const}$ in Figure 8.1. This finishes the proof of the assertion that the arcs $E'_{\text{lab}} = E'_{\text{bin}}$ and $E'_{\text{cm}} = \text{const}$ in Figure 8.1 intersect if and only if Eq. (B.5) is true.

B.2 Proof of the assertion

Consider the case Eq. (B.1) above. That is, suppose that

$$G_0(E'_{\text{bin}}, E'_{\text{cm}}, E) \geq 0 \quad (\text{B.11})$$

and

$$E'_{\text{trans}} + E'_{\text{cm}} \geq E'_{\text{bin}}. \quad (\text{B.12})$$

It is now shown that these two inequalities lead to the geometric condition Eq. (B.5) for intersection of the two arcs. The inequality Eq. (B.11) may be rewritten in the form

$$4E'_{\text{cm}}E'_{\text{trans}} - (E'_{\text{trans}} + E'_{\text{cm}} - E'_{\text{bin}})^2 \geq 0.$$

Because of the fact that $E'_{\text{trans}} + E'_{\text{cm}} - E'_{\text{bin}} \geq 0$, it is possible to take positive square roots to obtain the relation

$$2\sqrt{E'_{\text{cm}}E'_{\text{trans}}} \geq E'_{\text{trans}} + E'_{\text{cm}} - E'_{\text{bin}},$$

which may be rearranged as

$$E'_{\text{bin}} \geq \left(\sqrt{E'_{\text{trans}}} - \sqrt{E'_{\text{cm}}} \right)^2.$$

The first of the inequalities Eq. (B.5) is now verified.

The second inequality Eq. (B.5) follows trivially from the assumption Eq. (B.12),

$$E'_{\text{bin}} \leq E'_{\text{trans}} + E'_{\text{cm}} \leq E'_{\text{trans}} + E'_{\text{cm}} + 2\sqrt{E'_{\text{cm}}E'_{\text{trans}}}.$$

The other three cases may be analyzed in a similar fashion.

Bibliography

- [1] C. M. Mattoon et al., “Generalized Nuclear Data: a New Structure (with Supporting Infrastructure) for Handling Nuclear Data”, *Nuclear Data Sheets* **113** (2012) 2145.
- [2] B. R. Beck, “The `fudge` data processing code”, *AIP Conf. Proc.* **769** (2004) 503.
- [3] E. E. Lewis and W. F. Miller, *Computational methods of neutron transport*, Wiley, New York, 1984.
- [4] R. J. Howerton, R. E. Dye, P. C. Giles, J. R. Kimlinger, S. T. Perkins, and E. F. Plechaty, “Omega: a Cray 1 executive code for LLNL nuclear data libraries”, Report UCRL-50400 Vol. 25, Lawrence Livermore National Laboratory, Livermore, California, 1983.
- [5] G. W. Hedstrom, “An explanation of `ndfgen`”, Report PD-211, Nuclear Data Group, Lawrence Livermore National Laboratory, Livermore, California, 2000.
- [6] W. Gander and W. Gautschi, “Adaptive quadrature—revisited”, *BIT* **40** (2000) 84–101.
- [7] M. Herman, A. Trkov, and D. A. Brown, “ENDF-6 Formats Manual; Data Formats and Procedures for the Evaluated Nuclear Data Files ENDF/B-VI and ENDF/B-VII”, Report BNL-90365-2009 Rev. 2, National Nuclear Data Center, Brookhaven National Laboratory, Upton, New York, 2012.
- [8] G. W. Hedstrom, “Interpolation of nuclear reaction energy distributions”, *J. Nucl. Sci. Tech.*, to appear.
- [9] M. B. Chadwick *et al.*, “ENDF/B-VII.1 Nuclear Data for Science and Technology: Cross Sections, Covariances, Fission Product Yields and Decay Data”, *Nuclear Data Sheets* **112** (2011) 2887–2996.
- [10] G. W. Hedstrom, “An explanation of the `ENDEP` code”, Report PD-210, Nuclear Data Group, Lawrence Livermore National Laboratory, Livermore, California, 1999.
- [11] D. G. Madland and J. R. Nix, “New calculation of prompt fission neutron spectra and average prompt neutron multiplicities”, *Nucl. Sci. Eng.* **81** (1982), 213–271.

- [12] C. Kalbach, “Systematics of continuum angular distributions: Extensions to higher energies”, *Phys. Rev. C* **37** (1988) 2350–2369.
- [13] M. B. Chadwick, P. G. Young, and S. Chiba, “Angular distribution systematics in the pseudodeuteron regime”, *J. Nucl. Sci. Tech.*, **32** (1995) 1154.